

# **Multifunctional Water-Soluble Polymers for Dewatering of Oil Sands Tailings**

by

Sarang Prakash Gumfekar

A thesis submitted in partial fulfillment of the requirements for the degree of

Doctor of Philosophy

in

Chemical Engineering

Department of Chemical and Materials Engineering  
University of Alberta

© Sarang Prakash Gumfekar, 2018

## Abstract

Certain areas of oil sands in Canada are mined and processed for bitumen production using hot water processes that produce a slurry waste, referred to as tailings. Sand particles in tailings quickly settle and produce mature fine tailings (MFT), which are stored in large tailing ponds. Currently, tailing ponds occupy approximately 200 km<sup>2</sup> and the long-term storage of tailings in these ponds poses a serious environmental liability. Advances in existing tailings management technologies are necessary for the sustainability of oil sands industry.

One of the major operational and environmental challenges that the oil sands industry faces is how to effectively dewater MFT and strengthen the resulting deposits, so that the land can be reclaimed. Basically, this challenge may be addressed by enhancing the settling rate of solids in MFT, improving the dewaterability of the sediments, and recovering the water under industrially acceptable conditions. Research in this area has explored technologies such as composite tailings (CT), polymer-assisted flocculation, centrifugation, and freeze-thaw. Polymer-assisted flocculation is a promising technology to enhance settling rate, dewaterability, and water recovery, since the molecular structure of polymers can be changed to meet different application criteria. Unfortunately, existing commercial flocculants still lack the prerequisites to specifically address the issues associated with MFT treatment.

In this work, we synthesized three main types of flocculants: *i*) hydrophobically-modified anionic terpolymers, *ii*) hydrophobically-modified cationic terpolymers, and *iii*) hydrolytically-degradable cationic polymers. The first polymer was used to flocculate kaolin suspensions, which is the most common type of clay in MFT, and the terpolymer composition was optimized based on its flocculation performance. The composition of second terpolymer was designed considering binary comonomer reactivity ratios, and used to flocculate MFT. The first two flocculants contained hydrophobic groups resulting from the incorporation of a hydrophobic

comonomer. The third flocculant was designed to become hydrophobic upon hydrolytic degradation, and was used to dewater and densify MFT.

The main objective of this research was to develop a methodology to design multifunctional polymers specifically suited to flocculate and dewater MFT, taking into account its surface properties and water chemistry. To achieve this goal, we investigated flocculants containing several functional monomers, molecular weights, anionicity/cationicity, hydrophobicity, and degradability. Operational parameters such as MFT dilution (solids content) and flocculant dosage were also studied.

Flocculation performance was evaluated in terms of MFT settling rate, capillary suction time (dewaterability) of sediments, supernatant clarity, and floc formation ability. It would be ill-advised to make a general recommendation for ‘best-flocculant’ because the performance requirements of a flocculant may differ among oil operators. However, this work offers a rational methodology to systematically design flocculants considering the requirements of a given system. Systematically designed flocculants for MFT certainly offer more functionality than using conventional polymers that are used to treat other wastewater.

## Acknowledgement

After an intensive period of four years of doctoral study, writing this note of thanks is the finishing touch on my thesis. It has been a period of intense learning for me, not only in the scientific field but also on a personal level. I would like to reflect on the people who have supported and helped me throughout this period in various capacities.

Firstly, I would like to express my sincere gratitude to my advisor Prof. João Soares for giving me an opportunity to join his research group. I am thankful for his continuous support of my doctoral study and related research, for his patience, encouragement, and immense knowledge. In addition to guiding this research, he provided various opportunities to broaden my professional experience and prepared me for my career and future challenges. I am grateful to him. I could not have imagined having a better advisor and mentor for my doctoral study, and a role model for life. I wish I could be as lively, hardworking, and energetic as him.

Besides my advisor, I would like to thank Prof. Robin Hutchinson, Queens University Kingston, and his research group for the productive collaboration and introducing me to a new class of degradable polymers.

I sincerely thank Dr. Zhenge Xu, Dr. Ravin Narain, and the Institute of Oil Sands Innovation (IOSI), who provided me an access to their research facilities. I thank my fellow labmates in the Soares research group for the stimulating discussions and for all the fun we have had in the last four years. It is impossible to write about every labmate since the group always had more than 25 researchers and everyone helped my work in one or other way. I am also thankful to Chemical and Materials Engineering (CME) department for providing various teaching opportunities during my doctoral study.

I am grateful to Dr. Chandrashekar Mahajan and Dr. Shirish Sonawane for enlightening me the first glance of research in my undergraduate study.

Last but not the least, I would like to thank my family: my grandfather, my parents, brother, and lovely wife for supporting me through moral and emotional support during the PhD studies. I will miss my encouraging and always enthusiastic late grandmother for her screams of joy whenever a significant momentous was reached in my life.

## Table of Contents

<b>Chapter 1 Introduction</b> .....	<b>1</b>
1.1 Oil Sands Extraction.....	1
1.2 Challenges Associated with MFT Dewatering.....	2
1.3 Research Objectives .....	3
1.4 Thesis Outline .....	4
References .....	5
<b>Chapter 2 Theory and Literature Review</b> .....	<b>6</b>
2.1 Clays: Structure, Surface Reactions, and Cation Exchange Capacity.....	6
2.2 Electrical Double Layer: Derjaguin, Landau, Verwey, and Overbeek (DLVO) Theory .....	8
2.3 Coagulation and Flocculation Mechanisms .....	10
2.4 Polymers for Clays and MFT Settling: Literature Review .....	12
2.4.1 Acrylamide-based Polymers.....	12
2.4.2 Thermosensitive Polymers .....	16
2.4.3 Natural Polymers .....	18
2.4.4 Hydrophobically-modified Polymers .....	21
2.4.5 Challenges and Knowledge Gap.....	22
References .....	24
<b>Chapter 3 A Novel Hydrophobically-Modified Polyelectrolyte for Enhanced Dewatering of Clay Suspension</b> .....	<b>28</b>
3.1 Introduction .....	28
3.2 Experimental .....	31
3.2.1 Materials .....	31
3.2.2 Synthesis of p(NIPAM), p(NIPAM-AA), and p(NIPAM-AA-NTBM).....	31
3.2.3 Characterization of Polymers and Clay Suspension.....	32
3.2.4 Settling Tests .....	33
3.3 Results and Discussion.....	35
3.3.1 Synthesis of Hydrophobically-modified Polyelectrolytes.....	35
3.3.2 Thermo-Responsive Behavior of Polyelectrolytes.....	39
3.3.3 Flocculation of Kaolin Slurries.....	40
3.4 Conclusions .....	46
References .....	48

<b>Chapter 4 Rational Design of Multifunctional Terpolymer Based On the Reactivity Ratios and Its Application for Dewatering Oil Sands Tailings .....</b>	<b>52</b>
4.1 Introduction .....	52
4.2 Materials and Methods .....	55
4.2.1 Materials .....	55
4.2.2 Synthesis of p(NIPAM-MATMAC-BAAM) .....	55
4.2.3 Tailings Characterization and Flocculation Tests .....	56
4.3 Results and Discussion.....	58
4.3.1 Composition Drift in Binary Copolymers .....	58
4.3.2 Determination of Reactivity Ratios .....	59
4.3.3 Estimation of Terpolymer Composition.....	63
4.3.4 Floc Formation in MFT using Terpolymers .....	65
4.3.5 Initial Settling Rate of MFT using Terpolymers .....	68
4.3.6 Capillary Suction Time: The Ability to Dewater Sediments.....	69
4.4 Conclusions .....	71
References .....	73
<b>Chapter 5 Dewatering Oils Sands Tailings with Degradable Polymer Flocculants .....</b>	<b>76</b>
5.1 Introduction .....	76
5.2 Materials and Methods .....	80
5.2.1 Materials .....	80
5.2.2 Macromonomer Synthesis .....	80
5.2.3 Macromonomer Copolymerization.....	81
5.2.4 Ex-situ Degradation Study.....	82
5.2.5 Oil Sands Flocculation Tests .....	82
5.3 Results and Discussion.....	84
5.3.1 Synthesis of PCL <sub>2</sub> ChMA and TMAEMC-based Polymers.....	84
5.3.2 Effect of Solids Content in MFT .....	85
5.3.3 Initial Settling Rate (ISR).....	87
5.3.4 Supernatant Turbidity .....	88
5.3.5 Capillary Suction Time and Degradation Study.....	90
5.3.6 Significance of the Current Work and Environmental Implication.....	94
5.4 Conclusions .....	96

References .....	97
<b>Chapter 6 Conclusions and Recommendations.....</b>	<b>101</b>
6.1 Conclusions .....	101
6.2 Recommendations .....	102
<b>Bibliography .....</b>	<b>105</b>
<b>Appendix A Supplementary Information for Chapter 5.....</b>	<b>115</b>
<b>Appendix B Terpolymer Composition using the Reactivity Ratios Calculated by Different Methods.....</b>	<b>120</b>

## List of Figures

<b>Figure 1-1</b> Actual Alberta bitumen production rate as of 2008 and forecast to 2018. (Energy Resources Conservation Board, 2009).....	1
<b>Figure 1-2</b> Schematic of oil sands extraction emphasizing main elements of the process .....	2
<b>Figure 2-1</b> Layer structure of kaolin and illite clays. (Konan et al., 2007).....	6
<b>Figure 2-2</b> Protonation of aluminum hydroxyl surface at low pH and deprotonation at high pH. 7	7
<b>Figure 2-3</b> Schematic of the electric double layer and a graph of electric potential in the double layer as a function of distance from the particle surface. (Yingchoncharoen et al., 2016).....	9
<b>Figure 2-4</b> Effect of electrolyte concentration on DLVO interaction energy. (Guo et al., 2014) 11	11
<b>Figure 2-5</b> Various configurations of polymer chains on the particle surface and their suitability for flocculation.....	12
<b>Figure 2-6</b> Chemical structures of acrylamide-based neutral, anionic, and cationic polymers. ..	13
<b>Figure 2-7</b> Role of calcium ions in the flocculation of negatively charged surfaces. (Long et al., 2006) .....	13
<b>Figure 2-8</b> Schematic illustration of thermosensitive phase transition in PNIPAM. (Dimitrov et al., 2007) .....	17
<b>Figure 2-9</b> Effect of linear and graft architecture of starch-based cationic flocculants on floc size. (Wu et al., 2016) .....	20
<b>Figure 3-1</b> Schematic of experimental polymerization setup for NIPAM, AA, and NTBM.....	32
<b>Figure 3-2</b> Particle size distribution of clay particles in suspension.....	33
<b>Figure 3-3</b> Relationship between number average molecular weight ( $M_n$ ) of p(NIPAM) and initiator concentration. Red markers denote the experiments carried out to verify the correlation in the equation.....	37
<b>Figure 3-4</b> NMR spectra of p(NIPAM)549k (bottom), p(NIPAM-AA)20 (middle), and p(NIPAM-AA-NTBM)13 (top) along with corresponding molecular structures. The inset figures show the magnified view between $\delta = 7 - 8$ ppm to reveal NH proton.....	38
<b>Figure 3-5</b> Lower critical solution temperature (LCST) of the p(NIPAM)549k, p(NIPAM-AA)10 (middle), and p(NIPAM-AA-NTBM)7. ....	39



<b>Figure 3-6</b> Effect of number average molecular weight ( $M_n$ ) of p(NIPAM) on (A) settling profile and (B) initial settling rate (ISR) of kaolin suspension.....	40
<b>Figure 3-7</b> Effect of acrylic acid concentration in p(NIPAM-AA) on (A) settling profile and (B) initial settling rate (ISR) of kaolin suspension.....	41
<b>Figure 3-8</b> Effect of NTBM concentration in p(NIPAM-AA-NTBM) on (A) settling profile and (B) initial settling rate (ISR) of kaolin suspension .....	42
<b>Figure 3-9</b> Floc size distribution in kaolin suspension without and with 2000 ppm (NIPAM-AA-NTBM) terpolymer. ....	42
<b>Figure 3-10</b> Supernatant turbidity obtained after flocculation using: A) p(NIPAM) of different number average molecular weights, B) p(NIPAM-AA) of varying AA contents, and (C) p(NIPAM-AA-NTBM) of 20 mol % AA and varying NTBM content. ....	43
<b>Figure 3-11</b> Capillary suction time (CST) of the sediments obtained after the flocculation using (A) p(NIPAM) of different number average molecular weights, (B) p(NIPAM-AA) of varying AA concentration, and (C) p(NIPAM-AA-NTBM) of 20 mol % AA and varying NTBM content. ....	44
<b>Figure 3-12</b> Zeta potential of clay suspension with increase in terpolymer concentration.....	45
<b>Figure 3-13</b> Images of kaolin suspension without polymer and with 2000 ppm of optimized p(NIPAM-AA) and p(NIPAM-AA-NTBM).....	46
<b>Figure 4-1</b> Experimental polymerization setup for the polymers and chemical structures of the repeating units of p(NIPAM-MATMAC-BAAM) .....	56
<b>Figure 4-2</b> Schematic of initial settling rate calculation based on the settling profile.....	57
<b>Figure 4-3</b> Composition curves showing the drift in compositions of copolymers (A) p(NIPAM-MATMAC), (B) p(MATMAC-BAAM), and (C) p(NIPAM-BAAM) ( $f$ : fraction of comonomer in feed; $F$ : fraction of comonomer in the copolymer).....	59
<b>Figure 4-4</b> Determination of binary reactivity ratios using (A) Fineman-Ross method and (B) Kelen-Tudos method.....	60
<b>Figure 4-5</b> Determination of optimum fraction of MATMAC monomer in p(NIPAM-MATMAC) based on (A) initial settling rate of MFT and (B) capillary suction time of MFT sediments.....	64

<b>Figure 4-6</b> Real-time evolution of floc size in MFT using different dosages of (A) P(NMB-5), (B) P(NMB-10), and (C) P(NMB-15). The number $x$ in P(NMB- $x$ ) denotes the mol % BAAM in the terpolymer. ....	65
<b>Figure 4-7</b> Floc size distribution using different dosages of (A) P(NMB-5), (B) P(NMB-10), and (C) P(NMB-15). The number $x$ in P(NMB- $x$ ) denotes the mol% BAAM in terpolymer .....	67
<b>Figure 4-8</b> Surface response of initial settling rate as a function of varying BAAM content in terpolymer and its dosage .....	68
<b>Figure 4-9</b> Surface response of capillary suction time as a function of varying BAAM content in terpolymer and its dosage .....	70
<b>Figure 4-10</b> Flocculation images MFT using 5000 ppm of p(NIPAM-MATMAC-BAAM) terpolymer with varying fractions of BAAM. The first cylinder (left) is an example of poor flocculation due to insufficient dosage. Magnified images show the compaction of swelling clays (grey-colored). ....	71
<b>Figure 5-1</b> Chemical structures of cationic macromonomers used in radical homopolymerizations, as well as respective copolymerizations with acrylamide (AM) to produce flocculants investigated in this work.....	79
<b>Figure 5-2</b> Schematic representation of the flocculation procedure. ....	83
<b>Figure 5-3</b> Mudline height after flocculation using 5000 ppm of poly(PCL <sub>2</sub> ChMA) with MFT diluted to: a) 2 wt. % (30 min); b) 5 wt. % (30 min); c) 10 wt. % (24 h); and d) control sample with 5 wt. % MFT and 5000 ppm of PAM (30 min). ....	86
<b>Figure 5-4</b> Initial settling rates (ISR) using PCL <sub>2</sub> ChMA and TMAEMC-based polymers and copolymers at varying dosages with 5 wt. % MFT. Missing data for poly(PCL <sub>2</sub> ChMA) and poly(PCL <sub>2</sub> ChMA-AM) denotes insignificant settling. Inset images show the flocculation behavior after 24 h at respective dosages. ....	87
<b>Figure 5-5</b> Supernatant turbidity obtained after flocculation of 5 wt. % MFT using PCL <sub>2</sub> ChMA and TMAEMC homopolymers and copolymers at varying dosages. Turbidity values are indicated for each experiment, as the scale varies for each plot; ‘broken’ y-axes are used to visualize the relative changes among the lower turbidity values.....	89
<b>Figure 5-6</b> Capillary suction times for sediments obtained from flocculation of 5 wt. % MFT using the four cationic (co)polymers, measured before and after accelerated degradation of the sediments at 85 °C for one week. ....	91

**Figure 5-7** Cryo-FE-SEM images of: A) raw MFT, B) sediments obtained after flocculation C) internal structure of a floc, and D) the sediments obtained after the polymer hydrolysis ..... 94

**Figure A-1** <sup>1</sup>H-NMR spectrum and peak assignment for the average chain length of PCL<sub>2</sub>De in CDCl<sub>3</sub> at 25 °C.....115

**Figure A-2** <sup>1</sup>H NMR spectrum and peak assignment for PCL<sub>2</sub>DeMA in CDCl<sub>3</sub> at 25 °C.....116

**Figure A-3** <sup>1</sup>H NMR spectrum and peak assignment for PCL<sub>2</sub>ChMA in CDCl<sub>3</sub> at 25 °C... ..117

**Figure A-4** Molecular weight distributions for cationic macromonomer precursors measured in polyMMA equivalents by SEC with THF as eluent. ....118

**Figure A-5** Additional Cryo-FE-SEM images show the multiple similar microstructures across the sample. ....118

## List of Tables

<b>Table 3-1</b> Properties of flocculants synthesized in this study. ....	35
<b>Table 4-1</b> MFT composition determined using the Dean-Stark method.....	56
<b>Table 4-2</b> Ion composition in MFT measured using atomic absorption spectroscopy .....	56
<b>Table 4-3</b> Summary of binary reactivity ratios calculated by Fineman-Ross, Kelen-Tudos, and Yezrielev - Brokhina – Roskin method .....	61
<b>Table 4-4</b> Feed and terpolymer composition of the flocculants used in this study .....	65
<b>Table 5-1</b> Polymer charge densities, molecular weight averages and dispersities (effective values relative to PEO calibration). Copolymers contain 70 mol % AM .....	84
<b>Table A-1</b> Tabular format of CST values measured before the degradation of polymer (s) ....	119
<b>Table A-2</b> Tabular format of CST values measured before the degradation of polymer (s) ....	119
<b>Table B-1</b> Feed and terpolymer composition of the flocculants estimated using the reactivity ratios calculated by Fineman-Ross method. ....	120
<b>Table B-2</b> Feed and terpolymer composition of the flocculants estimated using the reactivity ratios calculated by Kelen-Tudos method. ....	120
<b>Table B-3</b> Feed and terpolymer composition of the flocculants estimated using the reactivity ratios calculated by Yezrielev - Brokhina – Roskin method. ....	120

# Chapter 1

## Introduction

This chapter describes the oil sands extraction process that is responsible for tailings generation. Further, it describes the composition of tailings and the challenges associated with its dewatering. Next, the specific research objectives of this work are stated. The chapter ends with a description of the thesis outline.

### 1.1 Oil Sands Extraction

Oil sands deposits are a resource of global strategic value and a guarantee of its energy future. Canada's total oil-in-place reserve is estimated at 1.7 trillion barrels, which are roughly equivalent to the total reserves for the entire Middle East region. Approximately 20% of the bitumen is accessible through surface mining processes, and 80% requires in-situ methods such as steam-assisted gravity drainage (SAGD) process. As shown in Figure 1-1, the estimated bitumen production rate in 2018 would be approximately  $450 \times 10^3 \text{ m}^3/\text{day}$ , as per the Energy Resources Conservation Board (ERCB) 2008 report. (Energy Resources Conservation Board, 2009)

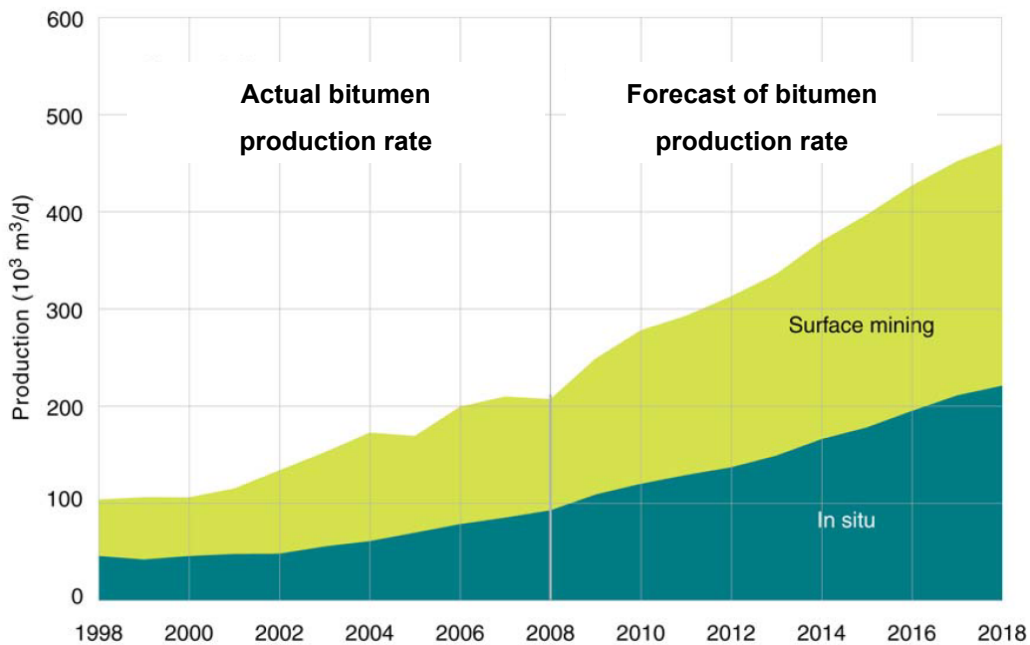


**Figure 1-1** Actual Alberta bitumen production rate as of 2008 and forecast to 2018. (Energy Resources Conservation Board, 2009)

Clark and Pasternack developed a process that used hot water to separate bitumen obtained via surface mining. (Clark and Pasternack, 1932) A simplified schematic of the oil sands extraction process is shown in Figure 1-2. In a typical process, oil sands are mined and crushed for size reduction and further processing. ‘Oil sands’ is used as a collective term for the lumps of sand coated with a water film, fines, and bitumen. These components exist as shown in Figure 1-2. Further, water and certain additives are added to prepare the slurry. In the extraction process, bitumen liberates from sand, attaching to air bubbles that were entrained during the slurry preparation step. Aerated bitumen froth, containing water and fine solids, rises to the top of the separation vessel. Bitumen can be enriched by diluting it with naphtha or paraffinic solvent. (Masliyah, J. H, Czarnecki, J. A, Xu, 2011) The tailings slurry, generated during bitumen extraction, is deposited in tailings ponds wherein coarse solids settle creating mature fine tailings (MFT).

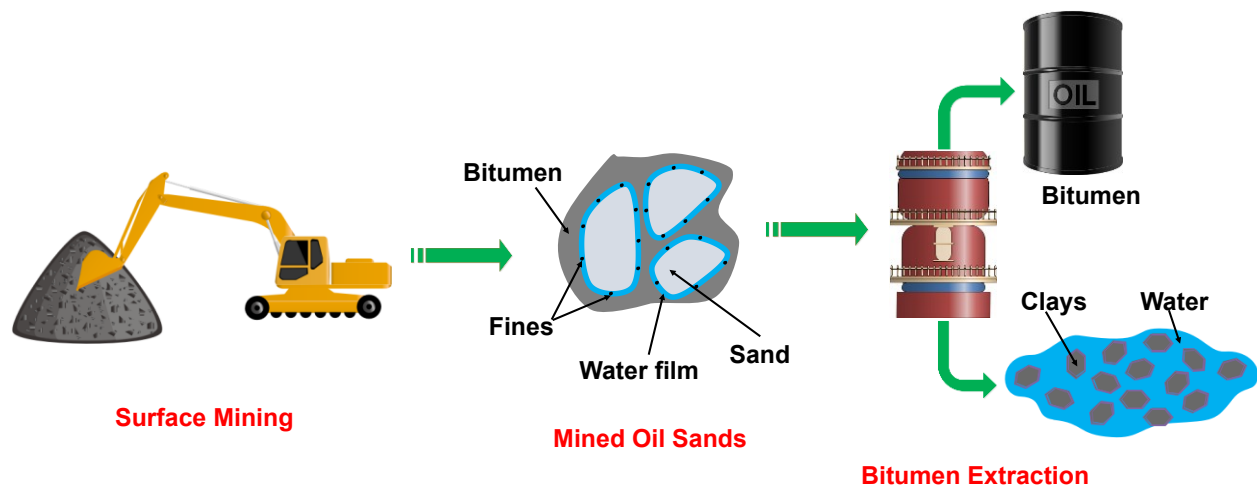


**Figure 1-2** Schematic of oil sands extraction emphasizing main elements of the process

## 1.2 Challenges Associated with MFT Dewatering

In a typical water-based bitumen extraction process, the production of one barrel of bitumen requires approximately 1.8 tons of oil sands mixed with 2.5 m<sup>3</sup> of hot water. (Sworska et al., 2000) After the recovery of one barrel of bitumen, approximately, 3.3 m<sup>3</sup> of tailings is generated and deposited in tailings ponds. Over several years, these tailings separate into three distinct layers: a layer of clear water on top, a transition layer composed of settling fines, and the MFT

zone at the bottom. MFT contains approximately 30 wt. % fine solids and 70 wt. % water. If bitumen is produced as forecasted, oil operators will generate several billion cubic meters of MFT in the next decade. The current tailings occupy a total area more than 200 km<sup>2</sup> and further accumulation of MFT will increase the operational cost and worsen critical environmental concerns.

- i) *Settling issue:* The poor settling rate of MFT is attributed to the use of caustic additives during the bitumen extraction process that causes the gelation of ultrafine particles (50-400 nm) in MFT. The gelation of ultrafine clays further leads to excessively high viscosity, making it difficult to consolidate. The surface charge of fine particles is also a key parameter to create a stable suspension in MFT. The clays in MFT (80 wt. % kaolin and 20 wt. % illite) bear negative charges that result in strong repulsion among them, leading to the formation of a stable suspension.
- ii) *Dewaterability issue:* MFT is known to hold a significant amount of water at alkaline pH that cannot be easily separated from the clays. Strong repulsion between the clay basal planes increases the gap between clay platelets, which is likely responsible for holding a substantial amount of water.
- iii) *Supernatant quality issue:* The water recovered from tailings is often recycled for bitumen extraction, and the efficiency of bitumen extraction from oil sands depends on the quality of the recycled water. Although charge neutralization of clays using inorganic cations such as Ca<sup>++</sup> or Al<sup>+++</sup> seem to be an easy solution, such cations significantly reduce the bitumen extraction efficiency from the oil sands matrix. Therefore, the recycled water is expected to be free of cations. Also, the fine particles, which do not consolidate upon treatment, get recycled back to bitumen extraction process and cause operational problems.

### **1.3 Research Objectives**

The purpose of the present study is to develop novel polymeric systems that are specifically customized for effective dewatering of MFT. The specific objectives of this study are:

- I. Synthesis of thermosensitive, hydrophobically-modified, anionic flocculant and examine the feasibility of thermosensitive polymers for MFT dewatering
- II. Synthesis of hydrophobically-modified, cationic polyelectrolytes for MFT dewatering

- III. Synthesis of hydrolytically-degradable flocculant for long-term dewatering of MFT
- IV. Flocculation of clays and MFT using the flocculants mentioned above and investigation of underlying flocculating mechanisms

The proposed flocculants are expected to be first-of-their-kind, specifically tailored for MFT dewatering.

## 1.4 Thesis Outline

This thesis consists of 6 chapters. The current chapter (**Chapter 1**) introduces the process of MFT generation from bitumen extraction plant followed by the challenges associated with MFT dewatering. **Chapter 2** discusses the relevant theory needed to understand the MFT system and its polymer-assisted flocculation. The discussion on theory is limited to colloidal suspensions and surface chemistry. Further, it reviews the flocculants used for MFT dewatering and the polymers used for other wastewater treatment that can be extended for MFT dewatering. **Chapter 3** presents the work on hydrophobically-modified anionic flocculant that benefits from its thermosensitive behavior. The flocculant was used to dewater kaolin suspension (a model of MFT). The results obtained in this work are published as- *S. P. Gumfekar and J. B. P. Soares, "A novel hydrophobically-modified polyelectrolyte for enhanced dewatering of clay suspension" Chemosphere, vol. 194, pp. 422–431, 2018.* **Chapter 4** of the thesis presents a systematic design of hydrophobically-modified cationic terpolymer based on binary reactivity ratios. The flocculant composition was optimized and was used for MFT dewatering. The results obtained in this chapter are submitted for the publication as- *S. P. Gumfekar and J. B. P. Soares, "Rational Design of Multifunctional Terpolymer Based On the Reactivity Ratios And Its Application for Dewatering Oil Sands Tailings", ACS Appl. Mater. Interfaces, submitted.* **Chapter 5** describes the results obtained from a collaborative research with Professor Robin Hutchinson's group at Queen's University, Kingston, Canada. The chapter describes the synthesis of hydrolytically-degradable cationic polycomb flocculant, which becomes partially hydrophobic upon degradation and enhances the MFT dewatering over the long term. The results presented in this chapter are published as- *S. P. Gumfekar, T. R. Rooney, R. A. Hutchinson, and J. B. P. Soares, "Dewatering Oil Sands Tailings with Degradable Polymer Flocculants," ACS Appl. Mater. Interfaces, vol. 9, no. 41, pp. 36290–36300, 2017.* **Chapter 6** provides a summary of the



investigations carried out in this work along with recommendations for future work on flocculant synthesis and MFT dewatering.

## **References**

Clark, K.A., Pasternack, D.S., 1932. Hot Water Separation of Bitumen from Alberta Bituminous Sand. *Ind. Eng. Chem.* 24, 1410–1416. doi:10.1021/ie50276a016

Energy Resources Conservation Board, 2009. Alberta's Energy Reserves 2008 and Supply/Demand Outlook 2009-2018, Outlook.

Masliyah, J. H, Czarnecki, J. A, Xu, Z., 2011. Handbook on theory and practice of bitumen recovery from Athabasca oil sands: theoretical basis, 1st ed. Kingsley Knowledge Publishing, Canada.

Sworska, A., Laskowski, J., Cymerman, G., 2000. Flocculation of the Syncrude fine tailings. *Int. J. Miner. Process.* 60, 143–152. doi:10.1016/S0301-7516(00)00012-0

## Chapter 2

### Theory and Literature Review

#### 2.1 Clays: Structure, Surface Reactions, and Cation Exchange Capacity

Clays are the major component among the fine particles in MFT. The type and amount of clay play an important role in bitumen extraction, froth treatment, tailings management, and the recycled water quality. Clay fines and their associated effects cause the formation of MFT. Typical characteristics of clays include high specific surface area, platelet-like morphology, and anisotropic dimensions. It is important to understand the properties of clays because they affect the bitumen recovery process and MFT dewatering.

The major clay minerals in MFT are kaolin and illite, but a small fraction of montmorillonite and smectite clays may also be present in clay fines. In general, clays are made up of tetrahedron sheets of silicon-oxygen and octahedron sheets of aluminum-oxygen-hydroxyl. Distinctive arrangements of the tetrahedron and octahedron sheets can result in different types of clays. Kaolin is formed by two-layer structures, whereas illite by three-layer structures, as shown in Figure 2-1.

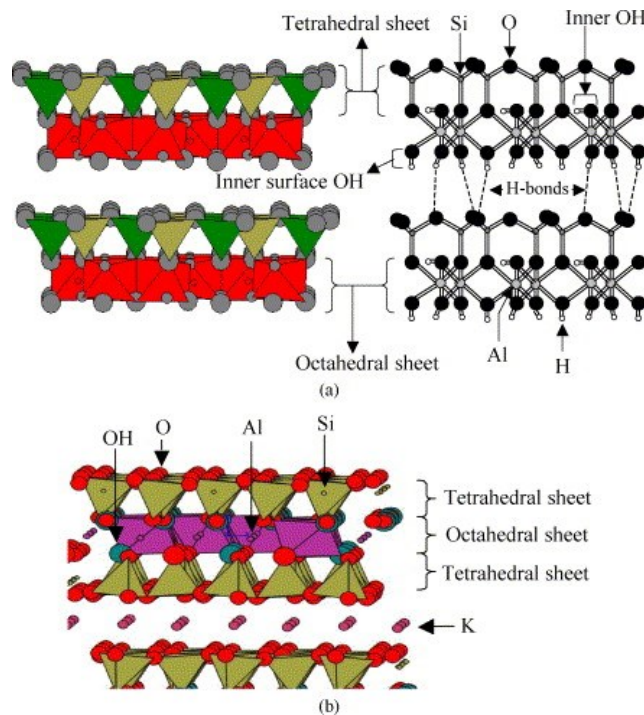


**Figure 2-1** Layer structure of kaolin and illite clays. (Konan et al., 2007)

The two layers in kaolin are covalently bonded to each other through the oxygen atoms in the tetrahedron sheet. Although kaolin and illite clays do not expand/swell, a small fraction of smectite clays (such as montmorillonite) in MFT undergoes significant expansion and forms a gel-like slurry. The tetrahedron and octahedron layers in kaolin carry permanent negative charges arising from the isomorphous substitution of higher valence cations by lower valence cations that create a charge deficiency. Clay surfaces carry permanent negative charges and are pH-insensitive; the edges, however, respond to pH and become negative at higher pH. (Tombácz and Szekeres, 2006) Low pH can protonate the aluminum hydroxyl group, whereas high pH can deprotonate it via hydrolysis reactions, as shown in Figure 2-2.

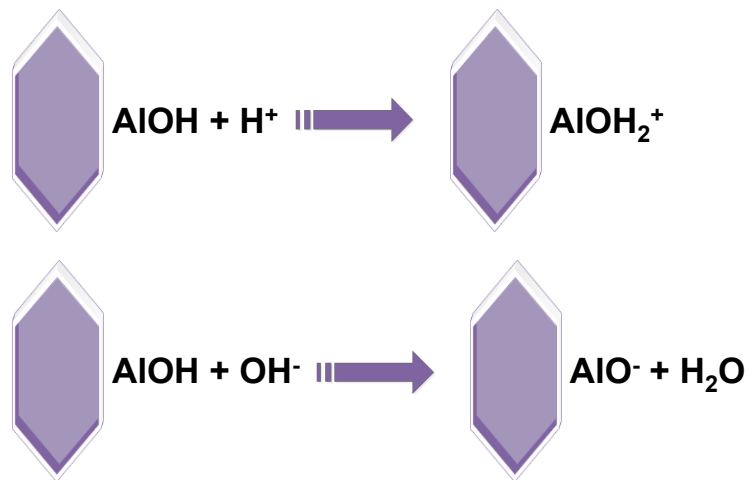
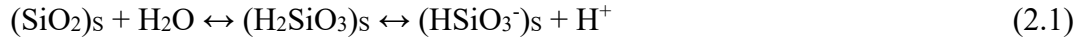


**Figure 2-2** Protonation of aluminum hydroxyl surface at low pH and deprotonation at high pH.

Isomorphous substitution on illite occurs mainly in the tetrahedron sheet, whereas it occurs in both tetrahedron and octahedron sheets in case of smectite clays. Cation exchange in kaolin and illite occurs mainly at their edges, while smectite clays undergo cation exchange at both edge and surface. Due to higher isomorphous substitution in three-layer clays (illite and smectite), they exhibit a more negative zeta potential than two-layer kaolin clays. As MFT contains a mixture of both two- and three-layer clays, it shows strong negative zeta potential that causes colloidal stabilization.

A common understanding of the source of surface charges is the adsorption of ions from neighboring solution on an initially neutral solid surface. Another source of surface charges is

the dissociation of surface groups. The silica surface of clays can react with water to form silicic acid, which can then dissociate to form silicic anion, as shown below:



As reaction (2.1) continues, negative charges build-up on the solid surface, and  $\text{H}^+$  ions diffuse into the bulk solution. The surface developed according to reaction (2.1) is sensitive to pH because all of the steps above are reversible, and the proton produced in the last step diffuses and stays in bulk solution. At high pH, the equilibrium of reaction (2.1) shifts to the right, generating negative charges on the clay surface whereas, at low pH, the surface is positively charged.

## 2.2 Electrical Double Layer: Derjaguin, Landau, Verwey, and Overbeek (DLVO) Theory

Although MFT clays have charges, the water present in MFT also carries an electric charge, equal and opposite in sign to that on the MFT solids. The absolute values of charges on the clay surfaces and water are the same, and collectively form a system of charges known as the electric double layer (EDL). (Maximova and Dahl, 2006) The EDL consists of several layers. The first layer is called the Stern layer, and the second layer of ions in solution is called the diffuse layer. The electric potential at the Stern layer is called the Stern potential, and at the diffuse layer is called the zeta potential. Figure 2-3 presents a schematic for the EDL of a spherical negatively charged particle. The plot embedded in the figure shows the electric potential in the double layer as a function of the distance from the particle surface. Ions in the diffuse layer are affected by electric interactions with the charged surface and thermal motion. (Masliyah and Bhattacharjee, 2006)

The thickness of the diffuse layer is proportional to the Debye length ( $1/\kappa$ ), which is assumed to approach zero with an increase in salt content.  $\kappa$  is called the Debye parameter. Based on the above discussion, there exists an electric potential distribution near the surface of charged solid particles immersed in an aqueous solution. In this context, we are interested to measure the surface potential of clays in MFT, but practically a potential difference can only be measured within a single phase. However, we can neglect all other interface boundaries in the system and calculate the sum of the surface potentials that lie very close to the solid particle surface. This potential, measured close to the surface, is called zeta potential (Figure 2-3). Often instruments

measure electrophoretic mobility of dilute colloidal dispersions to estimate their zeta potential. If the dispersed particles are coarse and can sediment, measurement of streaming potential is recommended. In this case, the liquid is forced through a plug made up of solid and the potential is measured for the known pressure.

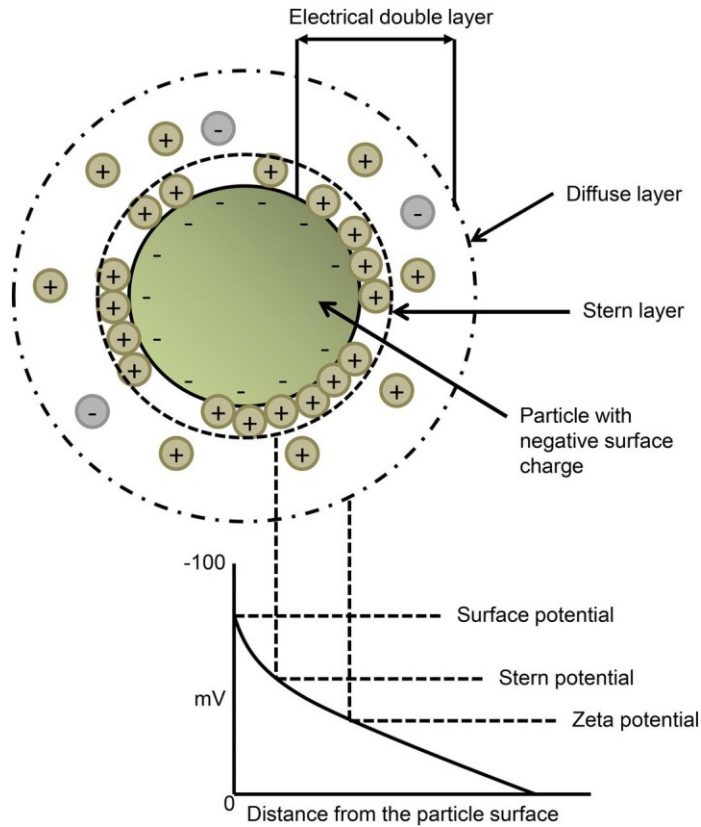


**Figure 2-3** Schematic of the electric double layer and a graph of electric potential in the double layer as a function of distance from the particle surface. (Yingchoncharoen et al., 2016)

The energy of a colloidal system is defined by the DLVO theory, which states that the energy of a system is the sum of attractive van der Waals energy and repulsive double layer energy as shown in the Equation 2-1. (Masliyah, J. H, Czarnecki, J. A, Xu, 2011)

$$E = E_{vdW} + E_{DL} \quad \text{Equation 2-1}$$

Although hydrodynamic forces are ignored in the DLVO theory, the stability of the system can be characterized based on the net interaction resulting from the attraction and repulsion between the particles. A system is considered a stable suspension if the net interaction between the

particles is repulsive. If the net interaction is attractive, the system is said to be unstable and may coagulate. In the context of MFT consolidation and dewatering, the DLVO theory can help design flocculants that effectively aggregate the solids, and subsequently dewater them. Repulsive forces arising from the electrical double layer significantly contribute to the stability of MFT. An effective flocculant would compress the electrical double layer and cause MFT to sediment.

Although the above discussion focusses on interaction energies among MFT particles, the water chemistry can significantly affect the surface charge on suspended particles. Since MFT contains clays with hydroxyl and oxide functionality, particles become negatively charged at neutral pH, and become even more negative as pH increases. Thus, the stability of clays in MFT increases with increase in pH. Current bitumen extraction processes use caustic additives to improve their efficiencies, generating alkaline tailings with pH of approximately 8.5. This basic medium increases the electrostatic repulsive forces between MFT clays through the mechanism described above and significantly increases the stability of MFT.

### **2.3 Coagulation and Flocculation Mechanisms**

Coagulants (mainly multivalent inorganic cations) suppress the electrical double layer, ultimately allowing van der Waals attractive forces to bring and hold particles together. Therefore, coagulants reduce the energy barrier that prevents particles from approaching each other. This energy barrier becomes zero at a critical coagulant concentration. The critical concentration depends on valence of the electrolyte used as a coagulant. The higher the valence, the lower the coagulant concentration needed to reach the zero-energy barrier. For constant-valence electrolytes, increasing concentration reduces the energy barrier and increases the net attraction forces, as shown in Figure 2-4.

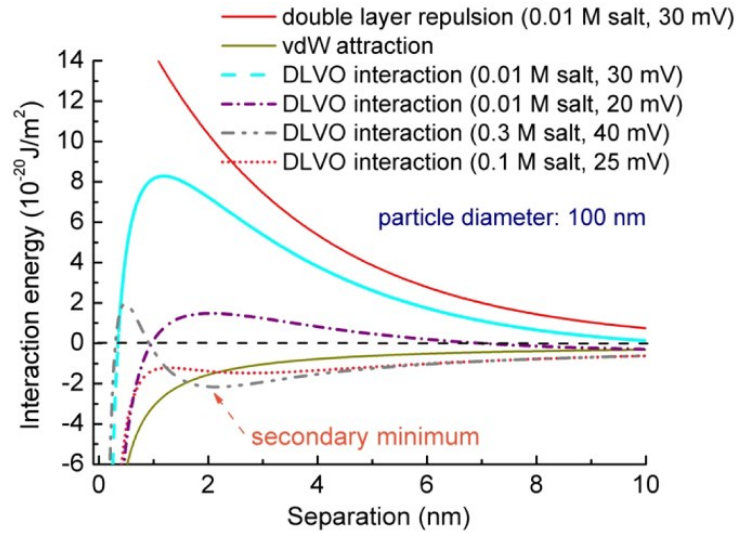


**Figure 2-4** Effect of electrolyte concentration on DLVO interaction energy. (Guo et al., 2014)

Consolidated tailings (CT) technology uses  $\text{Ca}^{2+}$  in gypsum as a coagulant. An overdose of a coagulant could be detrimental because the ions can adsorb on the clay surface and revert the net surface charge, inducing repulsive forces. When settling rate is monitored as a function of coagulant concentration, the settling rate decreases due to coagulant overdosing beyond a maximum. Although the addition of acid or base would result in similar behaviors, it is practically impossible to implement from a practical point of view, as it will require large amounts of acid or base. Potassium alum, aluminum sulfate, and gypsum are frequently used as coagulants in the industry.

Flocculation refers to the macroscopic aggregation of suspended particles into loosely packed flocs by addition of a polymeric flocculant. Flocs with a density higher than the surrounding medium settle rapidly and produce clear supernatants under optimal conditions. Polymeric chains adsorb on one or more sites of clay particles present in MFT via hydrogen bonding and electrostatic interactions. Figure 2-5 compares different polymer chain configurations on particle surfaces, and discusses their suitability for flocculation. Aggregates formed by flocculation have structures that are more open than those formed by coagulation due to the high molecular weight of the polymer. Often, this open structure causes flocs to hold a large amount of water within the aggregates. In flocculation, the proper design of the architecture of the polymer molecules is very

important to control adsorption and subsequent polymer configuration on the clay surfaces. In the case of charged polymers, an optimum charge density would ensure the polymer would have sufficient flexibility to form loops with moderate binding forces.

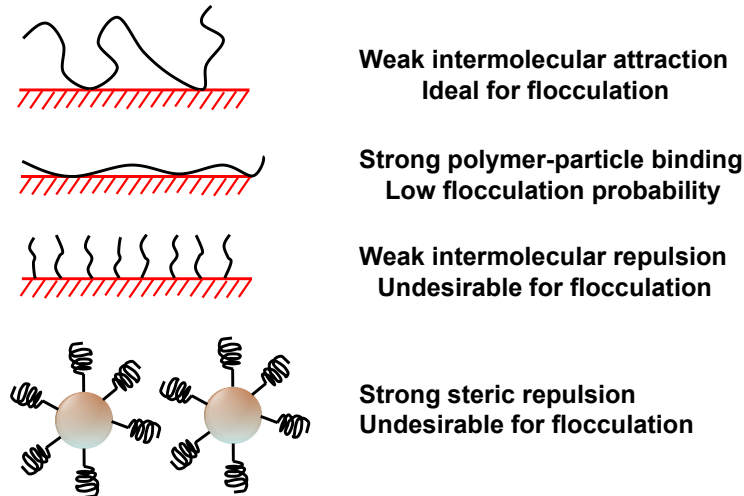


**Figure 2-5** Various configurations of polymer chains on the particle surface and their suitability for flocculation.

## 2.4 Polymers for Clays and MFT Settling: Literature Review

### 2.4.1 Acrylamide-based Polymers

Acrylamide-based polymers are widely used as flocculants in wastewater treatment. As polymer molecular weight plays a key role in flocculation processes, the majority of polyacrylamide (PAM) flocculants have average molecular weights up to  $16 \times 10^6$  Da. (Li et al., 2008) Acrylamide-based flocculants can be synthesized as neutral, anionic, and cationic polymers. Neutral PAM is rarely used as a flocculant since its lack of ionic charges makes it interact less effectively with suspended solids. (Griot and Kitchener, 1963) The field of tailings treatment has largely benefited from using anionic PAMs synthesized by hydrolysis of PAM (HPAM). However, since both MFT clays and HPAM are negatively charged,  $\text{Ca}^{2+}$  ions must be used with the HPAM flocculant to bridge polymer chains and clay surfaces. Copolymerization of acrylamide with acrylic acid can also produce anionic PAM. Cationic PAM can be synthesized by copolymerizing acrylamide with a variety of cationic comonomers. The chemical structures of acrylamide-based neutral, anionic, and cationic polymers are shown in Figure 2-6.



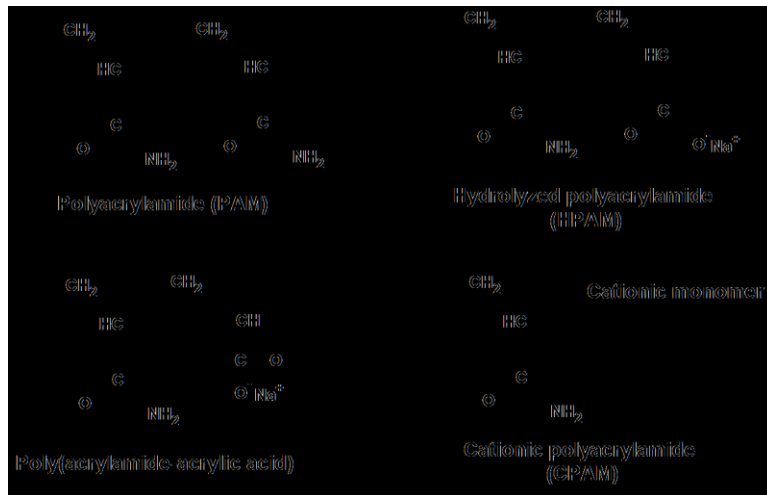


**Figure 2-6** Chemical structures of acrylamide-based neutral, anionic, and cationic polymers.

Long et al. used HPAM to flocculate oil sands tailings with co-addition of  $Ca^{2+}$  and  $Mg^{2+}$ . (Long et al., 2006) The presence of these divalent ions significantly enhanced the adhesion between HPAM and the fine solids, as measured by AFM, resulting in faster settling rates. The negatively charged carboxylic groups ( $COO^-$ ) on HPAM make their chains extend into solution due to intramolecular electrostatic repulsion, which is advantageous for effective flocculation. Divalent ions, such as  $Ca^{2+}$  and  $Mg^{2+}$  help forming bridges between clay surfaces and polymer chains, as shown in Figure 2-7. The complexation of  $Ca^{2+}$  or  $Mg^{2+}$  with HPAM chains and silica surfaces induces stronger bridging adhesion compared to that originated from purely hydrogen bonding, which explains the synergistic effect of HPAM with these divalent ions.

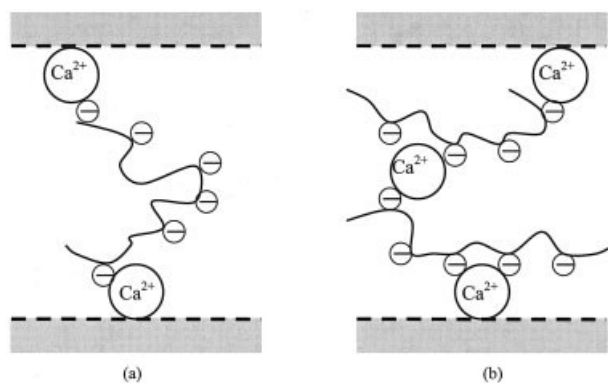


**Figure 2-7** Role of calcium ions in the flocculation of negatively charged surfaces. (Long et al., 2006)

High molecular weight (MW) HPAM is preferred over low MW HPAM because low MW polymers act as dispersants, keeping the clays suspended in MFT, whereas high MW polymers induce the formation of larger flocs via the bridging mechanism. Li et al. measured the interaction forces between kaolin and low and high MW HPAM, and demonstrated that repulsive forces significantly increased after the addition of low MW HPAM. (Li et al., 2008) Several researchers have reported that 30% hydrolyzed PAM, with average molecular weight of approximately  $17 \times 10^6$  Da, resulted in the optimal flocculant for MFT. Similar flocculants (high MW HPAM, medium charge density) were found to be effective for ceramic wastewater treatment, since it mainly contains silica and alumina. (Cengiz et al., 2009)

Recent studies have considered the use of cationic PAM (CPAM) in flocculation to avoid the use of divalent ions. (Vajihinejad et al., 2017) Cationic flocculants are univalent polyelectrolytes bearing only positively-charged functional groups, typically quaternary ammonium groups. Diallyldimethylammonium chloride (DADMAC) is one of cationic comonomers frequently used to synthesize cationic PAM flocculants. Zhou et al. investigated the effect of changing the charge density of CPAM on interactions between silica and flocculant. (Zhou et al., 2008) They reported CPAM with 10% charge density assumed an entangled loop conformation on silica surface, whereas the flocculant adopted a flatter conformation with increase in charge density up to 100%. Zhou and Franks reported that 10% cationic PAM facilitated bridging, 40% cationic PAM showed a combination of charge neutralization and bridging (depending on the polymer dosage) and 100% cationic PAM induced electrostatic patch flocculation. (Zhou and Franks, 2006) In another study, Wang et al. copolymerized acrylamide and acryloylamino-2-hydroxypropyl trimethyl ammonium chloride (AMHP) using ammonium persulfate (APS) as an initiator. (Wang et al., 2009) Their cationic PAM effectively flocculated 0.25 wt. % kaolin slurry via both bridging and charge neutralization mechanism. A lower dosage was needed to flocculate suspensions with acidic pH, and charge neutralization was found to be dominant mechanism at lower pH.

Aqueous-phase free radical polymerization is frequently used to synthesize water-soluble flocculants. Inchausti et al., however, copolymerized acrylamide and dimethyl aminoethyl acrylate-methyl chloride via inverse emulsion polymerization containing water and isoparaffinic

solvent. (Inchausti et al., 2005) Emulsion polymerization enables the synthesis of very high molecular weight polymer and fast monomer conversion.

The microstructure of the flocculant, which ultimately governs its flocculation performance, significantly depends on the polymerization method. Sun et al. reported the synthesis of branched cationic PAM using a potassium diperiodatocuprate initiator that induced self-condensing vinyl copolymerization of acrylamide and acryloxyethyltrimethyl ammonium chloride. (Sun et al., 2013) Dendritic polymers with highly branched structures can be produced using self-condensing vinyl polymerization in which, a vinyl monomer undergoes self-polymerization if it contains a pendant group that can be transformed into an initiating moiety by the action of an external stimulus such as initiator. Branched polymers have lower viscosity and are more soluble in water than linear polymers. Supernormal valence transition metals, such as potassium diperiodatocuprate, can create branching points on acrylamide that can further form a long chain branch. Branched copolymer was effective in turbidity removal than the linear copolymer.

Although researchers have shown that MFT can be effectively flocculated with acrylamide-based polymers, the sediments still hold significant amounts of water due to the hydrophilic nature of the flocculant. To increase their solids content, these sediments may be further processed using mechanical operations such as centrifugation and filtration. Beier et al. flocculated MFT as well as a fresh tailings stream using PAM to ‘thicken’ it, and further centrifuged it to increase the solids content and remove additional water. (Beier et al., 2013) In this process, the flocculant is mixed with MFT using an in-line mixer, so that the flocculation can be carried out continuously. Flocculation performance in an in-line mixer significantly depends on mixing energy that can be tuned by number of mixing elements in the mixer.

Fugitive bitumen in MFT significantly affects the settling rate of solids. Klein et al. investigated the effect of residual bitumen on the settling behavior of MFT. (Klein et al., 2013) They found bitumen decreases the size of flocs, and thus reduces their settling rate. Shearing is also important during flocculation. Excessive shearing breaks down formed flocs, may degrade the flocculant chains, and decreases solution viscosity. Sylvester and Toure studied the effect of shearing on the degradation of neutral, anionic, and cationic PAM used in flocculation.

(Sylvester and Toure, 1978) Regardless of their ionicity, the flocculation performance remarkably decreased due to degradation of polymer chains. In such cases, the polymer dosage needs to be increased to achieve the desired flocculation performance.

In general, cationic PAM flocculants effectively adsorb on clay surfaces than anionic or amphoteric PAM at a given polymer dosage. (Shaikh et al., 2017) Cationic PAM produces larger flocs at an optimum dosage than anionic or amphoteric PAM.

#### 2.4.2 Thermosensitive Polymers

Thermosensitive polymers change their conformation and phase behavior above or below a certain temperature, called the critical solution temperature. Polymers that change to ‘collapsed’ conformation above the critical solution temperature are called lower critical solution temperature (LCST) polymers. On the other hand, polymers that adopt a collapsed conformation below critical solution temperature are called upper critical solution temperature (UCST) polymers. In other words, LCST polymers are soluble in water below the critical temperature, whereas UCST polymers are soluble in water above the critical temperature.

In this thesis, LCST polymers were investigated as MFT flocculants; therefore, the discussion in the section is limited to LCST polymers. The LCST depends largely on hydrogen bonding among the constituent monomer units. (Dimitrov et al., 2007) Since the free energy of dissolution is equal to  $\Delta G = \Delta H - T\Delta S$ , it can change from negative (soluble) at low temperatures, to positive (insoluble) at high temperatures. At lower temperature,  $\Delta G$  is negative since polymer-solvent interactions results in higher entropic contribution (+ve  $T\Delta S$ ) and lower enthalpy change that favor the dissolution of polymer. At higher temperature, entropic contribution becomes smaller and enthalpy change increases due to increased hydrophobic interactions resulting in phase separation owing to positive  $\Delta G$ . This change in  $\Delta G$  significantly depends on  $T$ , thus polymers show thermosensitive behavior.

Poly(*N*-isopropylacrylamide) (PNIPAM) is one of the widely studied thermosensitive polymers. PNIPAM exhibits a very sharp LCST transition at 32 °C, above which it phase separates from water and assumes a collapsed conformation. Below the LCST, the random coils are favored, as they maximize hydrogen bond interactions among polymer and water molecules. Above the LCST, hydrogen bonding weakens and the entropy-controlled *hydrophobic effect*, the tendency

of the system to minimize the contact between water and hydrophobic PNIPAM groups increases, forcing the chains to transition from coiled to a denser globule structures. (Dimitrov et al., 2007) The smart behavior of PNIPAM arises from the entropic gain, as water molecules associated with the side chain isopropyl moieties are released into the bulk aqueous phase as the temperature increases above the LCST. Figure 2-8 illustrates the temperature-induced phase transition of PNIPAM in water.

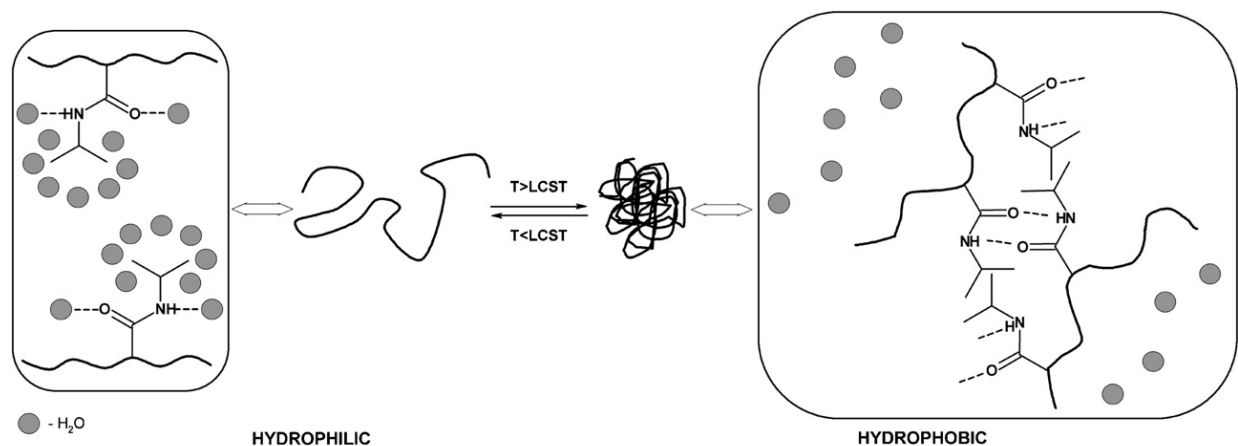


**Figure 2-8** Schematic illustration of thermosensitive phase transition in PNIPAM. (Dimitrov et al., 2007)

Recently, thermosensitive PNIPAM has been reported as a novel flocculant to accelerate the settling rate and enhance the consolidation of kaolin clays. (Li et al., 2007; Wang et al., 2014) PNIPAM can adsorb onto particle surfaces below its LCST via hydrogen bonding, forming large flocs. Raising the temperature above the LCST forces the PNIPAM chains to undergo a phase transition and become hydrophobic, resulting in the collapse of the polymer chains and in the expulsion of water from the sediments.

However, the use of PNIPAM homopolymers as flocculants is limited, since nonionic PNIPAM does not adsorb well onto negatively-charged clays. (Sakohara and Nishikawa, 2004) Wang et al. flocculated kaolin suspensions using linear and hyperbranched PNIPAM and showed they had superior solid-liquid separation performance owing to the hydrophobic interaction of PNIPAM segments on the particle surfaces. (Wang et al., 2014) They also reported the flocculation performance of a cationic copolymer of NIPAM and 2- aminoethyl methacrylamide (AEMA)

hydrochloride. The cationic PNIPAM flocculant led to lower supernatant turbidity and higher solids content in the sediments. Zhang et al. flocculated MFT using the same cationic copolymer, P(AEMA-NIPAM), and compared its performance with a conventional P(acrylamide-DADMAC) flocculant. (Zhang et al., 2017) Their investigations showed that P(AEMA-NIPAM) behaved as a polyelectrolyte, enhancing polymer adsorption onto clay particles via electrostatic interactions, thus further improving the settling rate and supernatant clarity.

In a typical flocculation, the thermosensitive polymer adsorbs on the clay surface in its water-soluble state (below the LCST). The polymer adopts a collapsed conformation above the LCST, and promotes hydrophobic interactions among polymer-coated clays. This process results in floc formation and causes sedimentation of solids. (Franks et al., 2009) The molecular weight of thermosensitive polymers has a significant effect on flocculation of solids from suspensions. PNIPAMs with higher molecular weights form stronger solid aggregates than PINIPAMs with lower molecular weights. (Li et al., 2009) Thus, lower dosages are needed for high molecular weight PNIPAM to induce effective solid aggregation.

Sakohara and Nishikawa also reported flocculation of TiO<sub>2</sub> suspensions using a cationic thermosensitive polymer synthesized by copolymerizing NIPAM with *N,N*-dimethylaminopropylacrylamide (DMAPAA). (Sakohara and Nishikawa, 2004) Although the cationicity of the thermosensitive flocculant enhanced its flocculation performance, it also increased the LCST of the copolymer because a higher thermal energy was required to collapse the polymer chains. Dual ionic polymer mixtures, containing anionic and cationic thermosensitive polymers, could facilitate the flocculation even at lower temperatures. (Sakohara et al., 2011) Sediments were also compacted by a combination of anionic and cationic thermosensitive polymers. (Sakohara et al., 2008)

### *2.4.3 Natural Polymers*

Natural polymers or biopolymers are attractive due to their lower cost, lower toxicity, and flocculation performance comparable to those of synthetic flocculants. Environmental effects of synthetic polymers is also an open debate. Commercial forms of synthetic organic flocculants may also contain toxic residual monomers. These issues are driving the use of natural polymers for flocculation applications.

Chitosan, a widely researched bioflocculant, is a linear copolymer of *D*-glucosamine and *N*-acetyl-*D*-glucosamine produced by the deacetylation of chitin. Chitosan has unique properties among biopolymers, especially due to the presence of primary amino groups. Chitosan has properties that are desirable in a flocculant, such as high cationic charge density and high molecular weight. Lu and coworkers used cationic chitosan along with anionic PAM to flocculate oil sands tailings, and concluded that the flocculants worked better when combined together than separately. In their two-step flocculation process, the anionic PAM bridged clay particles, whereas the cationic chitosan neutralized their charges, formed aggregates, and flocculated them. (Q. Lu et al., 2016) Roussy et al. flocculated bentonite suspensions with chitosan of varying molecular weights and degrees of deacetylation. (Roussy et al., 2005) Chitosan performed better in tap water and acidic pH than in demineralized water and alkaline pH. In an interesting study, Franks and coworkers flocculated alumina, silica, and zirconia suspensions using chitosan and changed the pH of the sediment bed to induce repulsive forces. (Franks et al., 2006) Due to these repulsive forces, the sediments continued to consolidate under the influence of gravity.

Starch-based flocculants are also widely used in many solid-liquid separation processes. Usually, cationic or anionic chains are grafted on starch backbones to improve their water solubility and induce charge density. Moreover, PAM-grafted starch has high molecular weight and promotes bridging flocculation. (Pal et al., 2012)

Recently, Wu et al. compared two cationic starch flocculants of different architectures: (i) starch-graft-poly[(2-methacryloyloxyethyl) trimethyl ammonium chloride, and (ii) starch-3-chloro-2-hydroxypropyl triethyl ammonium chloride. (Wu et al., 2016) The graft cationic polymer was a better flocculant than the linear cationic polymer, likely because of significantly enhanced bridging effects of the graft polymer. The effect of graft and linear starch-based flocculants on floc size is compared in Figure 2-9.

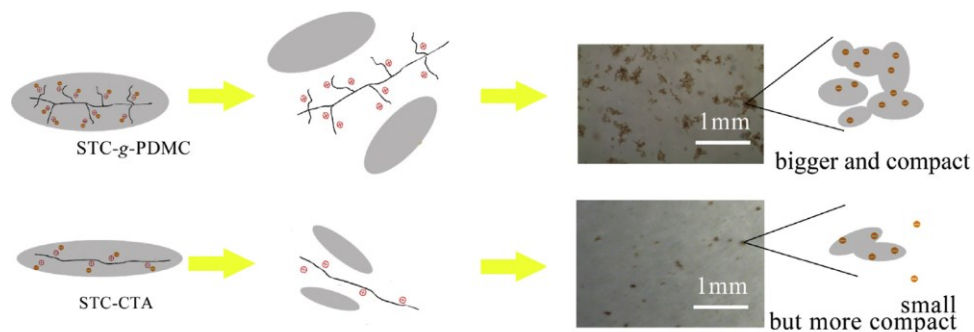


**Figure 2-9** Effect of linear and graft architecture of starch-based cationic flocculants on floc size. (Wu et al., 2016)

Yang et al. synthesized amphoteric starch-based grafting copolymers containing cations, anions and grafted branches that could be used to treat both positively- and negatively-charged suspension. (Yang et al., 2014) Amphoteric starch-based flocculants showed low pH-sensitivity in the consolidation of different types of colloidal systems.

Glycopolymers, which are carbohydrate-based polymers, possess low or no cytotoxicity and have high biocompatibility. Such polymers were also considered for solid-liquid separation. Lu et al. synthesized poly(2-lactobionamidoethyl methacrylamide) of varying molecular weights to flocculate kaolin slurries. (H. Lu et al., 2016) They reported increased polymer-particle adhesion with increase in molecular weight measured using the surface force apparatus. Glycopolymers of high molecular weight possess abundant hydroxyl groups that enhance hydrogen bonding among the fine clay particles.

Agar ( $C_{12}H_{18}O_9$ )<sub>n</sub> is another biopolymer that can be used as a flocculant to treat various wastewaters. It is commercially obtained from species of *Gelidium* and *Gracilariae*, which belongs to the Rhodophyceae class commonly known as Red seaweeds. Chemically, agar is a mixture of agarose and agaropectin. Rani and coworkers grafted acrylamide chains on the backbone of agar using free radical polymerization and microwave radiation. (Rani et al., 2012) Agar-grafted-PAM flocculated kaolin slurries better than pure agar.

Cellulose is one of the most abundant natural polysaccharides, and it can be modified in several ways to use as a flocculant. Hydroxypropyl methylcellulose (HPMC) is a modified form of cellulose that is currently used in biomedical science. Das et al. grafted acrylamide chains onto



HPMC backbones and investigated its flocculation performance in kaolin slurries. (Das et al., 2013) Their kinetic model of kaolin aggregation showed that the increase in flocculant dosage increased the aggregation rate constant and decreased the aggregate breakage constant. Graft polymers of such type can form particle-polymer-particle aggregates in which, the graft polymer serves as a bridge.

In general, there are fewer reports on the use of natural polymers to flocculation of oil sands tailings. Thus, it creates a scope to apply advancements in chitosan, starch, agar, and other natural polymers to address of oil sands tailings.

#### *2.4.4 Hydrophobically-modified Polymers*

Although researchers significantly contributed to addressing the MFT dewatering issue, the major outcomes included an increase in settling rate and improvement of supernatant turbidity. The majority of these advances used ionic comonomers to increase settling rate and decrease supernatant turbidity, but the flocs formed using such flocculants still hold a significant amount of water that cannot be further recovered.

Hydrophobically-modified polymers are potential candidates to enhance dewatering of MFT and obtain compact sediments. Lu et al. reported a hydrophobically-modified cationic flocculant to dewater kaolin suspensions. (Lu et al., 2015) They copolymerized NIPAM and 2-aminoethyl methacrylamide hydrochloride (AEMA) with 5-methacrylamido-1,2-benzoboroxole (MAAmBo) using free radical polymerization. Their hydrophobically-modified flocculant increased the settling rate due to the large contribution of hydrophobic forces. The hydrophobic monomer units also lower the viscosity of flocculant solution, facilitating efficient mixing of flocculant with suspension and increasing the probability of polymer adsorption onto clay particles.

Similarly, butylacrylate (BA) was used to hydrophobically modify a flocculant containing acrylamide (AM) and acryloyloxyethyl trimethyl ammonium chloride (DAC) to flocculate activated sludge. (Zheng et al., 2014) Additional interactions due to the hydrophobic monomer led to the formation of smaller and likely drier, flocs. Although smaller flocs lower the settling rate of solid particles, it improves the compaction of sediments and recovery of clear water.

Usually, hydrophobic comonomers are copolymerized with hydrophilic monomers in co-solvent systems or emulsion polymerization. Zheng et al. copolymerized acrylamide and a cationic monomer using ultraviolet (UV) radiation method, which was advantageous in terms of avoiding surfactants. (Liao et al., 2014) Sakohara et al. induced hydrophobicity in their flocculant by adding a hydrophobic monomer and a thermosensitive monomer that became hydrophobic above its LCST. (Sakohara et al., 2013) The hydrophobic monomer decreased the LCST of the whole polymer and achieved the flocculation at a lower temperature than for the homopolymer alone. In addition, the higher hydrophobicity due to both monomers above the LCST promoted higher water recovery and created compact kaolin sediments.

Fundamental investigations on the adsorption of hydrophobically-modified PAM on kaolin revealed that the hydrophobic monomer units promote multi-layer adsorption on the kaolin particle surface, and a bridging network of molecules in the aqueous suspension. (Ren et al., 2008) The flocculant synthesized by statistical free radical polymerization but containing macroblocks of hydrophobic monomer showed an enhanced adsorption ability on clays and better flocculation performance because such blocky distribution improved the hydrophobic interactions between polymer and clays.

Hydrophobically-modified flocculants have shown promising flocculation performance in clay suspensions and model wastewater with advantages of enhanced polymer-particle interactions, producing clearer supernatants, and creating compact sediments. However, to the best of author's knowledge, there are no reports of the application of hydrophobically-modified flocculants to dewater MFT. This stands as one of the motivations of this thesis work.

#### *2.4.5 Challenges and Knowledge Gap*

Efficient dewatering of oil sands tailings is of extreme importance to reduce the environmental footprint of oil sands operations. The current technologies for sewage water treatment, dewatering of clay suspensions, removal of the organic content in water, and treatment of ceramic wastewater are mature, but this is not the case for oil sands tailings. There is no mature technology capable of effectively treating oil sands tailings and eliminating the use of tailings ponds.

Consolidated tailings and paste technology are the most extensively used dewatering methods today. However, the high concentration of divalent ions in the water recovered using the consolidated tailings process impedes the re-utilization of this water in the bitumen extraction process. Accumulation of ions does not occur in the case of paste technology; however, this technology, similarly to the consolidated tailings process, recovers only part of the water from tailings and produces sediments having high water content (35-40 wt% solids) that still requires special storage.

The sediments produced by polyacrylamide (PAM)-based flocculants are not closely packed. Thus, sediments further require the application of other consolidation technologies such as freeze-thaw, filtration or centrifugation to obtain dry and self-supportive tailings. This knowledge gap necessitates the innovation of multifunctional flocculants, which will effectively flocculate the clays in oil sand tailings, using various mechanisms such as bridging and charge neutralization. The knowledge gap also underlines the need of point-of-use flocculants to treat fresh tailings.

## References

- Beier, N., Wilson, W., Dunmola, A., Segó, D., 2013. Impact of flocculation-based dewatering on the shear strength of oil sands fine tailings. *Can. Geotech. J.* 50, 1001–1007. <https://doi.org/10.1139/cgj-2012-0262>
- Cengiz, I., Sabah, E., Ozgen, S., Akyildiz, H., 2009. Flocculation of fine particles in ceramic wastewater using new types of polymeric flocculants. *J. Appl. Polym. Sci.* 112, 1258–1264. <https://doi.org/10.1002/app.29508>
- Das, R., Ghorai, S., Pal, S., 2013. Flocculation characteristics of polyacrylamide grafted hydroxypropyl methyl cellulose: An efficient biodegradable flocculant. *Chem. Eng. J.* 229, 144–152. <https://doi.org/10.1016/j.cej.2013.05.104>
- Dimitrov, I., Trzebicka, B., Muller, A.H.E., Dworak, A., Tsvetanov, C.B., 2007. Thermosensitive water-soluble copolymers with doubly responsive reversibly interacting entities. *Prog. Polym. Sci.* 32, 1275–1343. <https://doi.org/10.1016/j.progpolymsci.2007.07.001>
- Franks, G., Sepulveda, C., Jameson, G., 2006. pH sensitive flocculation: Settling rates and sediment densities. *AIChE J.* 52, 2774–2782. <https://doi.org/10.1002/aic>
- Franks, G. V., Li, H., O'Shea, J.-P., Qiao, G.G., 2009. Temperature responsive polymers as multiple function reagents in mineral processing. *Adv. Powder Technol.* 20, 273–279. <https://doi.org/10.1016/j.appt.2009.02.002>
- Griot, O., Kitchener, J.A., 1963. “Ageing” of Silica Suspensions in Water and its Influence on Flocculation by Polyacrylamide. *Nature* 200, 1004–1005. <https://doi.org/10.1038/2001004b0>
- Guo, D., Xie, G., Luo, J., 2014. Mechanical properties of nanoparticles: basics and applications. *J. Phys. D: Appl. Phys.* 47, 13001. <https://doi.org/10.1088/0022-3727/47/1/013001>
- Inchausti, I., Sasia, P.M., Katime, I., 2005. Copolymerization of dimethylaminoethylacrylate-methyl chloride and acrylamide in inverse emulsion. *J. Mater. Sci.* 40, 4833–4838. <https://doi.org/10.1007/s10853-005-2003-y>
- Klein, C., Harbottle, D., Alagha, L., Xu, Z., 2013. Impact of fugitive bitumen on polymer-based flocculation of mature fine tailings. *Can. J. Chem. Eng.* 91, 1427–1432. <https://doi.org/10.1002/cjce.21863>
- Konan, K.L., Peyratout, C., Bonnet, J.P., Smith, A., Jacquet, A., Magnoux, P., Ayrault, P., 2007. Surface properties of kaolin and illite suspensions in concentrated calcium hydroxide medium. *J. Colloid Interface Sci.* 307, 101–108. <https://doi.org/10.1016/j.jcis.2006.10.085>
- Li, H., Long, J., Xu, Z., Masliyah, J., 2007. Flocculation of kaolinite clay suspensions using a temperature-sensitive polymer. *AIChE J.* 53, 479–488. <https://doi.org/10.1002/aic>
- Li, H., Long, J., Xu, Z., Masliyah, J.H., 2008. Effect of molecular weight and charge density on the performance of polyacrylamide in low-grade oil sand ore processing. *Can. J. Chem.*

- Eng. 86, 177–185. <https://doi.org/10.1002/cjce.20029>
- Li, H., O’Shea, J.-P., Franks, G. V., 2009. Effect of molecular weight of poly( N -isopropyl acrylamide) temperature-sensitive flocculants on dewatering. *AIChE J.* 55, 2070–2080. <https://doi.org/10.1002/aic.11859>
- Liao, Y., Zheng, H., Qian, L., Sun, Y., Dai, L., Xue, W., 2014. UV-Initiated Polymerization of Hydrophobically Associating Cationic Polyacrylamide Modified by a Surface-Active Monomer: A Comparative Study of Synthesis, Characterization, and Sludge Dewatering Performance. *Ind. Eng. Chem. Res.* 53, 11193–11203. <https://doi.org/10.1021/ie5016987>
- Long, J., Li, H., Xu, Z., Masliyah, J.H., 2006. Role of colloidal interactions in oil sand tailings treatment. *AIChE J.* 52, 371–383. <https://doi.org/10.1002/aic.10603>
- Lu, H., Wang, Y., Li, L., Kotsuchibashi, Y., Narain, R., Zeng, H., 2015. Temperature- and pH-Responsive Benzoboroxole-Based Polymers for Flocculation and Enhanced Dewatering of Fine Particle Suspensions. *ACS Appl. Mater. Interfaces* 7, 27176–27187. <https://doi.org/10.1021/acsami.5b09874>
- Lu, H., Xiang, L., Cui, X., Liu, J., Wang, Y., Narain, R., Zeng, H., 2016. Molecular Weight Dependence of Synthetic Glycopolymers on Flocculation and Dewatering of Fine Particles. *Langmuir* 32, 11615–11622. <https://doi.org/10.1021/acs.langmuir.6b03072>
- Lu, Q., Yan, B., Xie, L., Huang, J., Liu, Y., Zeng, H., 2016. A two-step flocculation process on oil sands tailings treatment using oppositely charged polymer flocculants. *Sci. Total Environ.* 565, 369–375. <https://doi.org/10.1016/j.scitotenv.2016.04.192>
- Masliyah, J. H., Czarnecki, J. A., Xu, Z., 2011. *Handbook on theory and practice of bitumen recovery from Athabasca oil sands: theoretical basis*, 1st ed. Kingsley Knowledge Publishing, Canada.
- Masliyah, J.H., Bhattacharjee, S., 2006. *Electrokinetic and Colloid Transport Phenomena*. John Wiley & Sons, Inc., Hoboken, NJ, USA. <https://doi.org/10.1002/0471799742>
- Maximova, N., Dahl, O., 2006. Environmental implications of aggregation phenomena: Current understanding. *Curr. Opin. Colloid Interface Sci.* 11, 246–266. <https://doi.org/10.1016/j.cocis.2006.06.001>
- Pal, S., Sen, G., Ghosh, S., Singh, R.P., 2012. High performance polymeric flocculants based on modified polysaccharides—Microwave assisted synthesis. *Carbohydr. Polym.* 87, 336–342. <https://doi.org/10.1016/j.carbpol.2011.07.052>
- Rani, G.U., Mishra, S., Sen, G., Jha, U., 2012. Polyacrylamide grafted Agar: synthesis and applications of conventional and microwave assisted technique. *Carbohydr. Polym.* 90, 784–91. <https://doi.org/10.1016/j.carbpol.2012.05.069>
- Ren, H., Li, Y., Zhang, S., Wang, J., Luan, Z., 2008. Flocculation of kaolin suspension with the adsorption of N,N-disubstituted hydrophobically modified polyacrylamide. *Colloids Surfaces A Physicochem. Eng. Asp.* 317, 388–393. <https://doi.org/10.1016/j.colsurfa.2007.11.007>

- Roussy, J., Van Vooren, M., Dempsey, B.A., Guibal, E., 2005. Influence of chitosan characteristics on the coagulation and the flocculation of bentonite suspensions. *Water Res.* 39, 3247–3258. <https://doi.org/10.1016/j.watres.2005.05.039>
- Sakohara, S., Hinago, R., Ueda, H., 2008. Compaction of TiO<sub>2</sub> suspension by using dual ionic thermosensitive polymers. *Sep. Purif. Technol.* 63, 319–323. <https://doi.org/10.1016/j.seppur.2008.05.014>
- Sakohara, S., Kawachi, T., Gotoh, T., Iizawa, T., 2013. Consolidation of suspended particles by using dual ionic thermosensitive polymers with incorporated a hydrophobic component. *Sep. Purif. Technol.* 106, 90–96. <https://doi.org/10.1016/j.seppur.2012.12.030>
- Sakohara, S., Nishikawa, K., 2004. Compaction of TiO<sub>2</sub> suspension utilizing hydrophilic/hydrophobic transition of cationic thermosensitive polymers. *J. Colloid Interface Sci.* 278, 304–9. <https://doi.org/10.1016/j.jcis.2004.06.002>
- Sakohara, S., Yagi, S., Iizawa, T., 2011. Dewatering of inorganic sludge using dual ionic thermosensitive polymers. *Sep. Purif. Technol.* 80, 148–154. <https://doi.org/10.1016/j.seppur.2011.04.022>
- Shaikh, S.M.R., Nasser, M.S., Hussein, I.A., Benamor, A., 2017. Investigation of the effect of polyelectrolyte structure and type on the electrokinetics and flocculation behavior of bentonite dispersions. *Chem. Eng. J.* 311, 265–276. <https://doi.org/10.1016/j.cej.2016.11.098>
- Sun, W., Zhang, G., Pan, L., Li, H., Shi, A., 2013. Synthesis, Characterization, and Flocculation Properties of Branched Cationic Polyacrylamide. *Int. J. Polym. Sci.* 2013, 1–10. <https://doi.org/10.1155/2013/397027>
- Sylvester, N.D., Toure, M.P., 1978. Effect of Shear on Polymer Aided Flocculation of Suspensions. *Ind. Eng. Chem. Prod. Res. Dev.* 17, 347–351. <https://doi.org/10.1021/i360068a012>
- Tombácz, E., Szekeres, M., 2006. Surface charge heterogeneity of kaolinite in aqueous suspension in comparison with montmorillonite. *Appl. Clay Sci.* 34, 105–124. <https://doi.org/10.1016/j.clay.2006.05.009>
- Vajihinejad, V., Guillermo, R., Soares, J.B.P., 2017. Dewatering Oil Sands Mature Fine Tailings (MFTs) with Poly(acrylamide- co -diallyldimethylammonium chloride): Effect of Average Molecular Weight and Copolymer Composition. *Ind. Eng. Chem. Res.* 56, 1256–1266. <https://doi.org/10.1021/acs.iecr.6b04348>
- Wang, L.-J., Wang, J.-P., Zhang, S.-J., Chen, Y.-Z., Yuan, S.-J., Sheng, G.-P., Yu, H.-Q., 2009. A water-soluble cationic flocculant synthesized by dispersion polymerization in aqueous salts solution. *Sep. Purif. Technol.* 67, 331–335. <https://doi.org/10.1016/j.seppur.2009.03.044>
- Wang, Y., Kotsuchibashi, Y., Liu, Y., Narain, R., 2014. Temperature-Responsive Hyperbranched Amine-Based Polymers for Solid–Liquid Separation. *Langmuir* 30, 2360–

2368. <https://doi.org/10.1021/la5003012>

- Wu, H., Liu, Z., Yang, H., Li, A., 2016. Evaluation of chain architectures and charge properties of various starch-based flocculants for flocculation of humic acid from water. *Water Res.* 96, 126–135. <https://doi.org/10.1016/j.watres.2016.03.055>
- Yang, Z., Wu, H., Yuan, B., Huang, M., Yang, H., Li, A., Bai, J., Cheng, R., 2014. Synthesis of amphoteric starch-based grafting flocculants for flocculation of both positively and negatively charged colloidal contaminants from water. *Chem. Eng. J.* 244, 209–217. <https://doi.org/10.1016/j.cej.2014.01.083>
- Yingchoncharoen, P., Kalinowski, D.S., Richardson, D.R., 2016. Lipid-Based Drug Delivery Systems in Cancer Therapy: What Is Available and What Is Yet to Come. *Pharmacol. Rev.* 68, 701–787. <https://doi.org/10.1124/pr.115.012070>
- Zhang, D., Thundat, T., Narain, R., 2017. Flocculation and Dewatering of Mature Fine Tailings Using Temperature-Responsive Cationic Polymers. *Langmuir* 33, 5900–5909. <https://doi.org/10.1021/acs.langmuir.7b01160>
- Zheng, H., Sun, Y., Guo, J., Li, F., Fan, W., Liao, Y., Guan, Q., 2014. Characterization and Evaluation of Dewatering Properties of PADB, a Highly Efficient Cationic Flocculant. *Ind. Eng. Chem. Res.* 53, 2572–2582. <https://doi.org/10.1021/ie403635y>
- Zhou, Y., Franks, G. V., 2006. Flocculation mechanism induced by cationic polymers investigated by light scattering. *Langmuir* 22, 6775–86. <https://doi.org/10.1021/la060281+>
- Zhou, Y., Gan, Y., Wanless, E.J., Jameson, G.J., Franks, G. V., 2008. Interaction forces between silica surfaces in aqueous solutions of cationic polymeric flocculants: effect of polymer charge. *Langmuir* 24, 10920–8. <https://doi.org/10.1021/la801109n>

## Chapter 3

# A Novel Hydrophobically-Modified Polyelectrolyte for Enhanced Dewatering of Clay Suspension

This work investigates the effect of multifunctional poly (*N*-isopropyl acrylamide/acrylic acid/*N*-*tert*-butylacrylamide) [p(NIPAM-AA-NTBM)] ternary polymer on the sedimentation of kaolin clay – a major fraction of oil sands tailings. A series of linear, uncross-linked p(NIPAM), p(NIPAM/AA), and p(NIPAM/AA/NTBM) were synthesized as random copolymers, where all monomer units were randomly arranged along the polymer backbone and connected by covalent bonds. The ternary copolymer, used as a flocculant, exhibited thermo-sensitivity, anionic nature, and hydrophobic association due to NIPAM, AA, and NTBM, respectively. As the ternary polymer is thermosensitive, it undergoes extended to coil-like conformation, i.e. hydrophilic to hydrophobic transition, above its lower critical solution temperature (LCST). In the context of this work, thermosensitive polymers can be employed below its LCST to induce flocculation and temperature can be raised to promote the dewatering of sediments since the polymer turns to hydrophobic above its LCST. The comonomers NIPAM (above LCST) and NTBM help expel water out of sediments due to their hydrophobicity, while AA promotes charge neutralization of the kaolin clay particles. The effect of number average molecular weight, charge density, and concentration of NTBM on settling behavior of kaolin suspension was examined. Settling test at 50 °C resulted in significantly higher settling rates compared to that at room temperature. Further, the quality of water recovered in each experiment was tested in terms of its turbidity. These results indicate that this novel ternary polymer can be employed to enhance the recovery of water from oil sands tailings containing clays.

### 3.1 Introduction

The largest oil sand reserves in the world are located in eight countries: Canada, Venezuela, USA, Trinidad, Madagascar, Albania, Russia, and Romania. In the process of water-based bitumen extraction, oil sand ores are mined, crushed, and mixed with warm alkaline water followed by the separation of bitumen using a flotation process. (Masliyah et al., 2004; Wang et

---

A version of this chapter has been published as S. P. Gumfekar and J. B. P. Soares, “A novel hydrophobically-modified polyelectrolyte for enhanced dewatering of clay suspension” *Chemosphere*, vol. 194, pp. 422–431, 2018



al., 2014) The remainder of the slurry, referred to as tailings, is discharged into tailing ponds, which occupy an enormous area of land. Fine kaolin clays are the major ingredients of oil sands tailings and remain suspended in water for many years due to its water chemistry. Kaolin clays exhibit a strong tendency to repel each other due to double-layer repulsion that results in the formation of a stable suspension. (Botha and Soares, 2015; Long et al., 2006) Current polymer flocculation/dewatering technologies are centered on acrylamide-based polymers such as polyacrylamide (PAM), but sediments produced using PAM flocculants hold considerable amounts of water due to the formation of loosely packed flocs and their superhydrophilic nature. Additionally, recent studies have shown that the possible release of monomers from PAM-based flocculants pose a potential health risk as the released monomers can make way through the food chain. (Bolto and Gregory, 2007) Alamgir et al. considered the use of organic-inorganic flocculant synthesized of  $\text{Al}(\text{OH})_3$ -PAM; however, the potential risk of leaching aluminum into the environment could not be eliminated. (Alamgir et al., 2012) The incorporation of inorganic salts, such as aluminum hydroxide, or aluminum chloride, into flocculants is being avoided due to their potential role in Alzheimer's disease. (Divakaran and Sivasankara Pillai, 2001) Recently, many researchers used cationic polymers such as polyacrylamide quaternary amine comonomer to flocculate wastewater containing clay particles. (Liu et al., 2017; Wilkinson et al., 2017; Zhang et al., 2016) These researchers used cationic comonomers such as 3-(methacryloylamino) propyl trimethylammonium chloride, 2-methacryloxyethyltrimethyl ammonium chloride, and dimethyldiallylammonium chloride to impart a cationicity to the flocculant. Lu et al. used glycopolymer- poly(2-lactobionamidoethyl methacrylamide) of various molecular weights to flocculate kaolin suspension. (Lu et al., 2016) Our group recently exploited hydrolytically degradable polymers to dewater the clay slurries. (Gumfekar et al., 2017; Rooney et al., 2016) Researchers have also used bio-based flocculants such as starch, chitosan cellulose to flocculate wastewater containing clays. (Das et al., 2013; Divakaran and Sivasankara Pillai, 2001; Jia et al., 2016; Wu et al., 2016; Yang et al., 2014) Till date, oil sands industry has majorly relied on hydrolyzed polyacrylamide, copolymer of acrylamide and acrylic acid, and copolymer containing acrylamide and cationic monomers.

The prevailing mechanisms in destabilizing colloidal suspensions using polyelectrolytes are adsorption and bridging, charge neutralization, and charged patching. (Shifa M.R. Shaikh et al., 2017) In adsorption and bridging mechanism, polymeric chains first adsorb onto surface of

particles in colloidal suspension. Such polymer adsorbed particles bridge other particles in suspension to form a floc. This bridging phenomenon is observed up to a certain dosage of polymer beyond which flocculation deteriorates due to steric stabilization. At lower dosages, polymer is insufficient to form bridging links between particles. Overall, bridging produces stronger flocs than those produced with coagulation. The principle behind charge neutralization is the suppression of electric double layer of a particle due to flocculant's ionic nature. Suppression of electric double layer reduces electrostatic repulsion between particles causing them to aggregate. Charge neutralization is often confirmed by measuring zeta potential over the range of polyelectrolyte dosage. In flocculation induced by high molecular weight polyelectrolytes, both bridging and charge neutralization take place. Charge patching is often observed when high charge density cationic polymers are used in anionic suspensions because the high interaction energy favors flattened configuration of polymers on particle's surface instead of forming loops and trails. As a result, surface of particles exhibits regions/patches of cationic polymer and of existing anions. Such patches can interact with the surface of another particle forming a bridge between them. This mechanism is found to be dominant in a suspension of low particle concentration. (Bolto and Gregory, 2007; Tripathy and De, 2006)

Recently, researchers have used thermosensitive polymers such as pNIPAM for the treatment of various clay suspensions because these polymers can alter their conformation from hydrophilic to hydrophobic. (Gao et al., 2006; Sakohara et al., 2011, 2008) To a large extent, the past research on thermosensitive polymers focussed on their theoretical study, whereas the recent literature has focussed on their applications. Additional functionality can be added to pNIPAM by copolymerizing NIPAM with desired monomers such as acrylic acid, 2-aminoethyl methacrylamide hydrochloride, ethyleneimine, allylamine etc. (Gao et al., 2005; Han et al., 2015; Lu et al., 2015; Zintchenko et al., 2006) Polyelectrolytes, which exhibit charges on the backbone of the polymer, may form a multilayer assembly, aided by the thermosensitive polymer. (Glinel et al., 2003) Additionally, polyelectrolytes cause the coagulation of clay suspension by neutralizing the charges on clay edges, which are responsible for its stability. When hydrophobic monomers are added to the p(NIPAM) electrolyte, the LCST may be changed and hydrophobic domains may be induced. (Lowe et al., 1999) In the context of this work, such hydrophobic domains may further expel the water trapped in the sediments. The combination of both hydrophobic and ionic comonomers produces thermosensitive hydrophobically modified

polyelectrolytes. By balancing hydrophobic and hydrophilic comonomers and adjusting charge density in the chain, the structure and physical properties of hydrophobically modified polyelectrolytes may be changed to meet desired performance targets.

Taking the advent of the aforementioned factors, we synthesized hydrophobically modified polyelectrolyte flocculants. The synthesized flocculants were employed above their LCST to dewater kaolin suspensions, and the dewatering performance was studied. The performance of flocculants is measured in terms of initial settling rate (ISR), the supernatant turbidity, and capillary suction time (CST) of sediments.

## **3.2 Experimental**

### *3.2.1 Materials*

*N*-isopropyl acrylamide (NIPAM), acrylic acid (AA), *N*-*tert*-butylacrylamide (NTBM), ammonium persulfate (APS), and *N,N,N',N'*-tetramethylethylenediamine (TEMED), purchased from Sigma-Aldrich (analytical reagent grade), were used without further purification. NIPAM, AA, and NTBM were used as monomers while APS and TEMED were used as initiator and accelerator, respectively. Kaolin was purchased in powder form from Sigma-Aldrich (SKU: 18616) and used as received. Deionized water was used as a solvent for all syntheses.

### *3.2.2 Synthesis of p(NIPAM), p(NIPAM-AA), and p(NIPAM-AA-NTBM)*

The synthesis of polymers was carried out by modifying the procedures described elsewhere. (Sakohara et al., 2011, 2008; Sakohara and Nishikawa, 2004) In a typical procedure for p(NIPAM) synthesis, a desired quantity of NIPAM was dissolved in DI water. The solution was constantly stirred and purged with nitrogen for 0.5 h to remove dissolved oxygen. Next, the desired amount of TEMED and APS was added to the monomer solution. The polymerization was carried out at room temperature for 24 h. In a free radical polymerization, the polymer molecular weight increases rapidly, but longer polymerization times were adopted to ensure the highest possible monomer conversion. After the polymerization, the polymer was precipitated in hexane and washed 3 times, followed by vacuum drying. In all experiments, the total monomer concentration was maintained at 0.5 M. The homopolymer p(NIPAM) was synthesized with varying concentrations of APS to study its effect on polymer number average molecular weight.

The schematic of the experimental setup is shown in Figure 3-1. A similar procedure was followed for the synthesis of p(NIPAM-AA). The concentration of AA was varied to study its effect on the charge density of the copolymer. During these syntheses, the APS concentration which yielded the highest number average molecular weight for p(NIPAM) was selected, and the molar ratio of TEMED to APS was maintained at 15.

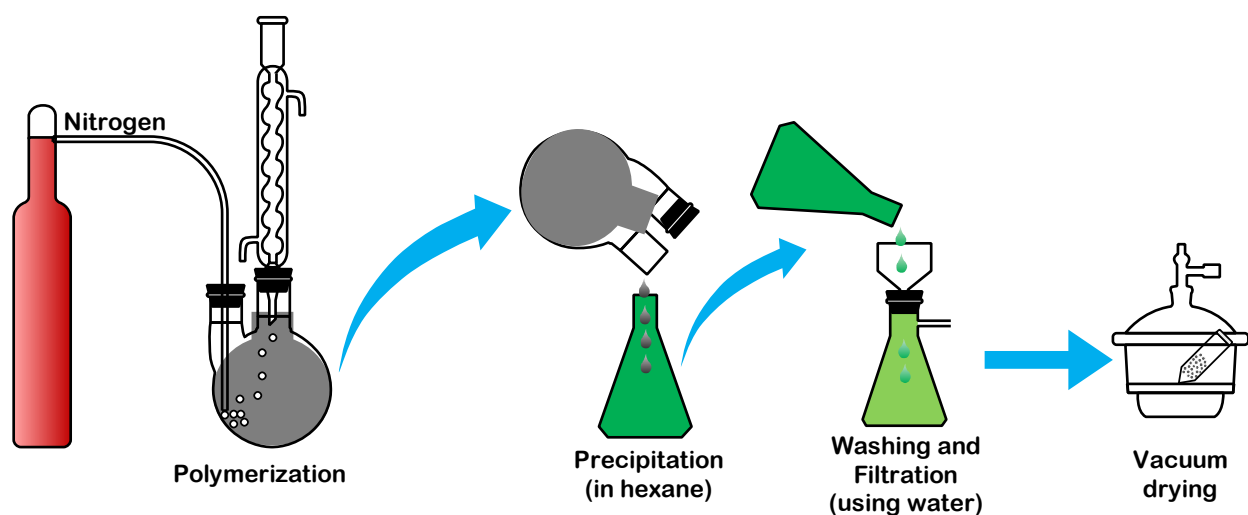


**Figure 3-1** Schematic of experimental polymerization setup for NIPAM, AA, and NTBM.

The synthesis of p(NIPAM-AA-NTBM) also followed a similar protocol. A mixture of water and acetonitrile in a volume ratio of 5:1 was used as the solvent when NTBM was used as one of the monomers to ensure all monomers were soluble in the polymerization medium. The concentration of AA was maintained at 20 mol %, which yielded the optimum charge density for the flocculation (as found during the study of p(NIPAM-AA) binary copolymers).

### 3.2.3 Characterization of Polymers and Clay Suspension

Each synthesized polymer was characterized using gel permeation chromatography (GPC) (1260 Infinity Multi-Detector GPC/SEC System, Agilent Technologies) to analyze its number average molecular weight ( $M_n$ ). The GPC system included three detectors: viscosity, refractive index, and light scattering.

We also used NMR and FTIR to qualitatively analyze the composition of these copolymers. NMR spectroscopy was performed using Agilent 400 MR with ProTune, and FTIR spectroscopy

was performed using an Agilent Technologies, Cary 600 series FTIR spectrometer. For NMR analysis, D<sub>2</sub>O and DMSO-*d*<sub>6</sub> were used as solvents.

Zeta potential measurements of polymers and clay suspensions were performed with a Malvern Zetasizer (Nanoseries Nano-ZS). A concentration of 10 mg/mL was chosen for all the analyses because it is high enough to produce a signal from the largest particles, and low enough so that particle-particle interactions do not significantly affect the signal. The zeta potential of clay suspension was found to be  $-28 \pm 3.1$  mV at pH  $8.3 \pm 0.3$ .

Clay average particle size and distribution was measured using a focused beam reflectance measurement (FBRM) technique. Figure 3-2 shows the particle size distribution of a typical kaolin suspension used in this study. Later in this work, FBRM was used to measure the floc size and distribution after addition of flocculant to investigate the floc formation process. Kaolin suspension of 2 wt. % exhibited the viscosity of  $6.851 \pm 0.4$  mPa.s at  $\tau = 500$  s<sup>-1</sup>.

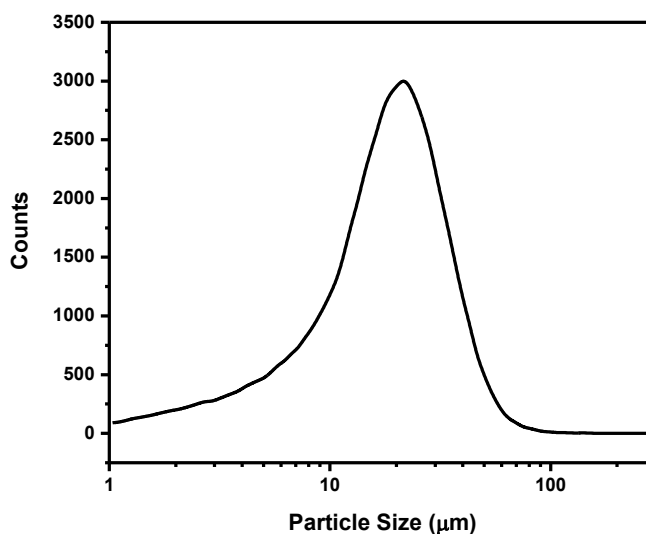


**Figure 3-2** Particle size distribution of clay particles in suspension.

### 3.2.4 *Settling Tests*

In this study, the flocculant dosage was kept constant at 1000 parts per million (ppm). It is worthwhile to note that the flocculant dosage is expressed on the basis of weight of solids in the slurry, not the volume. The term “polymer concentration with respect to solids in suspension” gives a better idea of the economic viability of the polymer flocculant. When the polymer dosage

is given as the ratio (weight polymer)/(weight of solid in suspension), it is easy to calculate how much it would cost to flocculate certain quantity of solid. Therefore, the dosage in ppm, reported in this manuscript, is equivalent to grams of polymer per ton of solids in suspension (g/t).

In each test, 2 g of kaolin clay was dispersed in 100 mL deionized water in a 250 mL baffled beaker. The pH of the suspension was adjusted to 8.3 using 1M NaOH solution. Flocculant stock solution of 2 wt. % was prepared in deionized water one day prior to its use. The mixing was performed in two stages. First, kaolin was mixed with deionized water at 600 rpm for 2 minutes. Next, we added the flocculant to the slurry under constant mixing at 300 rpm for 8 minutes. Further, the slurry was immediately transferred to a 100 mL measuring cylinder in a water bath at 50 °C, and the position of the suspension mudline (solid-liquid interface) was recorded during the settling period. Since the p(NIPAM) and its copolymers are thermosensitive, the solid-liquid separation below and above the LCST is well studied. Considering the prior knowledge, we carried out all flocculation experiments above the LCST of a flocculant. The purpose of mixing the polymers with kaolin at room temperature and then increasing the temperature to 50 °C was to alter the polymer conformation from hydrophilic to hydrophobic. The conformational change from hydrophilic to hydrophobic was desired because the sediments obtained after the flocculation could expel more water due to additional hydrophobicity and form compact sediments. The extent to which flocculation could be achieved mainly depends upon the polymer dosage; this investigation, however, does not aim at finding the optimum dosage for maximum settling rate, but rather we aim to establish polymer microstructure-performance relationships for the polymers under investigation.

The evaluation of the performance of the polymers on settling characteristics of the kaolin suspension is based on the normalized mudline height ( $h/H$ ) and the initial settling rate (ISR). Here,  $h$  is the mudline height at time  $t$ , and  $H$  is the initial mudline height at time zero; i.e. a suspension that is not responsive to the flocculant dosage would give an  $h/H$  value of unity. ISR was calculated from the slope of an initial linear portion of the settling curves. (Franks et al., 2009; Li et al., 2007) After the 24 h settling, the supernatant was collected and the turbidity was measured using Hach 2100AN turbidimeter. Capillary suction time (CST) of the consolidated solids was measured using Triton Electronics 319 multi-purpose CST apparatus. CST determines how fast sediments can be dewatered. The equipment measures the time taken by water to travel

certain radial distance. Measurement of CST is an important parameter in determining the sludge characteristics. (Sawalha and Scholz, 2007) Pipetting a fixed volume of the solids suspension gave more reproducible results than scooping an equivalent portion of the sediment with a spatula.

### 3.3 Results and Discussion

#### 3.3.1 Synthesis of Hydrophobically-modified Polyelectrolytes

We synthesized three different types of polymers: 1) thermosensitive polymers with varying molecular weight, 2) thermosensitive polyelectrolytes with a varying charge density of anions, and 3) hydrophobically modified polyelectrolytes with varying contents of hydrophobe. **Table 3-1** shows the initiator and comonomer concentration, the number average molecular weight ( $M_n$ ), charge density, and hydrophobe content of the polymers synthesized in this study. In the first type of polymer, linear p(NIPAM) with different molecular weights was synthesized by varying the NIPAM/initiator ratio during the polymerization. In free radical polymerization, the concentration of initiator plays an important role to determine the number average molecular weight ( $M_n$ ) of the polymer. The concentration of initiator was varied from 1 to 7 mM and the polymer molecular weights ( $M_n$ ) were obtained in the range of 549 to 62 kDa, respectively, as shown in **Table 3-1**.

**Table 3-1** Properties of flocculants synthesized in this study.

Flocculant	[I] (mM)	NIPAM:AA:NTBM concentration (M)	$M_n$ (kDa)	Charge density (mol %)	Hydrophobic component (mol %)
p(NIPAM)62k	7	0.5 : 0 : 0	62.158±10.11	0	0
p(NIPAM)142k	5	0.5 : 0 : 0	142.315±6.23	0	0
p(NIPAM)288k	3	0.5 : 0 : 0	238.453±9.67	0	0
p(NIPAM)549k	1	0.5 : 0 : 0	549.236±5.19	0	0
p(NIPAM-AA):5	1	0.475 : 0.025 : 0	535.000±6.64	5	0
p(NIPAM-AA):10	1	0.45 : 0.05 : 0	506.223±2.43	10	0
p(NIPAM-AA):15	1	0.425 : 0.075 : 0	487.331±5.16	15	0

p(NIPAM-AA):20	1	0.4 : 0.1 : 0	485.092±8.07	20	0
p(NIPAM-AA):25	1	0.375 : 0.125 : 0	448.502±9.18	25	0
p(NIPAM-AA-NTBM):4	1	0.38 : 0.1 : 0.02	461.801±5.23	20	4
p(NIPAM-AA-NTBM):7	1	0.365 : 0.1 : 0.035	407.217±10.26	20	7
p(NIPAM-AA-NTBM):10	1	0.35 : 0.1 : 0.05	354.336±7.55	20	10
p(NIPAM-AA-NTBM):13	1	0.335 : 0.1 : 0.065	291.082±9.69	20	13

To confirm the direct dependency of polymer number average molecular weight on initiator concentration, we considered the concept of kinetic chain length ( $\nu$ ),

$$\nu = \frac{R_p}{R_i} \quad \text{Equation 3-1}$$

As per the pseudo steady-state hypothesis,

$$R_i = R_t \text{ i. e. } 2fk_d[I] = 2k_t[M\bullet]^2 \quad \text{Equation 3-2}$$

Therefore,

$$\nu = \frac{R_p}{R_i} = \frac{k_p[M][M\bullet]}{2k_t[M\bullet]^2} \quad \text{Equation 3-3}$$

$$\text{where, } [M\bullet] = \sqrt{\frac{fk_d[I]}{k_t}} \quad \text{Equation 3-4}$$

$$\nu = \frac{k_p[M\bullet]}{2\sqrt{fk_tk_d[I]}} \quad \text{Equation 3-5}$$

where  $R_i$  is rate of initiation,  $R_p$  is rate of propagation,  $R_t$  is rate of termination,  $f$  is initiator efficiency,  $k_d$  is initiator decomposition constant,  $k_p$  is propagation constant,  $k_t$  is termination constant,  $[M]$  is monomer concentration,  $[I]$  is initiator concentration,  $[M\bullet]$  is concentration of polymer radicals.



According to Equation 3-5, the polymer kinetic chain length (or molecular weight) is inversely proportional to the square root of the concentration of initiator. Figure 3-3 shows that this dependency between the concentration of initiator and polymer number average molecular weight applies to our experiments. In addition, we experimentally confirmed that this relation could be extrapolated beyond the experimental range initially used for initiator concentration: see the last point for  $[I] = 9 \text{ mM}$  ( $1/\sqrt{[I]} = 0.33$ ). The higher polymer molecular weight results in the faster sedimentation of kaolin slurry. Therefore, in the second type of polymer, p(NIPAM-AA), the initiator concentration was kept at 1 mM, and NIPAM was copolymerized with AA to obtain a polyelectrolyte with negative charges. The charge density of the polyelectrolyte was varied by changing the concentration of acrylic acid in the feed. Here, the 20 mol % concentration of AA was considered optimum, based on the performance of a flocculant (initial settling rate and turbidity of supernatant) for the dewatering of kaolin slurry, as will be discussed in the subsequent sections in this chapter.

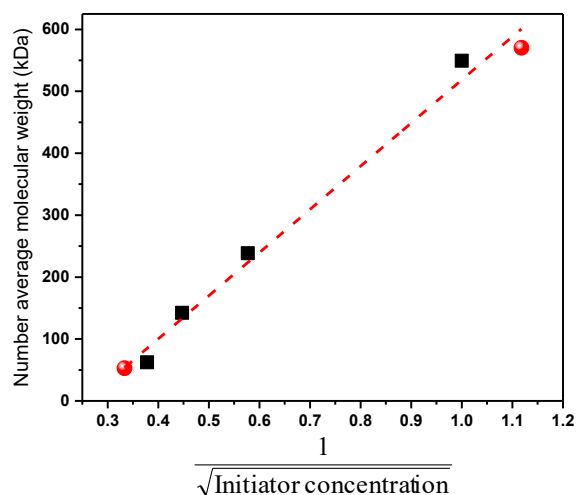


**Figure 3-3** Relationship between number average molecular weight ( $M_n$ ) of p(NIPAM) and initiator concentration. Red markers denote the experiments carried out to verify the correlation in the equation.

We observed that the number average molecular weight ( $M_n$ ) of p(NIPAM-AA) decreased with increasing AA concentration AA, as shown in Table 3-1. The lower reactivity of AA (as compared to NIPAM) is likely the main reason for this decrease. In the third type of polymer, p(NIPAM-AA-NTBM), the polyelectrolyte with 20 mol % AA was hydrophobically modified using NTBM as a third comonomer. The concentration of NTBM was varied from 4 mol % to 13

mol %. The NTBM concentration range was determined based on the solubility of a hydrophobically-modified polyelectrolyte in water. Higher concentration of hydrophobe in a polymer leads to a decreased solubility in water, rendering the product ineffective as a water-soluble flocculant.

NMR spectroscopy was performed on polymers from each class that showed the best flocculation and dewatering performance (Figure 3-4).

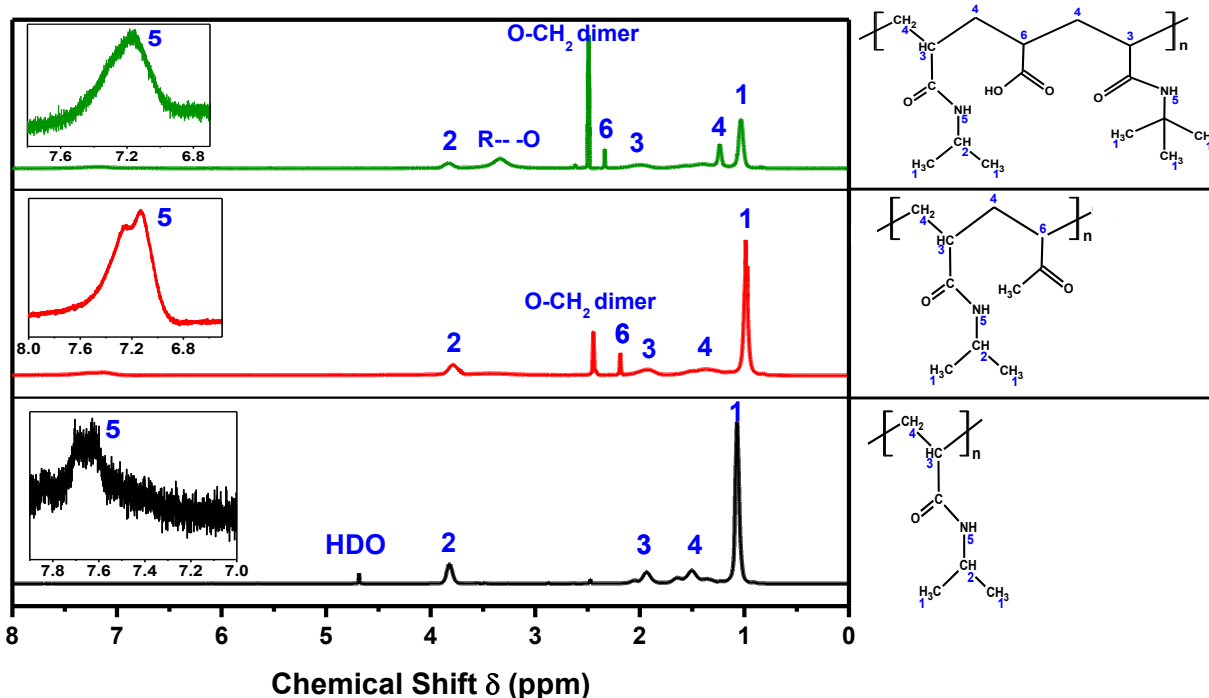


**Figure 3-4** NMR spectra of p(NIPAM)549k (bottom), p(NIPAM-AA)20 (middle), and p(NIPAM-AA-NTBM)13 (top) along with corresponding molecular structures. The inset figures show the magnified view between  $\delta = 7 - 8$  ppm to reveal NH proton.

Copolymer composition near to 100 % conversion was equivalent to feed comonomer composition, as expected. The NMR spectra show that the intensity of the shifts corresponding to methyl protons ( $\delta = 1.09$  ppm) and CH protons ( $\delta = 3.79$  ppm) decreases from homopolymer to terpolymer, (Gouveia et al., 2008) as expected since the fraction of NIPAM in the binary copolymer and terpolymer decrease with the incorporation of AA and NTBM comonomers. These peaks were also shifted to lower field for p(NIPAM-AA) and p(NIPAM-AA-NTBM) because their NMR analyses were carried out in DMSO-*d*<sub>6</sub>, whereas the NMR analysis of

p(NIPAM) was carried out in D<sub>2</sub>O. The spectrum for p(NIPAM) showed the presence of HDO at  $\delta = 4.69$  ppm because the residual moisture in polymer might have undergone the exchange with D<sub>2</sub>O. The broad peaks shown in insets reveal the protons corresponding to NH between  $\delta = 7.6 - 7.2$  ppm. The addition of comonomers to NIPAM showed the presence of peak corresponding to an interaction between carbonyl oxygen and methylene protons at  $\delta = 2.5$  ppm. (Zheng et al., 2013) The absence of peaks near 6 ppm (vinyl protons present in the monomers) evidences that the obtained polymers are purified and free from residual monomers.

### 3.3.2 Thermo-Responsive Behavior of Polyelectrolytes

As p(NIPAM) is known for its thermo-responsive behavior, we measured LCST of all three types of polymers under investigation: p(NIPAM), p(NIPAM-AA), and p(NIPAM-AA-NTBM) (Figure 3-5).

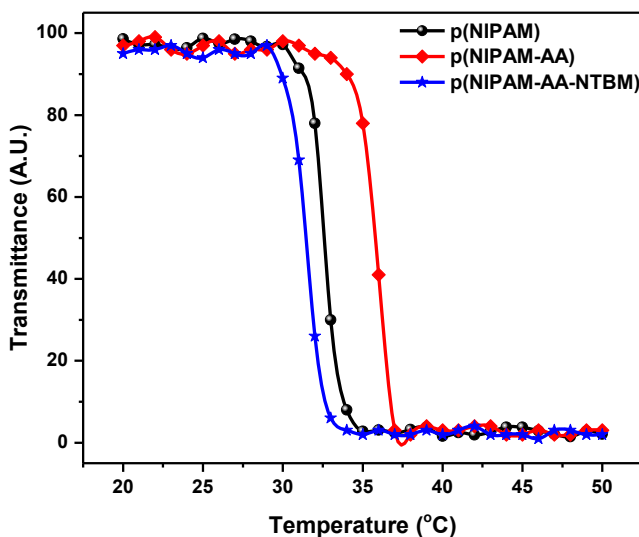


**Figure 3-5** Lower critical solution temperature (LCST) of the p(NIPAM)549k, p(NIPAM-AA)10 (middle), and p(NIPAM-AA-NTBM)7.

Typically, the LCST of thermo-responsive polymers depends on the extent of hydrogen bonding with the solvent. Therefore, we expected that the copolymerization of NIPAM with other monomers could alter hydrogen bonding ability, and affect LCST values. We observed that p(NIPAM) exhibited an LCST of 33 °C, whereas p(NIPAM-AA) and p(NIPAM-AA-NTBM) showed an LCST of 36 °C and 30 °C, respectively. The increase in LCST due to the addition of

AA was attributed to hydrophilic nature of AA, which enhances hydrogen bonding. Prior publications have shown that the LCST of p(NIPAM) increases due to copolymerization with an ionic monomer. (O’Shea et al., 2011; Sakohara and Nishikawa, 2004) On the other hand, incorporation of NTBM caused a marked decrease in LCST because the hydrophobic domains of NTBM greatly interfere the with hydrogen bonding. We attribute this behavior to NTBM monomer, as it minimizes the overall surface energy of the polymer in water by forming the aggregates. Jain et al. mentioned that hydrophobic moieties increase the surface tension at polymer-water interface, causing LCST to decrease. (Jain et al., 2015)

### 3.3.3 Flocculation of Kaolin Slurries

#### 3.1.1.1 Settling Profile

We flocculated 2 wt. % kaolin suspensions using p(NIPAM) of various molecular weights ( $M_n$ ) while keeping polymer dosage at 1000 ppm. The normalized mudline height measured over the period of 2 hours is shown in Figure 3-6A. We clearly observed that the higher molecular weight ( $M_n$ ) polymers promote faster settling of the solid particles. The position of mudline after 2 hours is a measurement of the compaction efficiency of the flocculant. The p(NIPAM) flocculant with  $M_n$  of 549 kDa promoted the highest settling rate and compaction effectiveness of all p(NIPAM) homopolymers. The slope of an initial linear portion of the settling curve is referred to as an initial settling rate (ISR); Figure 3-6B shows that ISR follows a linear relationship with p(NIPAM) molecular weight ( $M_n$ ). This observation supports the hypothesis of the formation of flocs due to polymeric chains and subsequent settling. Further, it supports the fact that the size of flocs depends on the molecular weight of the polymer flocculant.

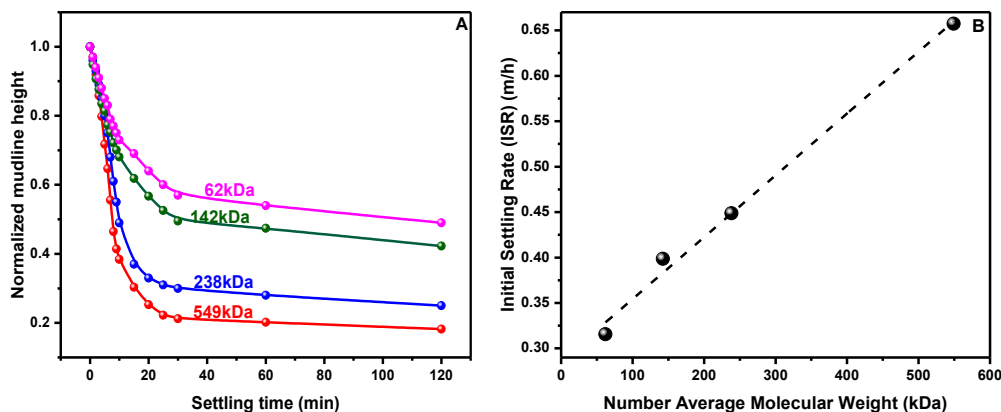


**Figure 3-6** Effect of number average molecular weight ( $M_n$ ) of p(NIPAM) on (A) settling profile and (B) initial settling rate (ISR) of kaolin suspension.

The polyelectrolyte p(NIPAM-AA) was also used to consolidate 2 wt. % kaolin suspensions; their settling profiles are shown in Figure 3-7A. We observed that the final mudline height decreased with increase in the concentration of AA in the polyelectrolyte up to 20 mol %, but decreased for 25 mol % AA. The trend of ISR shown in Figure 3-7B supported our observation that the ISR increases up to 20 mol % AA concentration and decreases later. The best value, followed by a marked decrease beyond that, can be explained based on the maximum possible destabilization of clay particles at an optimum concentration of AA, whereas excess anionicity caused the re-stabilization of clay particles. Therefore, the concentration of AA was kept constant at 20 mol % in further hydrophobic modification experiments.

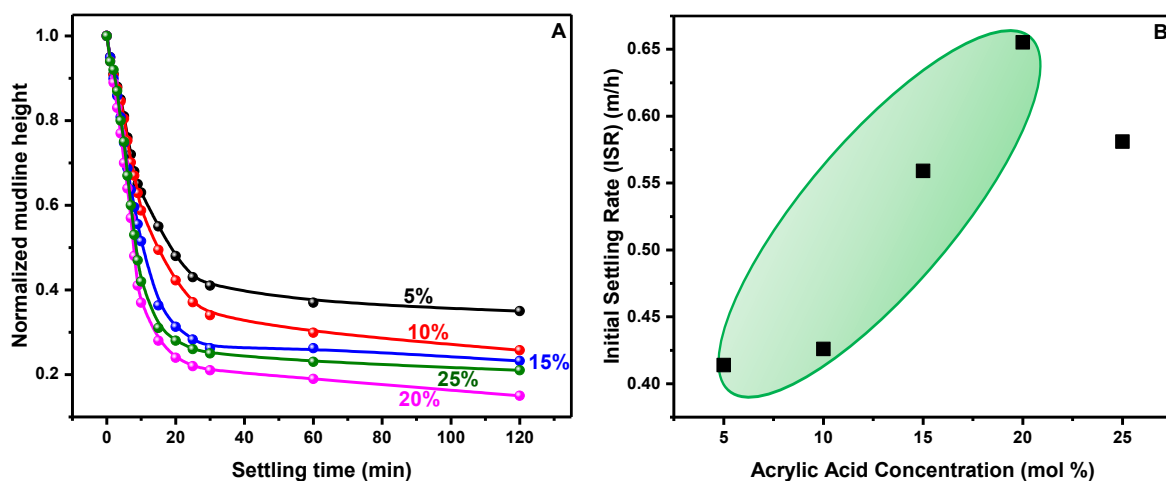


**Figure 3-7** Effect of acrylic acid concentration in p(NIPAM-AA) on (A) settling profile and (B) initial settling rate (ISR) of kaolin suspension.

Flocculation using hydrophobically-modified polyelectrolyte p(NIPAM-AA-NTBM) showed the interesting results depicted in Figure 3-8. The final mudline using the polyelectrolyte with 4 mol % NTBM reached 0.12, whereas that with 13 mol % NTBM reached 0.40. This observation implies that flocculants with higher hydrophobic content, due to combined hydrophobicity of NIPAM and NTBM, yield more compact sediments with lesser trapped water. This composition of flocculant enhanced the dewatering of MFT with the formation of possibly smaller flocs. The comprehensive comparison of Figures 6 to 8 reveal that the hydrophobically-modified polyelectrolytes strongly affect the final mudline height hence, the water content and compaction of the sediments.

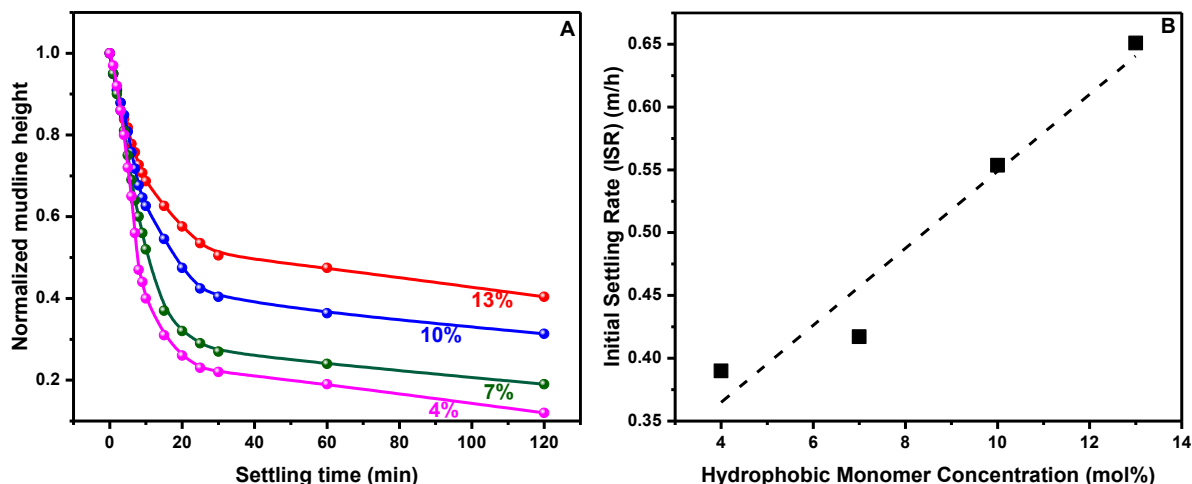


**Figure 3-8** Effect of NTBM concentration in p(NIPAM-AA-NTBM) on (A) settling profile and (B) initial settling rate (ISR) of kaolin suspension

In Figure 3-9, we demonstrate the formation of flocs using 2000 ppm of p(NIPAM-AA-NTBM) terpolymer that are larger than the clay size in suspension. The distribution shifted to higher size after the addition of 2000 ppm of terpolymer indicated that the terpolymer induced floc formation in kaolin suspension initiating the settling process.

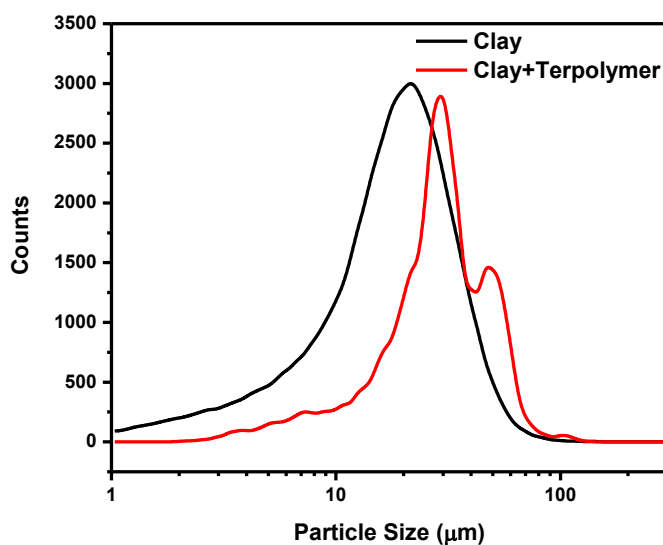


**Figure 3-9** Floc size distribution in kaolin suspension without and with 2000 ppm (NIPAM-AA-NTBM) terpolymer.

### 3.1.1.2 Clarity of Recovered Water: Turbidity of Supernatant

The quality of the water recovered after the consolidation was measured in terms of turbidity. Turbidity in water usually arises due to the presence of stable particulate matters. In the context of this work, lowering the turbidity of the supernatant signifies the ability of the flocculant to neutralize or bridge the fine clay particles, and subsequently consolidate them. Figure 3-10A shows the effect of the molecular weight ( $M_n$ ) of p(NIPAM) on the turbidity of the supernatant obtained after flocculation. Turbidity decreases linearly with increasing p(NIPAM) molecular weight ( $M_n$ ). It is worth to mention that the turbidity of the kaolin suspension without the addition of any flocculant was above 9000 NTU. In Figure 3-10B, the relation between the supernatant turbidity and the composition of p(NIPAM-AA) confirms the behavior we observed for ISR (Figure 3-7B): the supernatant turbidity decreases for p(NIPAM-AA) up to 20 mol % AA, beyond which it increases again. This behavior is likely observed because the increased anionicity of p(NIPAM-AA) with higher AA contents neutralizes the clay particles up to a certain AA content; however, once the surface of clay particles is completely covered by anions, electrostatic repulsion among the negative charges causes the re-stabilization of particles. (Shifa M R Shaikh et al., 2017) These re-stabilized particles make their way to the supernatant, resulting in an increase in turbidity. As expected, the hydrophobically-modified polyelectrolyte p(NIPAM-AA-NTBM) did not show a prominent change in turbidity when the hydrophobe content was varied, as can be seen in Figure 3-10C.

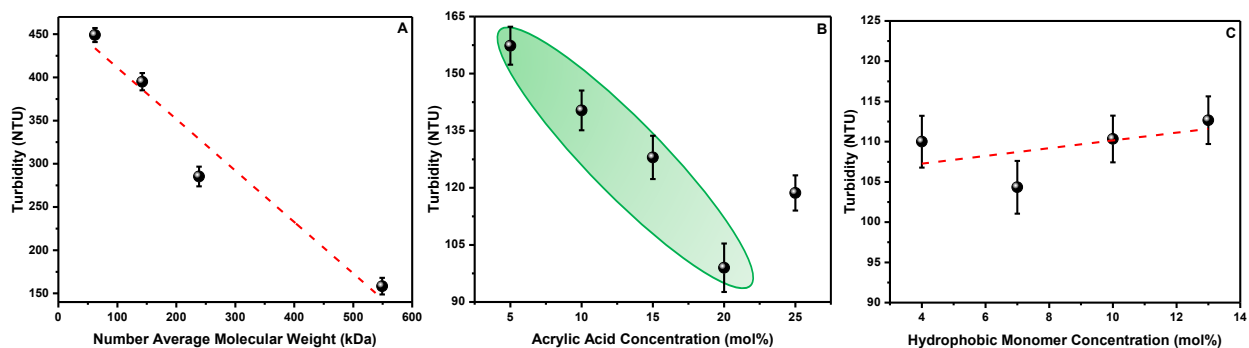


**Figure 3-10** Supernatant turbidity obtained after flocculation using: A) p(NIPAM) of different number average molecular weights, B) p(NIPAM-AA) of varying AA contents, and C) p(NIPAM-AA-NTBM) of 20 mol % AA and varying NTBM content.

### 3.1.1.3 Capillary Suction Time: The Ability to Dewater

Capillary suction time (CST) of the flocculated kaolin was measured using all three types of polymer flocculants. Figure 3-11A shows the effect of number average molecular weight of p(NIPAM) on the CST of the settled kaolin sediments. The lowest CST of 50 seconds was observed when p(NIPAM) of molecular weight ( $M_n$ ) 549 kDa was used. Overall, increasing molecular weight ( $M_n$ ) caused a significant reduction in CST, a behavior that differs from that usually observed with conventional hydrophilic polymers, as higher molecular weight flocculants tend to hold more water inside the flocs/sediments. Increasing the content of AA in p(NIPAM-AA) did not affect CST significantly, as seen in Figure 3-11B. In general, all p(NIPAM-AA) polymers had a NIPAM content ranging from 75-100 mol %. We speculate that the relatively high content of isopropyl functional groups in the copolymers maintained the water repulsion ability of the sediments. Another work in our research group has shown that CST depends more strongly on flocculant dosage (not investigated in this study) than on molecular weight. (Vajihinejad et al., 2017) The addition of hydrophobic monomer to the flocculant clearly made the CST to decrease, as depicted in Figure 3-11C. This behavior was expected, since increasing the hydrophobe content of the flocculant should make the sediments easier to dewater. Such behavior suggests that the hydrophobic nature of the comonomer is a dominant factor in determining dewaterability of the floc.

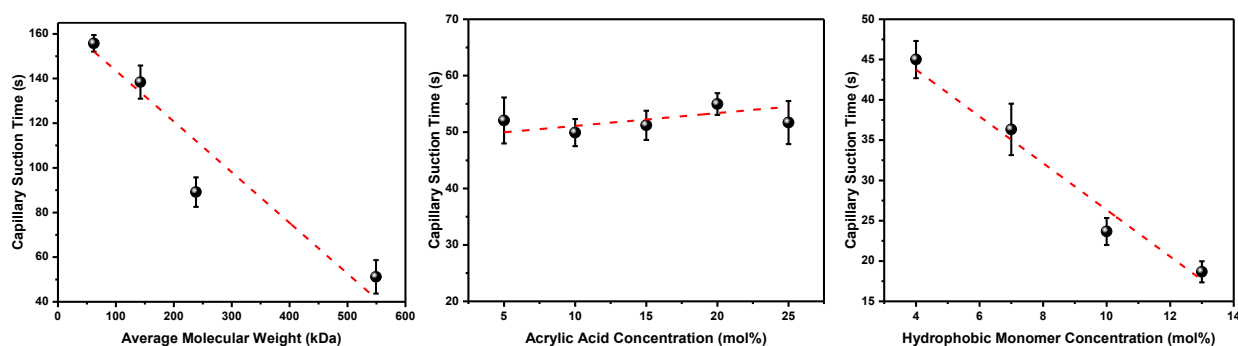


**Figure 3-11** Capillary suction time (CST) of the sediments obtained after the flocculation using (A) p(NIPAM) of different number average molecular weights, (B) p(NIPAM-AA) of varying AA concentration, and (C) p(NIPAM-AA-NTBM) of 20 mol % AA and varying NTBM content.



### 3.1.1.4 Flocculation Mechanism

In this work, we first used p(NIPAM) homopolymer of different molecular weights to flocculate kaolin suspension. Flocculation using the p(NIPAM), which is non-ionic, did not involve charge neutralization mechanism. The flocculation performance of p(NIPAM) described in this work was attributed to adsorption-bridging mechanism only. Further we used anionic p(NIPAM-AA) of varying charge density to flocculate kaolin suspension. Incorporation of AA showed marked effect on ISR and supernatant turbidity. The flocculation using p(NIPAM-AA) involved a combination of charge neutralization and bridging mechanism. Anions of copolymer possibly neutralized the edges of kaolin that are positively charged and surface of kaolin participated in bridging mechanism. (Shifa M R Shaikh et al., 2017; Shifa M.R. Shaikh et al., 2017) We verified this mechanism by measuring the zeta potential of clay suspension with increase in terpolymer concentration as shown in Figure 3-12. It was observed that zeta potential approached neutrality as we increased the dosage however, it did not reach to zero up to 5000 ppm. These results suggested that both charge neutralization and bridging mechanism co-exists during the flocculation.

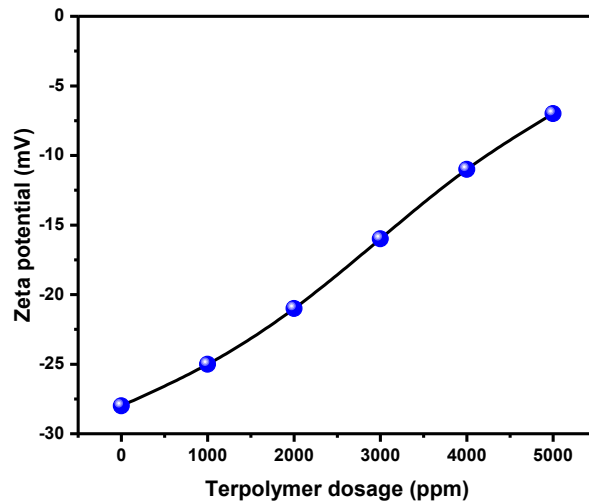


**Figure 3-12** Zeta potential of clay suspension with increase in terpolymer concentration.

Increase in charge density of copolymer beyond 20 mol % was detrimental to ISR and supernatant turbidity due to electrostatic stabilization of kaolin particles caused by excessive anions. The purpose of NTBM in p(NIPAM-AA-NTBM) was to add hydrophobicity to the flocculant that could enhance the dewatering of kaolin suspension. As NTBM is a non-ionic

monomer, it potentially did not contribute to charge neutralization mechanism. However, it helped in adsorption-bridging mechanism as evidenced in flocculation results. The Figure 3-13 shows that the sediments obtained using p(NIPAM-AA-NTBM) were significantly more compact than p(NIPAM-AA). This observation supports our claim that NTBM helps to expel the water from sediments due to its hydrophobic nature.

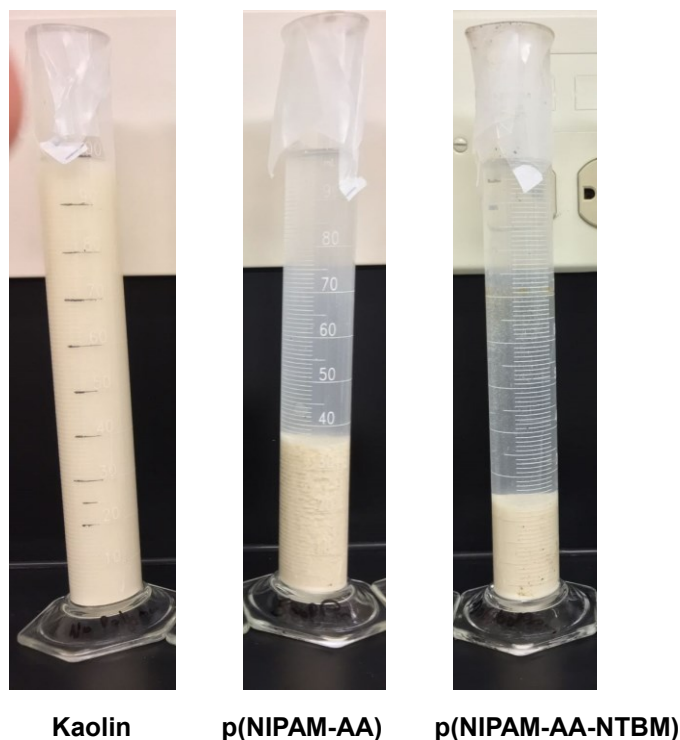


**Figure 3-13** Images of kaolin suspension without polymer and with 2000 ppm of optimized p(NIPAM-AA) and p(NIPAM-AA-NTBM).

### 3.4 Conclusions

In this work, we investigated the effect of multifunctional ternary polymer on the flocculation of kaolin suspensions. The higher molecular weight ( $M_n$ ) favored the initial settling rates due to the bridging mechanism. The addition of anionic comonomer, up to a certain extent, enhanced the initial settling rates and lowered the turbidity. Incorporation of hydrophobic comonomer led to the production of the best flocculant in terms of ISR, turbidity, and dewaterability. Above the optimum fraction of acrylic acid, the electrostatic repulsion between flocculant-coated particles dominated. Though hydrophobic comonomer enhanced the dewaterability of sediments, its

excess fraction lowered the water solubility of a flocculant. The LCST of a polymer increased when copolymerized with acrylic acid and decreased when copolymerized with the hydrophobic monomer. AA in ternary polymer played a vital role in neutralizing the charges onto clay particles whereas NTBM helped to improve the dewaterability of the sediments. Therefore, an optimum fraction of both comonomers is always desirable to balance the processing and performance of the flocculants. In this work, p(NIPAM) of molecular weight 549 kDa, p(NIPAM-AA) containing 20 mol % AA, and p(NIPAM-AA-NTBM) containing 20 mol % AA and 13 mol % NTBM were most effective in flocculating kaolin suspension.

## References

- Alamgir, A., Harbottle, D., Masliyah, J., Xu, Z., 2012. Al-PAM assisted filtration system for abatement of mature fine tailings. *Chem. Eng. Sci.* 80, 91–99. doi:10.1016/j.ces.2012.06.010
- Bolto, B., Gregory, J., 2007. Organic polyelectrolytes in water treatment. *Water Res.* 41, 2301–2324. doi:10.1016/j.watres.2007.03.012
- Botha, L., Soares, J.B.P., 2015. The Influence of Tailings Composition on Flocculation. *Can. J. Chem. Eng.* 93, 1514–1523. doi:10.1002/cjce.22241
- Das, R., Ghorai, S., Pal, S., 2013. Flocculation characteristics of polyacrylamide grafted hydroxypropyl methyl cellulose: An efficient biodegradable flocculant. *Chem. Eng. J.* 229, 144–152. doi:10.1016/j.cej.2013.05.104
- Divakaran, R., Sivasankara Pillai, V.N., 2001. Flocculation of kaolinite suspensions in water by chitosan. *Water Res.* 35, 3904–3908. doi:10.1016/S0043-1354(01)00131-2
- Franks, G. V., Li, H., O’Shea, J.-P., Qiao, G.G., 2009. Temperature responsive polymers as multiple function reagents in mineral processing. *Adv. Powder Technol.* 20, 273–279. doi:10.1016/j.appt.2009.02.002
- Gao, C., Chen, B., Möhwald, H., 2006. Thermosensitive poly(allylamine)-g-poly(N-isopropylacrylamide) copolymers: Salt-tuned phase separation, particle formation and their applicability on curved surface. *Colloids Surfaces A Physicochem. Eng. Asp.* 272, 203–210. doi:10.1016/j.colsurfa.2005.07.023
- Gao, C., Möhwald, H., Shen, J., 2005. Thermosensitive poly(allylamine)-g-poly(N-isopropylacrylamide): synthesis, phase separation and particle formation. *Polymer (Guildf)*. 46, 4088–4097. doi:10.1016/j.polymer.2005.02.115
- Glinel, K., Sukhorukov, G.B., Möhwald, H., Khrenov, V., Tauer, K., 2003. Thermosensitive Hollow Capsules Based on Thermoresponsive Polyelectrolytes. *Macromol. Chem. Phys.* 204, 1784–1790. doi:10.1002/macp.200350033
- Gouveia, L.M., Paillet, S., Khoukh, A., Grassl, B., Muller, A.J., 2008. The effect of the ionic strength on the rheological behavior of hydrophobically modified polyacrylamide aqueous solutions mixed with sodium dodecyl sulfate (SDS) or cetyltrimethylammonium p-toluenesulfonate (CTAT). *Colloids Surfaces A Physicochem. Eng. Asp.* 322, 211–218. doi:10.1016/j.colsurfa.2008.03.008
- Gumfekar, S.P., Rooney, T.R., Hutchinson, R.A., Soares, J.B.P., 2017. Dewatering Oil Sands Tailings with Degradable Polymer Flocculants. *ACS Appl. Mater. Interfaces* 9, 36290–36300. doi:10.1021/acsami.7b10302
- Han, D.-M., Matthew Zhang, Q., Serpe, M.J., 2015. Poly (N-isopropylacrylamide)-co-(acrylic acid) microgel/Ag nanoparticle hybrids for the colorimetric sensing of H<sub>2</sub>O<sub>2</sub>. *Nanoscale* 7, 2784–2789. doi:10.1039/C4NR06093H

- Jain, K., Vedarajan, R., Watanabe, M., Ishikiriyama, M., Matsumi, N., 2015. Tunable LCST behavior of poly(N-isopropylacrylamide/ionic liquid) copolymers. *Polym. Chem.* 6, 6819–6825. doi:10.1039/C5PY00998G
- Jia, S., Yang, Z., Yang, W., Zhang, T., Zhang, S., Yang, X., Dong, Y., Wu, J., Wang, Y., 2016. Removal of Cu(II) and tetracycline using an aromatic rings-functionalized chitosan-based flocculant: Enhanced interaction between the flocculant and the antibiotic. *Chem. Eng. J.* 283, 495–503. doi:10.1016/j.cej.2015.08.003
- Li, H., Long, J., Xu, Z., Masliyah, J., 2007. Flocculation of kaolinite clay suspensions using a temperature-sensitive polymer. *AIChE J.* 53, 479–488. doi:10.1002/aic
- Liu, B., Zheng, H., Deng, X., Xu, B., Sun, Y., Liu, Y., Liang, J., 2017. Formation of cationic hydrophobic micro-blocks in P(AM-DMC) by template assembly: characterization and application in sludge dewatering. *RSC Adv.* 7, 6114–6122. doi:10.1039/C6RA27400E
- Long, J., Li, H., Xu, Z., Masliyah, J.H., 2006. Role of colloidal interactions in oil sand tailings treatment. *AIChE J.* 52, 371–383. doi:10.1002/aic.10603
- Lowe, T.L., Virtanen, J., Tenhu, H., 1999. Hydrophobically modified responsive polyelectrolytes. *Langmuir* 15, 4259–4265. doi:10.1021/la981194n
- Lu, H., Wang, Y., Li, L., Kotsuchibashi, Y., Narain, R., Zeng, H., 2015. Temperature- and pH-Responsive Benzoboroxole-Based Polymers for Flocculation and Enhanced Dewatering of Fine Particle Suspensions. *ACS Appl. Mater. Interfaces* 7, 27176–27187. doi:10.1021/acsami.5b09874
- Lu, H., Xiang, L., Cui, X., Liu, J., Wang, Y., Narain, R., Zeng, H., 2016. Molecular Weight Dependence of Synthetic Glycopolymers on Flocculation and Dewatering of Fine Particles. *Langmuir* 32, 11615–11622. doi:10.1021/acs.langmuir.6b03072
- Masliyah, J., Zhou, Z.J., Xu, Z., Czarnecki, J., Hamza, H., 2004. Understanding Water-Based Bitumen Extraction from Athabasca Oil Sands. *Can. J. Chem. Eng.* 82, 628–654. doi:10.1002/cjce.5450820403
- O’Shea, J.-P., Qiao, G.G., Franks, G. V, 2011. Temperature responsive flocculation and solid-liquid separations with charged random copolymers of poly(N-isopropyl acrylamide). *J. Colloid Interface Sci.* 360, 61–70. doi:10.1016/j.jcis.2011.04.013
- Rooney, T.R., Gumfekar, S.P., Soares, J.B.P., Hutchinson, R.A., 2016. Cationic Hydrolytically Degradable Flocculants with Enhanced Water Recovery for Oil Sands Tailings Remediation. *Macromol. Mater. Eng.* 301, 1248–1254. doi:10.1002/mame.201600230
- Sakohara, S., Hinago, R., Ueda, H., 2008. Compaction of TiO<sub>2</sub> suspension by using dual ionic thermosensitive polymers. *Sep. Purif. Technol.* 63, 319–323. doi:10.1016/j.seppur.2008.05.014
- Sakohara, S., Nishikawa, K., 2004. Compaction of TiO<sub>2</sub> suspension utilizing hydrophilic/hydrophobic transition of cationic thermosensitive polymers. *J. Colloid Interface Sci.* 278, 304–9. doi:10.1016/j.jcis.2004.06.002

- Sakohara, S., Yagi, S., Iizawa, T., 2011. Dewatering of inorganic sludge using dual ionic thermosensitive polymers. *Sep. Purif. Technol.* 80, 148–154. doi:10.1016/j.seppur.2011.04.022
- Sawalha, O., Scholz, M., 2007. Assessment of Capillary Suction Time (CST) Test Methodologies. *Environ. Technol.* 28, 1377–1386. doi:10.1080/09593332808618898
- Shaikh, S.M.R., Nasser, M.S., Hussein, I.A., Benamor, A., 2017. Investigation of the effect of polyelectrolyte structure and type on the electrokinetics and flocculation behavior of bentonite dispersions. *Chem. Eng. J.* 311, 265–276. doi:10.1016/j.cej.2016.11.098
- Shaikh, S.M.R., Nasser, M.S., Hussein, I., Benamor, A., Onaizi, S.A., Qiblawey, H., 2017. Influence of polyelectrolytes and other polymer complexes on the flocculation and rheological behaviors of clay minerals: A comprehensive review. *Sep. Purif. Technol.* 187, 137–161. doi:10.1016/j.seppur.2017.06.050
- Tripathy, T., De, B., 2006. Flocculation: a new way to treat the waste water. *J. Phys. Sci.* 10, 93–127.
- Vajihinejad, V., Guillermo, R., Soares, J.B.P., 2017. Dewatering Oil Sands Mature Fine Tailings (MFTs) with Poly(acrylamide- co -diallyldimethylammonium chloride): Effect of Average Molecular Weight and Copolymer Composition. *Ind. Eng. Chem. Res.* 56, 1256–1266. doi:10.1021/acs.iecr.6b04348
- Wang, C., Harbottle, D., Liu, Q., Xu, Z., 2014. Current state of fine mineral tailings treatment: A critical review on theory and practice. *Miner. Eng.* 58, 113–131. doi:10.1016/j.mineng.2014.01.018
- Wilkinson, N., Metaxas, A., Bricchetto, E., Wickramaratne, S., Reineke, T.M., Dutcher, C.S., 2017. Ionic strength dependence of aggregate size and morphology on polymer- clay flocculation. *Colloids Surfaces A* 529, 1037–1046. doi:10.1016/j.colsurfa.2017.06.085
- Wu, H., Liu, Z., Yang, H., Li, A., 2016. Evaluation of chain architectures and charge properties of various starch-based flocculants for flocculation of humic acid from water. *Water Res.* 96, 126–135. doi:10.1016/j.watres.2016.03.055
- Yang, Z., Wu, H., Yuan, B., Huang, M., Yang, H., Li, A., Bai, J., Cheng, R., 2014. Synthesis of amphoteric starch-based grafting flocculants for flocculation of both positively and negatively charged colloidal contaminants from water. *Chem. Eng. J.* 244, 209–217. doi:10.1016/j.cej.2014.01.083
- Zhang, Z., Zheng, H., Huang, F., Li, X., He, S., Zhao, C., 2016. Template Polymerization of a Novel Cationic Polyacrylamide: Sequence Distribution, Characterization, and Flocculation Performance. *Ind. Eng. Chem. Res.* 55, 9819–9828. doi:10.1021/acs.iecr.6b01894
- Zheng, H., Sun, Y., Zhu, C., Guo, J., Zhao, C., Liao, Y., Guan, Q., 2013. UV-initiated polymerization of hydrophobically associating cationic flocculants: Synthesis, characterization, and dewatering properties. *Chem. Eng. J.* 234, 318–326. doi:10.1016/j.cej.2013.08.098

Zintchenko, A., Ogris, M., Wagner, E., 2006. Temperature Dependent Gene Expression Induced by PNIPAM-Based Copolymers: Potential of Hyperthermia in Gene Transfer. *Bioconjug. Chem.* 17, 766–772. doi:10.1021/bc050292z

## Chapter 4

# Rational Design of Multifunctional Terpolymer Based On the Reactivity Ratios and Its Application for Dewatering Oil Sands Tailings

We designed a series of multifunctional terpolymers, poly(*N*-isopropyl acrylamide/2-(methacryloyloxy) ethyl trimethyl ammonium chloride/*N*-*tert*-butylacrylamide) [p(NIPAM-MATMAC-BAAM)] and used them to flocculate oil sands mature fine tailings (MFT). The hydrophobic BAAM comonomer helped expel water out of sediments, while the cationic MATMAC comonomer promoted charge neutralization of the negatively charged particles in MFT. More importantly, the chemical composition distributions of these terpolymers were designed based on the knowledge of the reactivity ratios of all comonomers, not but random trial, as usually the case in polymer flocculants. Focused beam reflectance measurement (FBRM) experiments showed that larger flocs (120  $\mu\text{m}$ ) were formed in MFT containing average particles of 20  $\mu\text{m}$ . In general, the initial settling rate (ISR) decreased with increasing flocculant hydrophobicity, because the hydrophobic terpolymer segments do not take part in the bridging of MFT particles. Contrarily, the sediments dewaterability increased with increased terpolymer hydrophobicity. This study provides guidelines to design a polymer flocculant from first principles, and demonstrates the potential of using hydrophobically-modified cationic polymers to effectively flocculate MFT.

### 4.1 Introduction

Canada has the third largest oil sands deposits in the world, from which bitumen is extracted using large amounts of hot water and caustic. While the oil sands deposits are strategic resources for Canada, North America, and the global market, the extraction process generates fluid wastes called oil sands tailings, (Vajihinejad et al., 2017) which pose serious technical and environmental concerns for Canada. Typically, mature fine tailings (MFT) contain fine negatively-charged clays ( $\sim 33$  wt. %), water ( $\sim 65$  wt. %), and residual bitumen ( $\sim 2$ -5 wt. %).

---

A version of this chapter has been submitted as S. P. Gumfekar and J. B. P. Soares, "Rational Design of Multifunctional Terpolymer Based On the Reactivity Ratios and Its Application for Dewatering Oil Sands Tailings" to ACS Appl. Mater. Interfaces, 2018



(Botha and Soares, 2015) Although coarse particles settle quickly, the fine particles remain suspended in water, without further dewatering for many decades. Its water chemistry and solid components make MFT difficult to consolidate to levels required for land reclamation.

The main goals associated with MFT treatment are to enhance the settling and dewatering of solid sediments, and to recover the water trapped in the tailings. The recovery of water is important because for each barrel of bitumen produced in Canada's oil sands industry, approximately 0.5–2.5 barrels of freshwater is used from local waterways to aid in the processing of the mined ore. (Quinlan and Tam, 2015)

Existing technologies use water-soluble polymers, such as polyacrylamide (PAM) and its ionic copolymers, to form large MFT flocs and induce solid-liquid separation. (Vedoy and Soares, 2015) However, due to the strong water-affinity of PAM, the flocs entrap a significant amount of water, forming low-shear strength sediments that are difficult to dewater. PAM-based polymers produce gel-like networks through hydrogen bonding that retain large volumes of water, leading to poor sediment dewatering. Researchers have developed innovative polymers that induce hydrophobicity for effective dewatering as a response to change in temperature or pH. (Franks et al., 2006; Wang et al., 2014) Recently, Zhang et al. used a thermoresponsive cationic flocculant, which becomes hydrophobic above its lower critical solution temperature (LCST), to dewater MFT. (Zhang et al., 2017) However, the energy costs associated to achieve the temperature change of the enormous amount of MFT in tailings ponds limit its large-scale implementation. Polymers that change conformation from hydrophilic to hydrophobic upon exposure to acid or alkali (pH-sensitive polymers) are also a possible alternative, but the amount of acid or base required to change the pH of large volumes of tailings may limit their practical applications.

Other researchers have also attempted two reasonable strategies to address this issue: *i*) use of cationic polymers to neutralize negatively-charged particles, and *ii*) use of hydrophobically modified polymers to enhance dewatering. (Lee et al., 2011; Liao et al., 2014; Lu et al., 2015; Yang et al., 2010; Zheng et al., 2013) These approaches have been used to treat general wastewater, but not for MFT. The majority of the hydrophobically-modified polymers are synthesized using surfactant-assisted polymerization. (Candau and Selb, 1999) However, the presence of surfactants in the flocculants is undesirable as they form froth during flocculation. Functionalization of hydrophobic polymers to add hydrophilic functional groups, such as

polyethylene modified with acrylate, is one of the approaches used to maintain a balance between hydrophilicity and hydrophobicity within the polymer. (Botha et al., 2017)

Functionalities are added to the flocculants by copolymerizing a monomer with a cationic, anionic or hydrophobic monomer. (Gumfekar and Soares, 2018) The fraction of the functional comonomer in the copolymer (not in polymerization feed) plays an important role in the performance of the functional flocculant. Several investigations ignore differences in the reactivity ratios of the comonomers used to synthesize flocculants and implicitly assume that the polymerization feed composition is equal to the copolymer flocculant composition. This, however, is incorrect, since significant composition drift may take place during the copolymerization. (Escudero Sanz et al., 2007; Sakohara and Nishikawa, 2004; Wang et al., 2014) This problem becomes even more severe when terpolymers are used, since the proportions of the 3 comonomers may fluctuate widely throughout the polymerization.

In this work, we quantified compositional drift during the synthesis of a new terpolymer flocculant, and used this information to precisely synthesize a series of terpolymers with compositions suited for MFT dewatering. The comonomers used to make the terpolymer via free radical polymerization were 2-(methacryloyloxy) ethyl trimethyl ammonium chloride (MATMAC), a quaternary ammonium-based cationic monomer, *N-tert*-butylacrylamide (BAAM), a hydrophobic monomer, and *N*-isopropyl acrylamide (NIPAM). The multifunctionality of this terpolymer is regulated by the fractions of its cationic (MATMAC), hydrophobic (BAAM), and thermos-sensitive (NIPAM) monomers, and can be precisely controlled if we know their reactivity ratios for these three comonomers.

We systematically investigated the influence of terpolymer structure on MFT flocculation behavior to follow up the initial promising results demonstrated with kaolin, the principal clay component in MFT. (Gumfekar and Soares, 2018) The synthesized terpolymer flocculants were employed to dewater MFT, and the dewatering performance was studied. The performance of flocculants was measured in terms of floc size, initial settling rate (ISR), and capillary suction time (CST) of sediments.

## 4.2 Materials and Methods

### 4.2.1 Materials

*N*-isopropyl acrylamide (NIPAM), 2-(methacryloyloxy) ethyl trimethyl ammonium chloride (MATMAC), *N*-*tert*-butylacrylamide (BAAM), ammonium persulfate (APS), and *N,N,N',N'*-tetramethylethylenediamine (TEMED) were purchased from Sigma-Aldrich (analytical reagent grade) and used without further purification. NIPAM, MATMAC, and BAAM were used as monomers, while APS and TEMED were used as initiator and accelerator, respectively. Deionized (DI) water was used as a solvent for all syntheses. Mature fine tailings (MFT, 33.5 % solids by mass), obtained from Syncrude Canada Ltd., were diluted to 10 wt. % total solids for the flocculation experiments.

### 4.2.2 Synthesis of *p*(NIPAM-MATMAC-BAAM)

We used two procedures for synthesis of polymers with minor variation in terms of solvent selection. The first procedure was used to synthesize *p*(NIPAM-MATMAC) with DI water as a solvent. The second procedure was used for the synthesis of *p*(MATMAC-BAAM), *p*(NIPAM-BAAM), and *p*(NIPAM-MATMAC-BAAM) with a mixture of water and acetonitrile as co-solvents. Co-solvents ensured the all monomers become soluble in the polymerization medium.

In a typical synthesis, a desired quantity of monomers was dissolved in either DI water or a mixture of DI water and acetonitrile. We removed the dissolved oxygen from solution by constantly stirring and purging the solution with nitrogen for 0.5 h. Next, the desired amount of TEMED and APS was added to the monomer solution. The polymerization was carried out at room temperature for 10-15 min. In a free radical polymerization, the polymer molecular weight increases rapidly, but monomer conversion linearly increases with time. Lesser polymerization time ensured the overall monomer conversion below 10% and subsequently avoided substantial composition drift. After the polymerization, the polymer was precipitated in acetone and washed 3 times, followed by vacuum drying. In all experiments, the total monomer concentration was maintained at 0.5 M. The schematic of the experimental setup and chemical structures of repeating units of the terpolymer is shown in Figure 4-1.

We used proton nuclear magnetic resonance spectroscopy ( $^1\text{H-NMR}$ ) (Agilent 400 MR) to quantitatively analyze the composition of these copolymers and terpolymers. For NMR analysis,  $\text{D}_2\text{O}$  and  $\text{DMSO-}d_6$  were used as solvents and all spectra were recorded at  $27\text{ }^\circ\text{C}$  and  $400\text{MHz}$ .

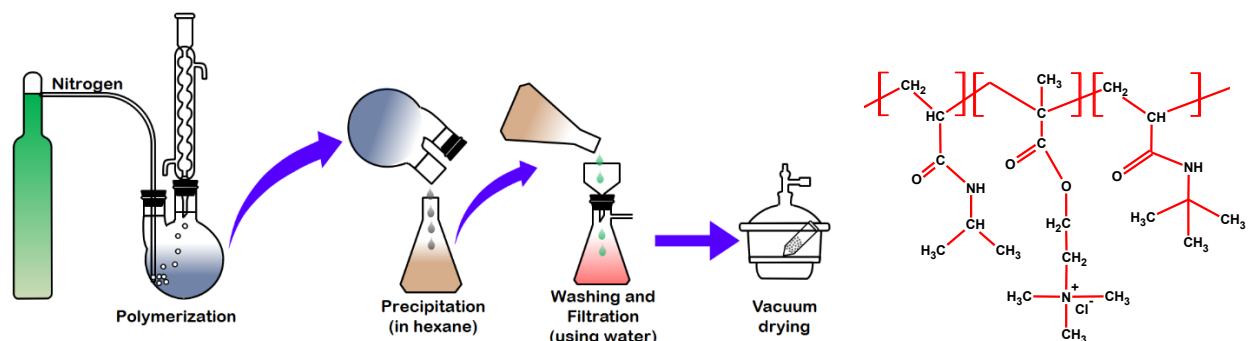


**Figure 4-1** Experimental polymerization setup for the polymers and chemical structures of the repeating units of p(NIPAM-MATMAC-BAAM)

#### 4.2.3 Tailings Characterization and Flocculation Tests

The Dean–Stark extraction method was used to determine the amount of solids, water, and bitumen in the MFT sample, as shown in Table 4-1. The details of this method are described elsewhere. (Vajihinejad et al., 2017; Zhu et al., 2017) We used atomic absorption spectroscopy (AAS) to quantify the concentration of major ions in the MFT sample (Table 4-2).

**Table 4-1** MFT composition determined using the Dean-Stark method

Compound	Weight %
Water	61.8
Solids	33.6
Bitumen	4.6

**Table 4-2** Ion composition in MFT measured using atomic absorption spectroscopy

Ion	Quantity (ppm)
$\text{Na}^+$	238.9
$\text{K}^+$	21.5
$\text{Ca}^{2+}$	12.4
$\text{Mg}^{2+}$	17.7

Each flocculation experiment was carried out with 100 mL of a 10 wt. % solids mixture, prepared by diluting MFT with DI water. The pH of the diluted MFT varied between 8.0 and 8.5. The flocculant dosage was varied from 1000 to 7000 parts per million (ppm), on a weight basis relative to the weight of solids in the MFT. This MFT suspension was transferred to a 250 mL baffled beaker (7 cm diameter and 9.5 cm height) in which the flocculant and the MFT suspension were mixed in two steps using a 316 stainless steel 4-blade propeller with 2 inch diameter: *i*) the MFT mixture was stirred at 300 rpm for 2 min, followed by addition of the desired quantity of the flocculant; *ii*) mixing was maintained at 300 rpm for an additional 5 min, followed by 2 min at 100 rpm. The MFT suspension mixed with flocculant was immediately transferred to a 100 mL graduated cylinder, and the mudline (solid-liquid interface) was recorded during the initial settling period.

The evaluation of the flocculant performance on the settling rate of the MFT suspension was based on the normalized mudline height ( $h/H$ ) and the initial settling rate (ISR) as shown in Figure 4-2. Here,  $h$  is the mudline height at time  $t$ , and  $H$  is the initial mudline height at time zero.; i.e. a suspension that is not responsive to the flocculant dosage would give an  $h/H$  value of unity. ISR was calculated from the slope of an initial linear portion of the settling curves.

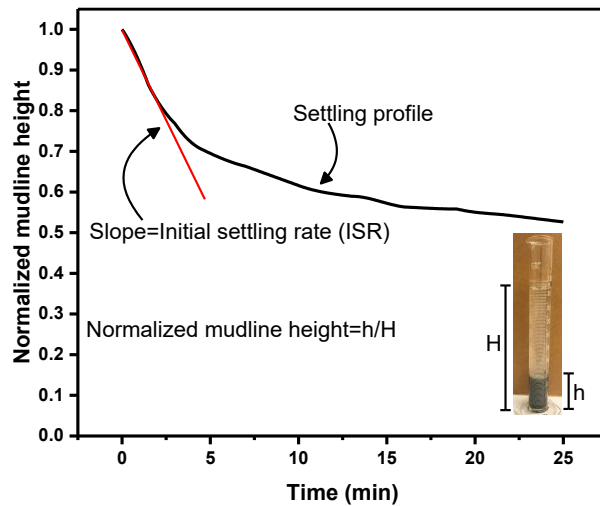


**Figure 4-2** Schematic of initial settling rate calculation based on the settling profile

We used focused beam reflectance measurement instrument (FBRM G400, Mettler-Toledo, USA) to measure the real-time evolution of floc size before and after the addition of the flocculant. Several studies have used FBRM to investigate flocculation. (Gregory, 2009; Senaputra et al., 2014; Wang et al., 2016) The FBRM probe consists of a fast rotating laser beam, which is immersed in a beaker containing the MFT suspension. The clay particles in the MFT reflect the incident laser beam that is captured by the FBRM probe. Further, the system translates the reflected signal into ‘the chord length’ using the multiplication of the beam reflectance speed and the duration of the reflected signal, which is considered as a floc/particle size. We obtained the chord length before and after the addition of terpolymer on a real-time basis. In this work, we used the square weighted mean chord length because it resolves even small changes in floc size. Various researchers have also recommended that the square weighted mean chord length represents an unbiased change in the system. (Gregory, 2009; Senaputra et al., 2014) The data were acquired at a frequency of every 2 seconds in the range of 1 to 1000  $\mu\text{m}$  in the primary electronic mode.

Capillary suction time (CST) of the MFT sediments was measured using Triton Electronics 319 multi-purpose CST apparatus. CST determines how fast sediments can be dewatered. The equipment measures the time taken by water to travel certain radial distance. Measurement of CST is an important parameter in determining the sludge characteristics. (Sawalha and Scholz, 2007) Pipetting a fixed volume of the solids suspension gave more reproducible results than scooping an equivalent portion of the sediment with a spatula. In cases where large flocs were obtained, the pipette tip was sawed off to provide a wider opening, to prevent shearing of the flocs.

## **4.3 Results and Discussion**

### *4.3.1 Composition Drift in Binary Copolymers*

We estimated the binary reactivity ratios of the comonomers by synthesizing copolymers of NIPAM-MATMAC, MATMAC-BAAM, and NIPAM-BAAM with varying mole fraction of each monomer in the feed, and measured the corresponding fraction of the monomer in the copolymers using proton nuclear magnetic resonance spectroscopy ( $^1\text{H-NMR}$ ). The overall monomer conversion in these experiments was kept below 10 % to avoid substantial composition

drift that may occur at high conversion. Figure 4-3 shows the composition curves of the copolymers synthesized in this study, where  $f$  denotes the fraction of monomer in feed and  $F$  denotes the fraction of monomer in the copolymer.

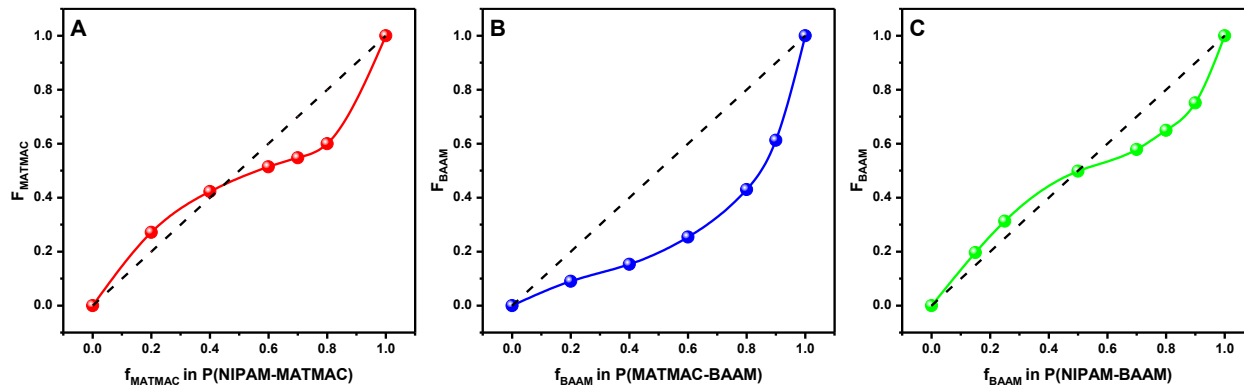


**Figure 4-3** Composition curves showing the drift in compositions of copolymers (A) p(NIPAM-MATMAC), (B) p(MATMAC-BAAM), and (C) p(NIPAM-BAAM) ( $f$ : fraction of comonomer in feed;  $F$ : fraction of comonomer in the copolymer).

Figure 4-3A and C show that p(NIPAM-MATMAC) and p(NIPAM-BAAM) exhibited an azeotropic point at approximately  $f = 0.4$  and  $0.5$ , respectively. At the azeotropic point, composition drift does not take place; however, a small change in reaction conditions can affect the molar fraction of monomers in the copolymer. The results showed that NIPAM has good reactivity with MATMAC and BAAM, but, MATMAC has poor reactivity with BAAM. In the case of p(NIPAM-MATMAC), MATMAC is poorly incorporated in the copolymer when  $f > 0.4$ , probably because the electrostatic repulsion between the positively charged MATMAC units becomes dominant. On the other hand, it is difficult to reach high incorporation of BAAM in the BAAM-MATMAC copolymer, likely due to differences in polarity and solution compatibility of both comonomers. The incorporation of BAAM in p(NIPAM-BAAM) is significantly reduced when  $f > 0.5$ . BAAM showed better compatibility with NIPAM than with MATMAC.

#### 4.3.2 Determination of Reactivity Ratios

We estimated the binary reactivity ratios of our system using the Fineman-Ross, Kelen-Tudos, Yezrielev - Brokhina - Roskin (YBR), and non-linear least square methods. (Fineman and Ross,

1950; Kelen and Tüd[Otilde]s, 1975) The Fineman-Ross method linearizes the Mayo-Lewis equation (Mayo and Lewis, 1944)

$$F_1 = 1 - F_2 = \frac{r_1 f_1^2 + f_1 f_2}{r_1 f_1^2 + 2f_1 f_2 + r_2 f_2^2} \quad \text{Equation 4-1}$$

By rearranging the terms of Equation 4-1, one obtains

$$\frac{F}{f}(f - 1) = r_1 \frac{F^2}{f} - r_2 \quad \text{Equation 4-2}$$

Equation 4-2 can be made more compact making the following variable transformation  $G = \frac{F}{f}(f - 1)$  and  $H = \frac{F^2}{f}$ . Therefore, Equation 4-2 becomes

$$G = r_1 H - r_2$$

Figure 4-4A shows the plot of  $G$  vs  $H$  for p(NIPAM-MATMAC), p(MATMAC-BAAM), and p(NIPAM-BAAM). The slope of the curve and negative of the intercept give the reactivity ratios listed in Table 4-3. This method offers a considerable advantage of using linear least squares to fit the experimental data. However, one notes that the data was aggregated towards the lower  $H$  values, which may bias these estimates.

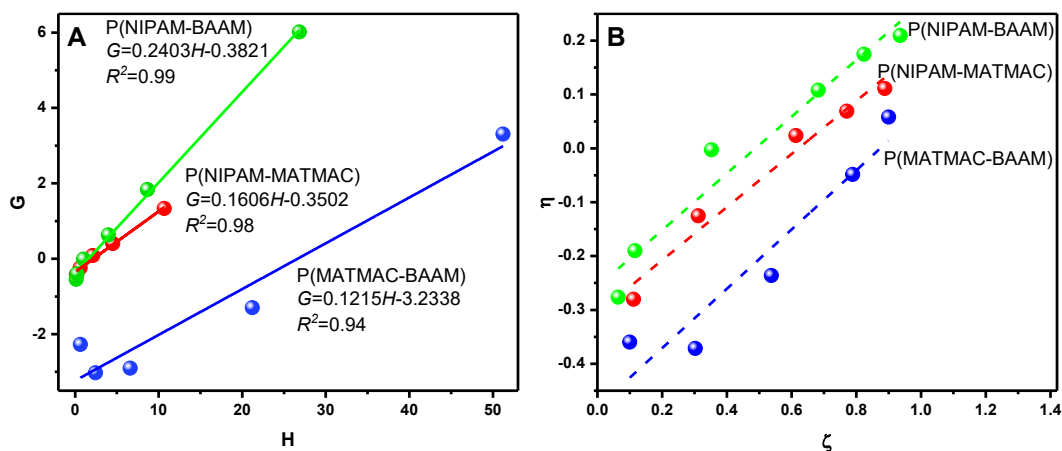


**Figure 4-4** Determination of binary reactivity ratios using (A) Fineman-Ross method and (B) Kelen-Tudos method



The Kelen-Tudos method prevents this drawback, and can scatter the data well over the full range of conditions. This method uses two more transformation variables in addition to  $G$  and  $H$

$$\eta = \frac{G}{\alpha + H}$$

$$\zeta = \frac{H}{\alpha + H}$$

The Fineman-Ross equation can now be written as

$$\eta = \left( r_1 + \frac{r_2}{\alpha} \right) \zeta - \frac{r_2}{\alpha} \quad \text{Equation 4-3}$$

where

$$\alpha = \sqrt{H_{\text{minimum}} \times H_{\text{maximum}}}$$

Figure 4-4B shows the plots of  $\eta$  vs  $\zeta$  for p(NIPAM-MATMAC), p(MATMAC-BAAM), and p(NIPAM-BAAM) that can lead to the calculation of  $r_1$  and  $r_2$ . The reactivity ratios of monomers obtained by Kelen-Tudos method are listed in Table 4-3.

**Table 4-3** Summary of binary reactivity ratios calculated by Fineman-Ross, Kelen-Tudos, and Yezrielev - Brokhina – Roskin method

Copolymer	Non-linear fitting*	Fineman-Ross method	Kelen-Tudos method	Yezrielev - Brokhina - Roskin method
$r_{N,M}$	0.407	0.350	0.410	0.425
$r_{M,N}$	0.180	0.160	0.186	0.181
$r_{M,B}$	3.493	3.233	2.732	2.463
$r_{B,M}$	0.123	0.121	0.069	0.044
$r_{N,B}$	0.475	0.382	0.476	0.469
$r_{B,N}$	0.270	0.240	0.269	0.230

\* Non-linear fitting was carried out using *MATLAB*. Subscripts: N = NIPAM, M = MATMAC, B = BAAM.

We also estimated the reactivity ratios by the YBR method that basically transforms the Mayo-Lewis equation into a symmetrical form. The solution of the YBR equation was used to calculate the reactivity ratios, as per Equation 4-4 and Equation 4-5.

$$\eta = \left(r_1 + \frac{r_2}{\alpha}\right) \zeta - \frac{r_2}{\alpha} \quad \text{Equation 4-4}$$

$$r_2 = \frac{A_1 C_2 + n C_1}{A_1 A_2 - n^2} \quad \text{Equation 4-5}$$

where

$$A_1 = \sum_{i=1}^n \frac{X_i^2}{Y_i}$$

$$A_2 = \sum_{i=1}^n \frac{Y_i}{X_i^2}$$

$$C_1 = \sum_{i=1}^n X_i \left(1 - \frac{1}{Y_i}\right)$$

$$C_2 = \sum_{i=1}^n \frac{Y_i}{X_i} \left(\frac{1}{Y_i} - 1\right)$$

$$X = \frac{f_1}{f_2}$$

$$Y = \frac{F_1}{F_2}$$

and  $n$  is the number of data points.

The reactivity ratios obtained by the YBR method are listed in Table 4-3. Reactivity ratios of MATMAC-BAAM and BAAM-MATMAC pairs varied with the calculation method because the graphical methods rely on accurately determining the slope and intercept, and the reactivity of MATMAC with BAAM was small.

We further used the non-linear least square fitting method using *MATLAB* to fit the experimental data in Mayo-Lewis equation (Equation 4-1). The obtained fitting parameters are the reactivity ratios and are listed in Table 4-3. We used the reactivity ratios obtained by the non-linear least square fitting method to estimate the terpolymer composition because of its accuracy over other methods. However, we reported the data of other methods because the majority of past literature used either all or one of those methods to calculate the reactivity ratios. Therefore, readers/researchers can use and compare the literature values with those reported in this work.

#### 4.3.3 Estimation of Terpolymer Composition

We used the Alfrey-Goldfinger equation to estimate the terpolymer composition. (Hagiopol, 1999) The Alfrey-Goldfinger equation estimates the composition of a terpolymer from the knowledge of the binary reactivity ratios.

$$\overline{F}_N : \overline{F}_M : \overline{F}_B = f_N \lambda_N : f_M \lambda_M : f_B \lambda_B \quad \text{Equation 4-6}$$

$$\lambda_N = \left\{ \frac{f_N}{r_{B,N} r_{M,N}} + \frac{f_M}{r_{M,N} r_{B,M}} + \frac{f_B}{r_{B,N} r_{M,B}} \right\} \times \left\{ f_N + \frac{f_M}{r_{N,M}} + \frac{f_B}{r_{N,B}} \right\} \quad \text{Equation 4-7}$$

$$\lambda_M = \left\{ \frac{f_N}{r_{N,M} r_{B,N}} + \frac{f_M}{r_{N,M} r_{B,M}} + \frac{f_B}{r_{B,M} r_{N,B}} \right\} \times \left\{ f_M + \frac{f_N}{r_{M,N}} + \frac{f_B}{r_{M,B}} \right\} \quad \text{Equation 4-8}$$

$$\lambda_B = \left\{ \frac{f_N}{r_{N,B} r_{M,N}} + \frac{f_M}{r_{M,B} r_{N,M}} + \frac{f_B}{r_{N,B} r_{M,B}} \right\} \times \left\{ f_B + \frac{f_N}{r_{B,N}} + \frac{f_M}{r_{B,M}} \right\} \quad \text{Equation 4-9}$$

$$\overline{F}_N = \left( 1 + \frac{\lambda_M f_M + \lambda_B f_B}{\lambda_N f_N} \right)^{-1} \quad \text{Equation 4-10}$$

$$\overline{F}_M = \left( 1 + \frac{\lambda_N f_N + \lambda_B f_B}{\lambda_M f_M} \right)^{-1} \quad \text{Equation 4-11}$$

$$\overline{F}_B = 1 - \overline{F}_N - \overline{F}_M \quad \text{Equation 4-12}$$

where,  $f$  is the monomer fraction in the feed,  $F$  is the monomer fraction in terpolymer, and  $r$  is reactivity ratio. N, M, and B stand for NIPAM, MATMAC, and BAAM, respectively.

We synthesized three terpolymers that contain 40 mol % of the cationic monomer ( $F_M = 0.4$ ) and varying fractions of BAAM ( $F_B = 0.05, 0.10,$  and  $0.15$ ). The monomer fractions required in the feed to synthesize these three terpolymers were determined using Equation 4-10, 4-11, and 4-12. The composition of these three terpolymers was particularly chosen to study the effect of varying hydrophobicity ( $F_B$ ) on MFT flocculation, while the cationicity ( $F_M$ ) remained the same.

The value of 40% for the cationicity was based on the flocculation of MFT using p(NIPAM-MATMAC) with varying MATMAC content. Figure 4-5 shows the initial settling rate (ISR) and capillary suction time (CST) of MFT treated with p(NIPAM-MATMAC) having varying fractions of MATMAC.

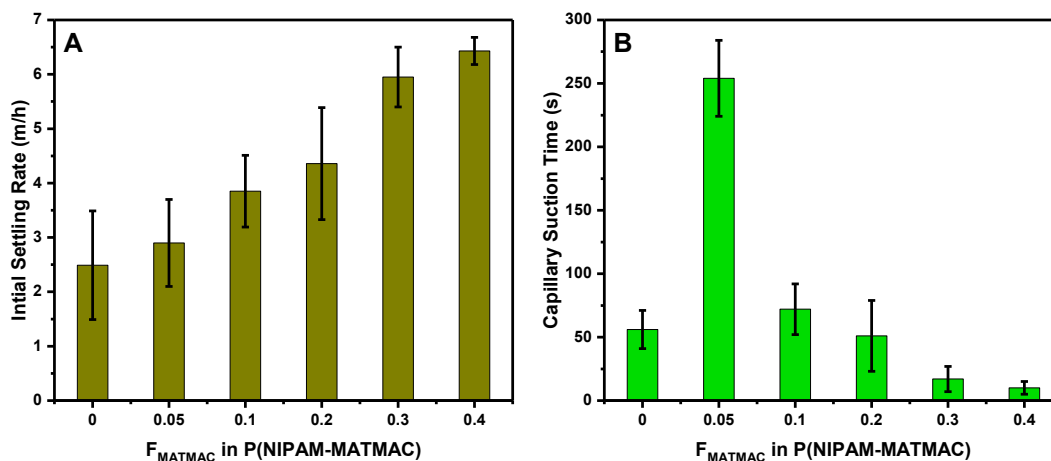


**Figure 4-5** Determination of optimum fraction of MATMAC monomer in p(NIPAM-MATMAC) based on (A) initial settling rate of MFT and (B) capillary suction time of MFT sediments

ISR increased continuously with increasing MATMAC fraction in the copolymer, whereas CST decreased with increasing MATMAC fraction, down to an outstanding value of  $10 \text{ s} \pm 5$ . Absence of MATMAC in copolymer ( $F_M = 0$ ) resulted in CST of  $56 \text{ s} \pm 15$  whereas 5 mol % addition of MATMAC ( $F_M = 0.05$ ) in copolymer increased the CST to  $254 \pm 29$ . The change in chemical composition and molecular weight caused by the addition of 5 mol % MATMAC resulted in the CST increase. We could further increase the fraction of MATMAC to try for further increase ISR, but our aim was to synthesize a terpolymer, and the reactivity of MATMAC with BAAM is low ( $r_{M,B} = 2.810$ ). Therefore, we synthesized three terpolymers

containing 40 mol % cationicity ( $F_M = 0.4$ ) and varying fractions of BAAM. The fraction of each monomer in the feed and in the terpolymer for these three flocculants is listed in Table 4-4.

**Table 4-4** Feed and terpolymer composition of the flocculants used in this study

Terpolymer	NIPAM		MATMAC		BAAM	
	$f$	$F$	$f$	$F$	$f$	$F$
P(NMB-5)	0.75	0.55	0.22	0.40	0.03	0.05
P(NMB-10)	0.71	0.50	0.23	0.40	0.06	0.10
P(NMB-15)	0.66	0.45	0.24	0.40	0.1	0.15

#### 4.3.4 Floc Formation in MFT using Terpolymers

We monitored the floc formation in MFT, from the addition of the terpolymer until the flocs became stable. The real-time evolution of floc size in MFT using different dosages of P(NMB-5), P(NMB-10), and P(NMB-15) is shown in Figure 4-6. Here, the numbers 5, 10, and 15 in P(NMB- $x$ ) denotes the mol % BAAM in the terpolymer.

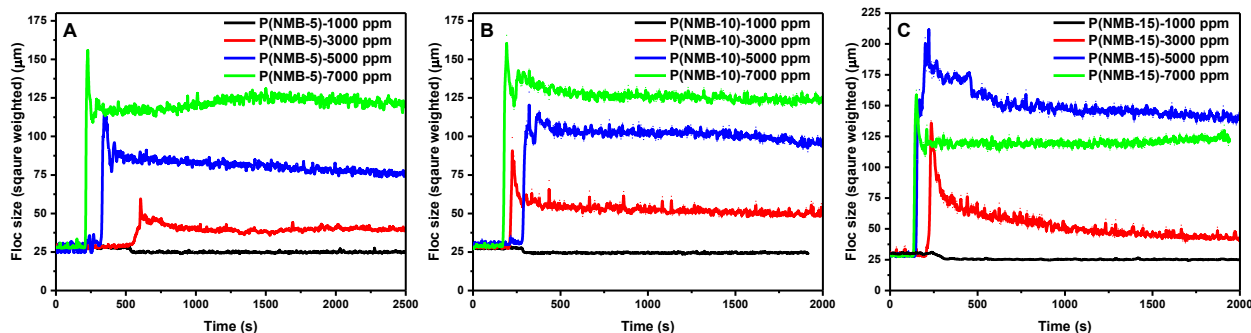


**Figure 4-6** Real-time evolution of floc size in MFT using different dosages of (A) P(NMB-5), (B) P(NMB-10), and (C) P(NMB-15). The number  $x$  in P(NMB- $x$ ) denotes the mol % BAAM in the terpolymer.

In the case of P(NMB-5), the flocs formed quickly as we increased the flocculant dosage. Before the addition of the flocculant, the average MFT particle/floc size was approximately 25  $\mu\text{m}$ ; however, the addition of 1000 ppm of all P(NMB) flocculants slightly reduced average particle sizes, instead of increasing it. This was a consistently reproducible behavior. The reduction in

particle size may have occurred because at lower dosages, the flocculant molecules may act as spacers between clay platelets, and possibly break/exfoliate some clay aggregates. Since the terpolymers contain MATMAC, which has quaternary ammonium cations, they may lower the surface energy of clay by cation exchange and improve their wetting characteristics. (Liu, 2007; Sinha Ray and Okamoto, 2003) This phenomenon was only observed at lower dosages, and the terpolymer acted as flocculant as well as coagulant at higher dosages.

We also observed that the flocs grew quickly as we increased the flocculant dosage from 1000 to 7000 ppm. For example, P(NMB-5) formed flocs at 560 s, 325 s, and 208 s at dosages of 3000, 5000, and 7000 ppm respectively. The probability of polymer adsorbing on the particle surfaces increased with higher dosages because the cationic MATMAC unit favored attractive interactions with the negatively charged clay surfaces. It may be possible that BAAM also participated in additional hydrophobic interactions with fugitive bitumen and organic coatings. Zhang et al. also reported that the hydrophobic interactions increase the adsorption of flocculant chains on clay particles in MFT. (Zhang et al., 2017)

The initial slope of the curve after flocculant addition correlates with the rate of adsorption of flocculant onto the clay surfaces. Gregory and Barany described the polymer adsorption rate onto clay particles as the rate of disappearance of polymer from the solution. (Gregory and Barany, 2011) Equation (13) describes the characteristic adsorption time at a given concentration of solid particles in the system (Gregory, 2009)

$$t_{ads} = \frac{-\ln(1-x)}{k N} \quad \text{Equation 4-13}$$

where  $x$  is the fraction of polymer required to adsorb onto the clay surface to initiate the flocculation,  $k$  is the collision frequency between polymer chains and clay particles per unit time, and  $N$  is the initial number of particles per unit volume in the suspension. The required polymer fraction  $x$  decreases with increasing polymer dosage, while the collision frequency  $k$  remains virtually constant because the viscosity of the suspension does not significantly change during flocculation. Since  $k$  remains constant, the possibility of polymer adsorption on clay surface increases with increase in polymer dosage. Equation 4-13 evidently explains our observations on why increasing polymer dosage reduces the characteristics adsorption time. The flocculants

reported in this study showed an excellent rate of adsorption except at 3000 ppm of P(NMB-5), which could not form flocs quickly.

After flocculant addition, the flocs grew to their largest size, and finally dropped slightly to their steady state dimensions. Increasing the dosage of all P(NMB) flocculants increased floc sizes, except for 7000 ppm of P(NMB-15). We attribute this observation to flocculant overdosing, causing steric and electrostatic repulsion among the flocs, which is also reflected in ISR and CST measurements discussed later below. The sharp initial increase in floc size indicates that the polymer chains quickly neutralized and partially bridged several clay particles. As they polymer chains relax on the clay surfaces, the flocs become more compact and their size decreases slightly. We may speculate that when the flocculant is used at lower dosages, the formed flocs are more loosely bound together, and break more easily under shearing forces. When higher dosages are used, on the other hand, the flocs are held together more strongly by the flocculant, and are less sensitive to shearing effects during the FBRM experiments.

Figure 4-7 compares the size distributions of MFT and stable flocs made with different dosages of the flocculants. Higher dosages shifted the floc size distribution to higher averages. Two main aspects are important when interpreting these distributions: their peak positions (or averages), and peak areas (or heights). When larger flocs are formed, the FBRM distribution moves to the right, but their peak height and areas indicate the number of such larger flocs in the system.

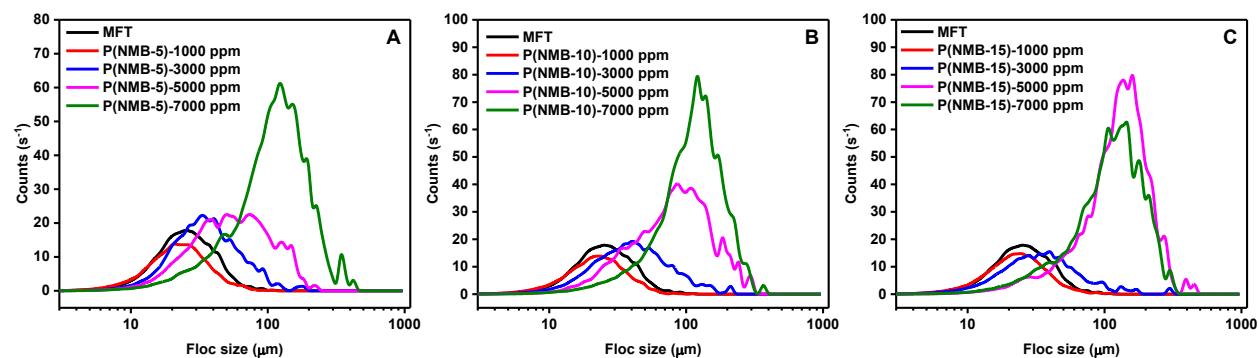


**Figure 4-7** Floc size distribution using different dosages of (A) P(NMB-5), (B) P(NMB-10), and (C) P(NMB-15). The number  $x$  in P(NMB- $x$ ) denotes the mol% BAAM in terpolymer

The distributions that were shifted to larger floc size but remained at same intensity revealed that, at such dosages, flocs grow in size but smaller particles also exist in the system. On the other hand, the distributions that were significantly shifted to larger size and exhibit considerably higher intensity showed that the majority of smaller particles in MFT were incorporated in flocs and caused a large shift. The comparison of distributions with an increase in dosage revealed that the flocs grew randomly where smaller flocs could combine with other smaller flocs or larger flocs. Combination of only smaller flocs shifts the lower end of the distribution to higher size but the combination of both smaller and larger flocs shifts both ends of the distribution to a larger size. The distribution corresponding to 1000 ppm (red curves) of all P(NMB) flocculants was suppressed as compared to MFT (black curves) which explained our previous observations that lower dosage of the P(NMB) flocculant acted as a spacer and exfoliated the clays. The comparison of distributions of 5000 and 7000 ppm of P(NMB-15) (Figure 4-7C) agreed well with the observation in Figure 4-6C. 7000 ppm of P(NMB-15) was found to be a clear overdose that possibly caused steric and electrostatic repulsion among the flocs.

#### 4.3.5 Initial Settling Rate of MFT using Terpolymers

Figure 4-8 shows how ISR varies as a function of flocculant hydrophobicity and dosage. In general, ISR decreases when the terpolymer becomes more hydrophobic.

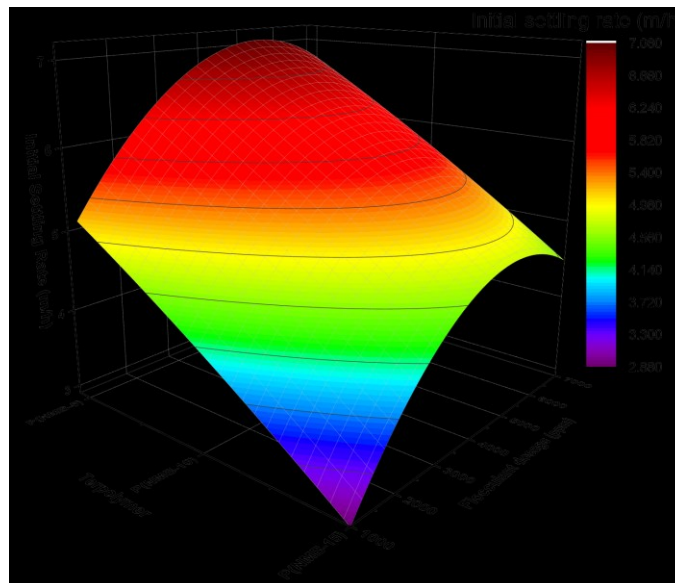


**Figure 4-8** Surface response of initial settling rate as a function of varying BAAM content in terpolymer and its dosage



The lowest ISR of 2.9 m/h was measured for 1000 ppm of P(NMB-15), which still compares well with ISRs reported in the literature for similar systems. (Gumfekar et al., 2017; Gumfekar and Soares, 2018; Liu et al., 2017; Lu et al., 2016; Vajihinejad et al., 2017; Zhang et al., 2017) ISR increased when more flocculant was added, but it further decreased at 7000 ppm. MFT flocculated at approximately 7.0 m/h using 5000 ppm of P(NMB-5), which was the highest ISR obtained in this study. ISR considerably decreased after the optimum dosage of 5000 ppm of P(NMB-15). This observation was expected and is consistent with the previous the results shown in Figure 4-6C and Figure 4-7C. The existence of optimum dosage and a further decrease in ISR confirmed the overdosing of flocculant in the system. Lu and coworkers reported similar observations for dewatering of fine particle suspensions. (Lu et al., 2015) In this situation, possibly excessive polymer chains significantly covered the clay surface resulting into the less free surface for further interaction and floc formation. Such correlation between free surface and probability of flocculation is given by Equation 4-14.

$$P_f = \Phi(1 - \Phi) \quad \text{Equation 4-14}$$

where,  $P_f$  is the probability of flocculation and  $\Phi$  is the surface coverage by flocculant. The probability of flocculation ( $P_f$ ) is largest when  $\Phi = 0.5$ . Therefore, we speculate that 7000 ppm of P(NMB-15) might have covered more than half of the particles' surface leading to reduced ISR due to repulsion among particles. This repulsion was mainly attributed to brush-like conformation polymer on particle's surface rather than loop-like conformation that leads to flocculation. (Lu et al., 2016) Wang et al. confirmed the similar observations of a decrease in ISR by measuring the surface potential of the particles covered by the flocculant. (Wang et al., 2014) It is important to control the flocculant dosage because the adsorption of polymer chains on particle's surface generates a strong steric force that is usually difficult to overcome.

#### 4.3.6 Capillary Suction Time: The Ability to Dewater Sediments

Capillary suction time (CST) was used to measure the dewaterability of the settled sediments. A lower CST value indicates more efficient sediments dewatering. As expected, CST was reduced with an increase in flocculant hydrophobicity (BAAM fraction in the terpolymer) because once the MFT solids settle, the hydrophobic flocculant chains can more easily expel the water out of sediments. Figure 4-9 shows how increasing the BAAM fraction in terpolymer facilitated

sediments dewatering. Several previous publications demonstrated the role of hydrophobicity in densifying sediments. (Gumfekar et al., 2017; Gumfekar and Soares, 2018; Lu et al., 2015; Rooney et al., 2016)

Interestingly, flocculant dosage had a significant impact on CST. Increasing the dosage of all terpolymers from 1000 to 7000 ppm reduced the CST at least 10 times, from approximately 200 to 20 s. The higher charge densities and hydrophobicities resulting from higher flocculant dosages jointly affect CST. Vajihinejad et al. demonstrated that copolymer composition and charge density regulate the dewaterability of MFT flocs. (Vajihinejad et al., 2017) Botha et al. reported that increasing the dosage of highly hydrophilic flocculants, such as polyacrylamide (PAM), increased the CST of MFT sediments because the PAM trapped significant amounts of water in the flocs. (Botha et al., 2017) We did not observe such behavior, and CST continued to decrease even for the highest dosage of all P(NMB) flocculants.

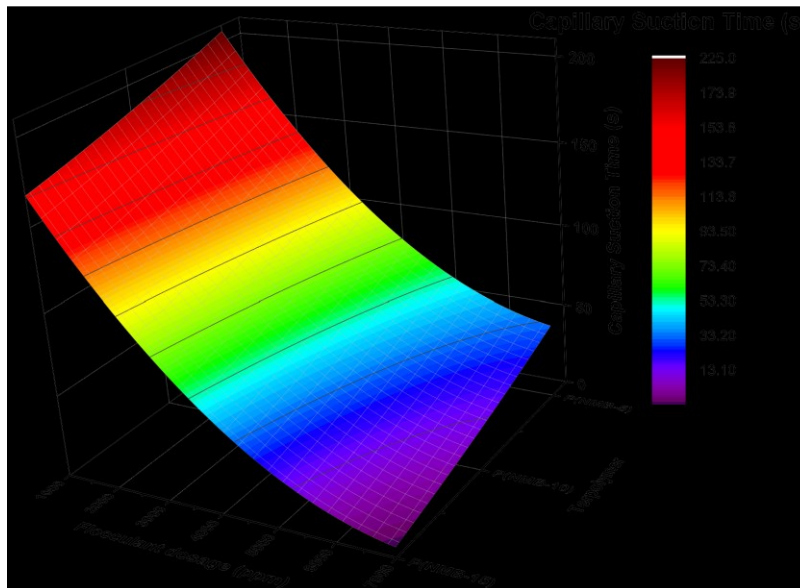


**Figure 4-9** Surface response of capillary suction time as a function of varying BAAM content in terpolymer and its dosage

A thoughtful design of the molecular architecture of P(NMB) can significantly avoid the negative effects of flocculant overdosing on CST. Figure 4-10 shows the flocculation images of MFT consolidation.

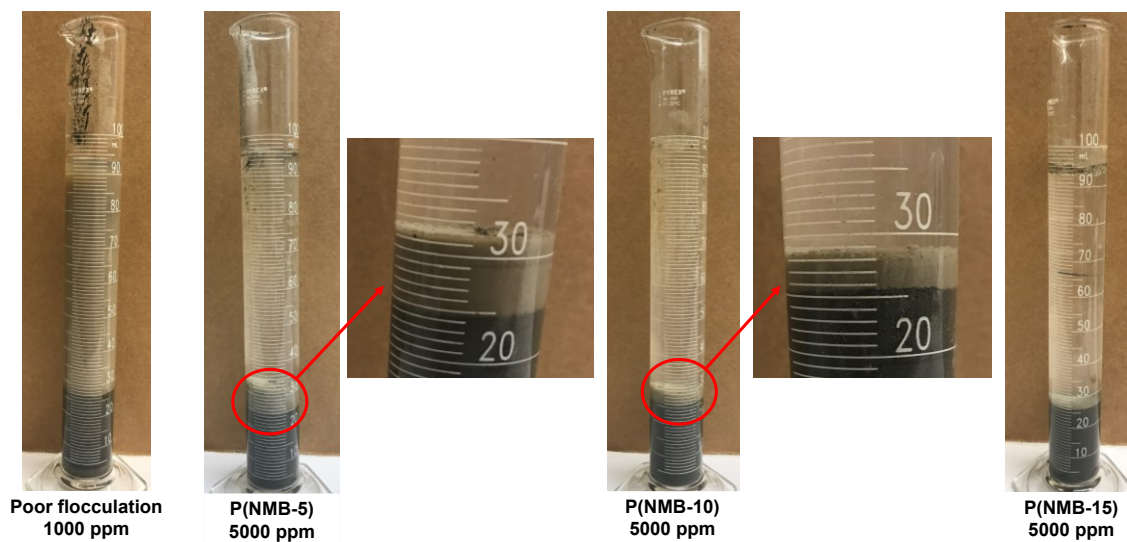


**Figure 4-10** Flocculation images MFT using 5000 ppm of p(NIPAM-MATMAC-BAAM) terpolymer with varying fractions of BAAM. The first cylinder (left) is an example of poor flocculation due to insufficient dosage. Magnified images show the compaction of swelling clays (grey-colored).

In general, 1000 ppm was identified as insufficient dosage to dewater, resulting in poor flocculation as seen in the first cylinder (Figure 4-10). Further images show the mudline heights and supernatant clarity using 5000 ppm of all P(NMB) flocculants. It can be seen that the supernatants are very clear and significant solid compaction occurred. A closer look at mudline heights revealed the interesting information about dewatering and solids compaction. Magnified images related to P(NMB-5) and P(NMB-10) showed the presence of grey-colored layer, which was attributed to swelling clays (illite, smectite and layered illite-smectite) in MFT. (Kaminsky, 2008) This layer was not compact and held significant water within, due to cation exchange abilities of the clays. However, the height of the grey-colored layer reduced with increase in hydrophobicity of the flocculant and 5000 ppm of P(NMB-15) did not show the presence of the grey layer. We speculate that the hydrophobic segments of the flocculant could expel the water through such swelling clays that significantly reduced the CST of sediments.

#### 4.4 Conclusions

Although several polymers have been used as flocculants to treat various types of wastewater, they do not perform well when used with oil sands mature fine tailings (MFT). We synthesized a

series of ternary multifunctional polymer poly(*N*-isopropyl acrylamide/ 2-(methacryloyloxy) ethyl trimethyl ammonium chloride/ *N*-*tert*-butylacrylamide) [p(NIPAM-MATMAC-BAAM)] in which, MATMAC offered cationicity and BAAM offered hydrophobicity to the flocculant to address the unusual challenges encountered in MFT treatment. A simple free radical polymerization with co-solvents enabled the synthesis with varied functionality that can be extended to other comonomers as well. The cationicity of the terpolymer flocculant was optimized to 40 mol % based on preliminary flocculation experiments. We varied the hydrophobicity (in terms of mol % of BAAM) of the flocculant from 5 to 15 mol % and showed how it affected flocculation and dewatering performance. The flocculation performance was assessed in terms of floc average size and stability, kinetics of floc formation, initial settling rate (ISR), and capillary suction time (CST). In this study, the highest floc size of 200  $\mu\text{m}$ , highest ISR of 7 m/h and lowest CST of 20 s was achieved. In this work, we developed a framework to systematically synthesize multifunctional polymers and demonstrated the application of such hydrophobically-modified cationic terpolymers to effectively dewater oil sands tailings.

## References

- Botha, L., Davey, S., Nguyen, B., Swarnakar, A.K., Rivard, E., Soares, J.B.P., 2017. Flocculation of oil sands tailings by hyperbranched functionalized polyethylenes (HBfPE). *Miner. Eng.* 108, 71–82. doi:10.1016/j.mineng.2017.02.004
- Botha, L., Soares, J.B.P., 2015. The Influence of Tailings Composition on Flocculation. *Can. J. Chem. Eng.* 93, 1514–1523. doi:10.1002/cjce.22241
- Candau, F., Selb, J., 1999. Hydrophobically-modified polyacrylamides prepared by micellar polymerization. *Adv. Colloid Interface Sci.* 79, 149–172. doi:10.1016/S0001-8686(98)00077-3
- Escudero Sanz, F.J., Ochoa Gómez, J.R., Sasia, P.M., De Apodaca, E.D., Río, P., 2007. Synthesis of cationic flocculants by the inverse microemulsion copolymerization of acrylamide with 60% 2-acryloxyethyltrimethyl ammonium chloride in the monomer feed. I. Initiation by ammonium persulfate/sodium disulfite redox system. *J. Appl. Polym. Sci.* 103, 2826–2836. doi:10.1002/app.24381
- Fineman, M., Ross, S.D., 1950. Linear method for determining monomer reactivity ratios in copolymerization. *J. Polym. Sci.* 5, 259–262. doi:10.1002/pol.1950.120050210
- Franks, G., Sepulveda, C., Jameson, G., 2006. pH sensitive flocculation: Settling rates and sediment densities. *AIChE J.* 52, 2774–2782. doi:10.1002/aic
- Gregory, J., 2009. Monitoring particle aggregation processes. *Adv. Colloid Interface Sci.* 147–148, 109–123. doi:10.1016/j.cis.2008.09.003
- Gregory, J., Barany, S., 2011. Adsorption and flocculation by polymers and polymer mixtures. *Adv. Colloid Interface Sci.* 169, 1–12. doi:10.1016/j.cis.2011.06.004
- Gumfekar, S.P., Rooney, T.R., Hutchinson, R.A., Soares, J.B.P., 2017. Dewatering Oil Sands Tailings with Degradable Polymer Flocculants. *ACS Appl. Mater. Interfaces* 9, 36290–36300. doi:10.1021/acsami.7b10302
- Gumfekar, S.P., Soares, J.B.P., 2018. A novel hydrophobically-modified polyelectrolyte for enhanced dewatering of clay suspension. *Chemosphere* 194, 422–431. doi:10.1016/j.chemosphere.2017.12.009
- Hagiopol, C., 1999. Copolymerization. Springer US, Boston, MA. doi:10.1007/978-1-4615-4183-7
- Kaminsky, H.A.W., 2008. Characterization of an Athabasca oil sand ore and process streams. University of Alberta.
- Kelen, T., Tüd[Otilde]s, F., 1975. Analysis of the Linear Methods for Determining Copolymerization Reactivity Ratios. I. A New Improved Linear Graphic Method. *J. Macromol. Sci. Part A - Chem.* 9, 1–27. doi:10.1080/00222337508068644
- Lee, K.E., Morad, N., Poh, B.T., Teng, T.T., 2011. Comparative study on the effectiveness of hydrophobically modified cationic polyacrylamide groups in the flocculation of kaolin.

Desalination 270, 206–213. doi:10.1016/j.desal.2010.11.047

- Liao, Y., Zheng, H., Qian, L., Sun, Y., Dai, L., Xue, W., 2014. UV-Initiated Polymerization of Hydrophobically Associating Cationic Polyacrylamide Modified by a Surface-Active Monomer: A Comparative Study of Synthesis, Characterization, and Sludge Dewatering Performance. *Ind. Eng. Chem. Res.* 53, 11193–11203. doi:10.1021/ie5016987
- Liu, B., Zheng, H., Deng, X., Xu, B., Sun, Y., Liu, Y., Liang, J., 2017. Formation of cationic hydrophobic micro-blocks in P(AM-DMC) by template assembly: characterization and application in sludge dewatering. *RSC Adv.* 7, 6114–6122. doi:10.1039/C6RA27400E
- Liu, P., 2007. Polymer modified clay minerals: A review. *Appl. Clay Sci.* 38, 64–76. doi:10.1016/j.clay.2007.01.004
- Lu, H., Wang, Y., Li, L., Kotsuchibashi, Y., Narain, R., Zeng, H., 2015. Temperature- and pH-Responsive Benzoboroxole-Based Polymers for Flocculation and Enhanced Dewatering of Fine Particle Suspensions. *ACS Appl. Mater. Interfaces* 7, 27176–27187. doi:10.1021/acsami.5b09874
- Lu, H., Xiang, L., Cui, X., Liu, J., Wang, Y., Narain, R., Zeng, H., 2016. Molecular Weight Dependence of Synthetic Glycopolymers on Flocculation and Dewatering of Fine Particles. *Langmuir* 32, 11615–11622. doi:10.1021/acs.langmuir.6b03072
- Mayo, F.R., Lewis, F.M., 1944. Copolymerization. I. A Basis for Comparing the Behavior of Monomers in Copolymerization; The Copolymerization of Styrene and Methyl Methacrylate. *J. Am. Chem. Soc.* 66, 1594–1601. doi:10.1021/ja01237a052
- Quinlan, P.J., Tam, K.C., 2015. Water treatment technologies for the remediation of naphthenic acids in oil sands process-affected water. *Chem. Eng. J.* 279, 696–714. doi:10.1016/j.cej.2015.05.062
- Rooney, T.R., Gumfekar, S.P., Soares, J.B.P., Hutchinson, R.A., 2016. Cationic Hydrolytically Degradable Flocculants with Enhanced Water Recovery for Oil Sands Tailings Remediation. *Macromol. Mater. Eng.* 301, 1248–1254. doi:10.1002/mame.201600230
- Sakohara, S., Nishikawa, K., 2004. Compaction of TiO<sub>2</sub> suspension utilizing hydrophilic/hydrophobic transition of cationic thermosensitive polymers. *J. Colloid Interface Sci.* 278, 304–9. doi:10.1016/j.jcis.2004.06.002
- Sawalha, O., Scholz, M., 2007. Assessment of Capillary Suction Time (CST) Test Methodologies. *Environ. Technol.* 28, 1377–1386. doi:10.1080/09593332808618898
- Senaputra, A., Jones, F., Fawell, P.D., Smith, P.G., 2014. Focused beam reflectance measurement for monitoring the extent and efficiency of flocculation in mineral systems. *AIChE J.* 60, 251–265. doi:10.1002/aic.14256
- Sinha Ray, S., Okamoto, M., 2003. Polymer/layered silicate nanocomposites: a review from preparation to processing. *Prog. Polym. Sci.* 28, 1539–1641. doi:10.1016/j.progpolymsci.2003.08.002

- Vajihinejad, V., Guillermo, R., Soares, J.B.P., 2017. Dewatering Oil Sands Mature Fine Tailings (MFTs) with Poly(acrylamide- co -diallyldimethylammonium chloride): Effect of Average Molecular Weight and Copolymer Composition. *Ind. Eng. Chem. Res.* 56, 1256–1266. doi:10.1021/acs.iecr.6b04348
- Vedoy, D.R.L., Soares, J.B.P., 2015. Water-soluble polymers for oil sands tailing treatment: A Review. *Can. J. Chem. Eng.* 93, 888–904. doi:10.1002/cjce.22129
- Wang, C., Han, C., Lin, Z., Masliyah, J., Liu, Q., Xu, Z., 2016. Role of Preconditioning Cationic Zetag Flocculant in Enhancing Mature Fine Tailings Flocculation. *Energy and Fuels* 30, 5223–5231. doi:10.1021/acs.energyfuels.6b00108
- Wang, Y., Kotsuchibashi, Y., Liu, Y., Narain, R., 2014. Temperature-Responsive Hyperbranched Amine-Based Polymers for Solid–Liquid Separation. *Langmuir* 30, 2360–2368. doi:10.1021/la5003012
- Yang, Z.L., Gao, B.Y., Li, C.X., Yue, Q.Y., Liu, B., 2010. Synthesis and characterization of hydrophobically associating cationic polyacrylamide. *Chem. Eng. J.* 161, 27–33. doi:10.1016/j.cej.2010.04.015
- Zhang, D., Thundat, T., Narain, R., 2017. Flocculation and Dewatering of Mature Fine Tailings Using Temperature-Responsive Cationic Polymers. *Langmuir* 33, 5900–5909. doi:10.1021/acs.langmuir.7b01160
- Zheng, H., Sun, Y., Zhu, C., Guo, J., Zhao, C., Liao, Y., Guan, Q., 2013. UV-initiated polymerization of hydrophobically associating cationic flocculants: Synthesis, characterization, and dewatering properties. *Chem. Eng. J.* 234, 318–326. doi:10.1016/j.cej.2013.08.098
- Zhu, Y., Tan, X., Liu, Q., 2017. Dual polymer flocculants for mature fine tailings dewatering. *Can. J. Chem. Eng.* 95, 3–10. doi:10.1002/cjce.22628

## Chapter 5

### Dewatering Oils Sands Tailings with Degradable Polymer Flocculants

We synthesized hydrolytically-degradable cationic polymers by micellar radical polymerization of a short-chain polyester macromonomer, polycaprolactone choline iodide ester methacrylate (PCL<sub>2</sub>ChMA) with two polyester units, and used them to flocculate oil sands mature fine tailings (MFT). We evaluated the flocculation performance of the homopolymer and copolymers with 30 mol% acrylamide (AM) by measuring initial settling rate (ISR), supernatant turbidity, and capillary suction time (CST) of the sediments. Flocculants made with trimethylaminoethyl methacrylate chloride (TMAEMC), the monomer corresponding to PCL<sub>n</sub>ChMA with  $n = 0$ , have improved performance over poly(PCL<sub>2</sub>ChMA) at equivalent loadings due to their higher charge density per gram of polymer. However, MFT sediments flocculated using the PCL<sub>2</sub>ChMA-based polymers are easier to dewater (up to an 85% reduction in CST) after accelerated hydrolytic degradation of the polyester side chains. This study demonstrates the potential of designing cationic polymers that effectively flocculate oil sands tailings ponds, and also further dewater the resulting solids through polymer degradation.

#### 5.1 Introduction

Oil sands deposits in the province of Alberta, Canada, are the third largest oil reserve in the world, with deposits estimated at 28.3 billion cubic meters. (Kaminsky, 2008; Masliyah et al., 2004) While they are a strategic resource for Canada, North America, and the global market, the extraction of bitumen from oil sands form waste tailings that cause technical and environmental problems. Typically, these tailings contain negatively charged clays (~30-35 wt. %), water (~65 wt. %), and residual bitumen (3-5 wt. %). (Botha and Soares, 2015) The composition and water chemistry of the mixture makes it harder to dewater the tailings than to recover oil from the reserves. Although coarse particles settle quickly, the fine particles remain suspended in water, with no further dewatering for many decades. The two main challenges associated with such *mature fine tailings* (MFT) are: *i*) to recover water trapped in the tailings, and *ii*) to further dewater the sediments obtained after the flocculation. Existing technologies use water-soluble

---

A version of this chapter has been published as S. P. Gumfekar, T. R. Rooney, R. A. Hutchinson, J. B. P. Soares, "Dewatering Oils Sands Tailings with Degradable Polymer Flocculants", ACS Applied Materials & Interfaces, 9 (41), 36290-36300, 2017



polymers, such as polyacrylamide (PAM) and its ionic copolymers, to form large flocs and induce solid-liquid separation. However, due to the strong water-affinity of PAM, the flocs entrap a significant amount of water, forming low-shear strength sediments that are difficult to dewater.

Research in this area aims at improving dewatering technology and developing more effective flocculating agents. Several researchers have investigated combinations of chemical and mechanical dewatering techniques, such as flocculation using polymers followed by filtration or centrifugation, as summarized in a recent article. (Masliyah, J. H, Czarnecki, J. A, Xu, 2011) Such energy-intensive combinations are useful only if the sediments recovered have little water, and the transportation of these high-solid content mixtures to tailing ponds remains a challenge.

Ionic polyelectrolyte copolymers, in which at least one of the monomers is anionic and/or cationic, are promising candidates for MFT treatment. (O'Shea et al., 2011a; Sakohara et al., 2011; Vajihinejad et al., 2017) Cationic polymers are favored because the clays suspended in tailings have net negative charges. Flocculation of clays occurs through a combination of bridging and charge neutralization: the (generally high molecular weight) polymer chains 'bridge' the solid particles in suspension, while the randomly distributed ionic monomers in the polymer chains neutralize the charges on the clay surface. However, the flocs still contain water because the polymer flocculants are hydrophilic. Some researchers are addressing this problem by synthesizing hydrophobically-modified polymers, (Botha et al., 2017; Isik et al., 2016; Li et al., 2013; Li and Kwak, 2004; Reis et al., 2016; Zheng et al., 2014) because hydrophobic groups present in the flocculant cause the sediments to retain less water.

Functionalization of hydrophobic polymers such as polyethylene is one of the approaches used to maintain a balance between hydrophilicity and hydrophobicity within the polymer. (Botha et al., 2017) Often, such hydrophobically-modified polymers are synthesized by surfactant-assisted emulsion polymerization or precipitation polymerization. (Sakohara et al., 2013; Zhu et al., 2007) However, the presence of surfactants in the flocculants is undesirable as they form froth during flocculation.

A range of innovative flocculating agents are currently under investigation, including thermo-responsive, pH-responsive, and CO<sub>2</sub>-switchable copolymers synthesized with cationic

monomers, as well as hydrophobically modified monomers. (Deng et al., 1996; O’Shea et al., 2011b; Pinaud et al., 2012; Sakohara et al., 2011; Sand et al., 2010; Zheng et al., 2013) While using polymers that can reversibly change from hydrophilic (for efficient flocculation of the MFT) to hydrophobic (for efficient release of the water remaining in the sediment) is promising, significant challenges remain regarding their implementation in the field. For example, thermoresponsive polymers such as poly (*N*-isopropylacrylamide) (PNIPAM) and its ionic derivatives have been studied due to their temperature-sensitive switching from hydrophilic to hydrophobic, but the associated energy costs limit their large-scale implementation. (Li et al., 2009) pH-Responsive polymers that switch from hydrophilic to hydrophobic upon the addition of acid or alkali are also attractive, but the amount of acid or base required to alter pH may limit their practical applications. (Franks, 2005) Researchers have also explored the use of CO<sub>2</sub>-switchable flocculants such as *N, N, N', N'*-tetramethyl-1,4-diaminobutane, imidazolyl cellulose nanocrystals, long-chain alkylamidines and poly(dimethylamino)ethyl methacrylate (PDMAEMA) (Chen et al., 2013; Eyley et al., 2015) that become cationic upon exposure to CO<sub>2</sub>. However, considering the 176 km<sup>2</sup> area occupied by tailings ponds in Alberta, mass transfer limitations associated with purging CO<sub>2</sub> and maintaining those conditions may not be a feasible solution either.

The approach we report herein involves the synthesis of a flocculant that is cationic and water-soluble in the ‘as-synthesized’ state, but contains polyester grafts that degrade by hydrolysis to increase the flocculant’s hydrophobicity. In a previous publication we showed that this strategy enhanced the dewaterability of “model tailings” sediments consisting of pure kaolin. (Rooney et al., 2016) The novel material is produced by radical polymerization of a short-chain polyester macromonomer, polycaprolactone choline iodide ester methacrylate (PCL<sub>*n*</sub>ChMA), where *n* is the average number of polycaprolactone units in the methacrylic ester side chain. The cationic tips of the resulting comb-like polymer accelerate the settling rate of the oil sands tailings, while partial hydrolysis of the polyester grafts expose the hydrophobic segments, increasing the dewaterability of the sediments over time.

The structure of the macromonomer, shown in Figure 5-1, differs from trimethylaminoethyl methacrylate chloride (TMAEMC) by the degradable polyester spacers in the side chain. Radical polymerization of the macromonomer yields comb-polymers whose hydrolytic degradability is

controlled by the number and type of polyester units specified in the macromonomer synthesis, a feature which has been demonstrated for similar hydroxyl-functionalized polyester macromonomers investigated for biomedical applications. (Colombo et al., 2014; Ferrari et al., 2011) The number and type of polyester units in the macromonomer structure also affects the hydrophobicity and cation density of the resulting comb-polymer; such properties can be further modified through copolymerization with a common water-soluble monomer such as acrylamide (AM).

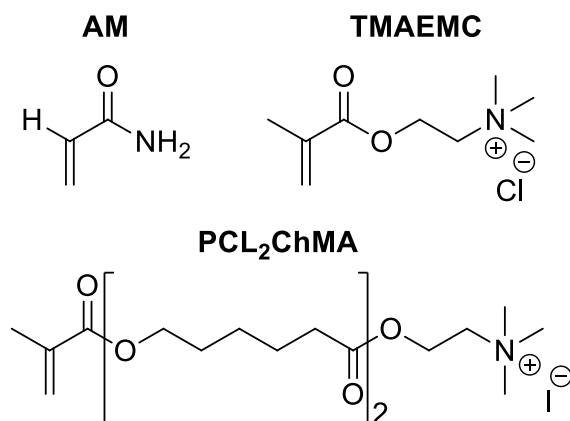


**Figure 5-1** Chemical structures of cationic macromonomers used in radical homopolymerizations, as well as respective copolymerizations with acrylamide (AM) to produce flocculants investigated in this work.

In this work, we systematically investigated the influence of the copolymer structure on MFT flocculation behavior to follow up the initial promising results demonstrated with kaolin, (Rooney et al., 2016) the principle clay component in oil sands mixtures. The average number of degradable units in the polyester side chain was adjusted to 2 to afford a homopolymer with both appreciable cationic density and hydrophobic content, while still maintaining its hydrolytic degradation characteristics. As well as moving to the more challenging MFT system, we investigated the influence of copolymerizing PCL<sub>2</sub>ChMA with AM to further control polymer charge density and hydrophobicity; a recent study determined that 60-70 mol % AM content in a cationic polymer provides a good balance of flocculation parameters. (Vajihinejad et al., 2017) The main feature of poly(PCL<sub>2</sub>ChMA) – its increased hydrophobicity in response to hydrolysis which does not require external triggers such as changes in temperature or pH – is demonstrated

by comparing the MFT sediment dewaterability, as characterized by capillary suction time, immediately following flocculation to that after one week of accelerated degradation. In addition, the performance of the material is compared to that of a structurally similar cationic copolymer produced by radical copolymerization of trimethylaminoethyl methacrylate chloride (TMAEMC) as well as non-ionic AM (see Figure 5-1), whose hydrolytic degradation products are not expected to elicit an increase in polymer hydrophobicity.

## 5.2 Materials and Methods

### 5.2.1 Materials

$\epsilon$ -Caprolactone (CL, 97 %), 2-(dimethylamino)ethanol (De, >98 %), stannous octoate ( $\text{Sn}(\text{oct})_2$ , 92.5-100.0 %) triethylamine (TEA,  $\geq 99.5$  %), basic alumina (Brockmann 1), methyl iodide ( $\text{ICH}_3$ , 99 %), acrylamide (AM,  $\geq 99$  %), 2,2-azobis(2-methylpropionamide)dihydrochloride (V-50, 97 %), [2-(methacryloyloxy)ethyl] trimethylammonium chloride solution (TMAEMC; 80 wt % in  $\text{H}_2\text{O}$ ), and nonionic polyacrylamide (PAM, 5-6 million Da) were purchased from Sigma Aldrich and used as received. Tetrahydrofuran (THF, >99 %, ACP Chemicals), anhydrous diethyl ether ( $\geq 99.0$  %, ACP Chemicals), chloroform-d ( $\text{CDCl}_3$ , 99.8 % D, Cambridge Isotope Laboratories), and deionized water (Millipore Synergy water purification system) were used as received. Methacryloyl chloride (MACl, 97 %, Sigma Aldrich) was distilled immediately before use to remove reactive dimers. Mature fine tailings (MFT, 33.5 % solids by mass) obtained from Syncrude Canada Ltd. were diluted to 5 wt. % total solids for the flocculation experiments.

### 5.2.2 Macromonomer Synthesis

The synthesis of polycaprolactone 2-(*N,N*-dimethylamino)ethyl ester methacrylate ( $\text{PCL}_2\text{DeMA}$ ) with average  $n = 2$  was performed according to a previously published procedure modified to reduce reaction time. (Rooney et al., 2016) A catalyst/monomer mixture with molar ratio of 1:500 consisting of  $\text{Sn}(\text{oct})_2$  (35.1 mg, 86.6  $\mu\text{mol}$ ) and CL (4.94 g, 43.3 mmol), was loaded into a 50 mL sealed round bottom flask, purged with nitrogen, and then heated to 130 °C. De (1.93 g, 21.7 mmol) was added to the catalyst/monomer mixture by syringe and allowed to react for 110 min at 130 °C to yield polycaprolactone 2-(*N,N*-dimethylamino)ethyl ester ( $\text{PCL}_2\text{De}$ ) with

number average  $n = 2.0$  and CL conversion  $\approx 94\%$  (as determined by  $^1\text{H-NMR}$  in Figure A-1 in Appendix A).

Next,  $\text{PCL}_2\text{De}$  (6.87 g, 21.7 mmol -OH) was dissolved in 35 mL tetrahydrofuran (THF) in a sealed 3 neck 100 mL round bottom flask, to which 24 mL triethylamine (TEA, 173.0 mmol) was then added. The solution was cooled to  $0\text{ }^\circ\text{C}$  using an ice bath, bubbled with  $\text{N}_2$  for 10 minutes, and then 2.8 mL freshly distilled methacryloyl chloride (MACl, 28.2 mmol) diluted by 4.1 mL THF was fed over 1 h using a glass syringe. The reaction mixture was maintained at  $0\text{ }^\circ\text{C}$  for an additional 3 h, filtered to remove the TEA salt, and then passed through a column of basic alumina. The solvent was evaporated in vacuo to afford 6.19 g  $\text{PCL}_2\text{DeMA}$  in 74 % yield including MACl impurities (Figure A-2 in Appendix A).

$\text{PCL}_2\text{DeMA}$  (6.19 g, 16.1 mmol) was dissolved in 140 mL diethyl ether, cooled to  $0\text{ }^\circ\text{C}$ , and kept under constant flow of nitrogen. Approximately 3 mL  $\text{ICH}_3$  was injected by syringe then the reaction was allowed to warm to room temperature and proceed for 48 h. The white waxy precipitate was collected by filtration, washed three times with 200 mL cold diethyl ether, and dried under vacuum at  $40\text{ }^\circ\text{C}$  overnight to afford 5.48 g polycaprolactone choline iodide ester methacrylate ( $\text{PCL}_2\text{ChMA}$ ) (77 % methylation yield). According to the  $^1\text{H-NMR}$  in Figure A-3, the  $\text{PCL}_2\text{ChMA}$  macromonomer contains up to 10 mol% [2-(methacryloyloxy)ethyl] trimethylammonium iodide (TMAEMI), resulting from unreacted De initiator in the ROP step.

All  $^1\text{H}$  NMR characterizations (Figures A-1 to A-3 in Appendix A) were performed on a Bruker Avance instrument operating at 400 MHz. The oligomeric distributions of  $\text{PCL}_2\text{DeMA}$  (Figure A-4 in Appendix A) was assessed by size exclusion chromatography (SEC). The SEC setup consists of a Waters 2960 separation module instrument with a Waters 410 differential refractometer (DRI), and four Styragel columns (HR 0.5, 1, 3, 4) maintained at  $35\text{ }^\circ\text{C}$  with distilled THF as eluent at  $0.3\text{ mL}\cdot\text{min}^{-1}$ . The DRI detector was calibrated using 14 narrow poly(MMA) standards (302–853,000 Da).

### 5.2.3 Macromonomer Copolymerization

For homopolymerizations, 2.0 g of  $\text{PCL}_2\text{ChMA}$  or TMAEMC was dissolved in 18.0 g  $\text{H}_2\text{O}$  (containing 0.22 and 0.40 wt. % V-50, respectively) and bubbled with nitrogen for 1 h in a sealed 50 mL single neck round bottom flask. Next, the solution was heated to reaction temperature ( $70$

°C for PCL<sub>2</sub>ChMA and 50 °C for TMAEMC), allowed to proceed for 2 h then cooled to room temperature and stored in the refrigerator at 4 °C. The same conditions were employed for the copolymerizations, except that the 2.0 g of (macro)monomer loading comprised an amount of AM which corresponds to 30 mol % cationic (macro)monomer (56 and 76 wt. % TMAEMC and PCL<sub>2</sub>ChMA relative to AM, respectively). In all cases, quantitative conversions were verified by complete disappearance of the vinyl signals by <sup>1</sup>H NMR.

Each synthesized polymer was characterized using gel permeation chromatography (GPC) (1260 Infinity Multi-Detector GPC/SEC System, Agilent Technologies) to analyze its molecular weight and dispersity (*D*). The GPC system included three detectors: viscosity, refractive index, and light scattering. Two columns (TKS gel G6000PW XL-CP) connected in series were used to obtain a better resolution and increase the detection range of the instrument. The system was calibrated using polyethylene oxide standards provided by Agilent Technologies. Water containing 0.3 M sodium nitrate and 0.01 M monosodium phosphate was used as a mobile phase for the analysis.

#### *5.2.4 Ex-situ Degradation Study*

The poly(PCL<sub>2</sub>ChMA) homopolymer was diluted to 1 wt. % in H<sub>2</sub>O and held at 85 °C for 1 day increments then cooled to room temperature for analysis before increasing the temperature back to 85 °C. The solution pH was measured using a Mettler Toledo SevenExcellence pH meter, while dispersion size was determined with a Malvern Zetasizer Nano ZS (size range 0.3 nm –10 µm) at 25 °C with backscattering optics (173°), using a 4 mW He–Ne (633 nm) laser. All measurements were made in quartz cuvettes, and the reported sizes represent an intensity average of at least 30 scans.

#### *5.2.5 Oil Sands Flocculation Tests*

The flocculant dosage was varied from 1000 to 5000 parts per million (ppm), on a weight basis relative to the weight of solids in the MFT. Figure 5-2 shows the schematic illustrating the flocculation procedure. For each flocculation test, 100 mL of a 5 wt. % solids mixture was prepared by diluting MFT with deionized water. The pH of the diluted MFT varied between 7.9 and 8.2. This suspension was transferred to a 250 mL baffled beaker (7 cm diameter and 9.5 cm

height), in which the polymer flocculant and the MFT suspension were mixed in two stages using 316 stainless steel 4-blade propeller with 2 inch diameter. 1) the MFT mixture was stirred at 600 rpm for 2 min, followed by addition of the desired quantity of the polymer flocculant; 2) mixing was maintained at 600 rpm for an additional 5 min, followed by 2 min at 300 rpm. The mixture was immediately transferred to a 100 mL graduated cylinder, and the mudline (solid-liquid interface) was recorded during the initial settling period.

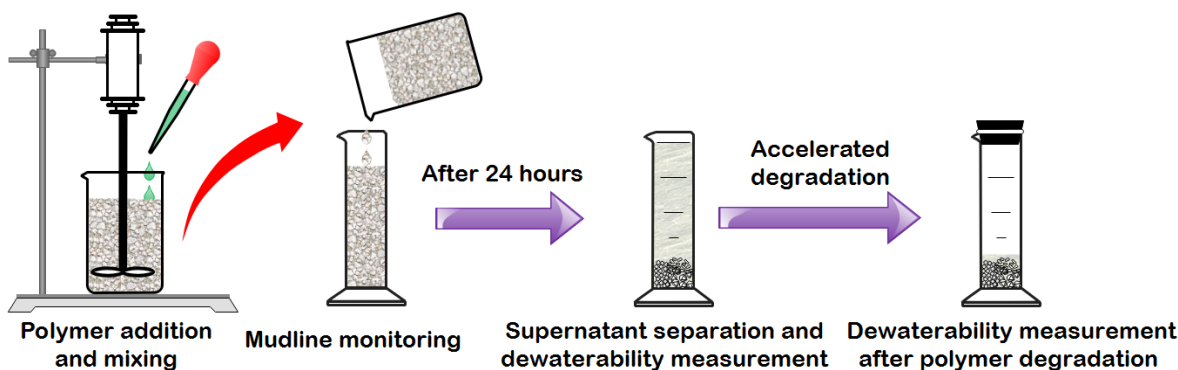


**Figure 5-2** Schematic representation of the flocculation procedure.

Three measurements were used to assess flocculation performance of the polymers: 1) initial settling rate (ISR), 2) supernatant turbidity, and 3) capillary suction time (CST). ISR was calculated from the slope of an initial linear portion of the settling curves. (Franks et al., 2009; Li et al., 2007) An ISR value of zero was assigned when the MFT suspension did not start settling upon addition of the polymer solution. After the settling, the supernatant was collected and the turbidity was measured using a Hach 2100AN turbidimeter. Capillary suction time (CST) of the consolidated solids remaining after removal of the supernatant was measured with a Triton Electronics 319 multi-purpose CST apparatus. Pipetting a fixed volume of the solids suspension gave more reproducible results than scooping an equivalent portion of the sediment with a spatula.

The remaining sediments were kept in the graduated cylinder, which was sealed with a rubber cork to prevent water from evaporating. The mixture was held at 85 °C for 1 week to allow the accelerated *in situ* degradation of the polymer within the sediments. The CST of these samples

was measured after one week to assess the effect of polymer degradation on the dewaterability of the sediments.

The morphology of the solids in the sediments obtained after flocculation, as well as the raw MFT, were analyzed using cryo-field emission-scanning electron microscope (FE-SEM). The samples were prepared by lyophilizing the raw MFT and the sediments followed by gold coating of 8 nm using Denton Gold Sputter Unit. FE-SEM images were obtained using a Zeiss Sigma FESEM w/ EDX and EBSD at accelerating voltage of 10 kV using an *inlens* detector.

## 5.3 Results and Discussion

### 5.3.1 Synthesis of PCL<sub>2</sub>ChMA and TMAEMC-based Polymers

All four cationic copolymers were synthesized by batch radical polymerization in aqueous solution. Although TMAEMC and AM polymerize in solution, the added hydrophobicity of the PCL spacers makes PCL<sub>2</sub>ChMA a reactive surfactant, which, in an aqueous environment, propagates by micellar polymerization. (Rooney et al., 2016) While all polymers have similar number average molecular weights ( $M_n$ ) (Table 5-1), the four copolymers differ primarily in their charge densities which is defined during the macromonomer synthesis step and is independent of the number of cationic (macro)monomers in the final homopolymer.

**Table 5-1** Polymer charge densities, molecular weight averages and dispersities (effective values relative to PEO calibration). Copolymers contain 70 mol % AM

Polymer	Charge Density (mmol/g)	$M_n$ (g/mol)	$M_w$ (g/mol)	$\mathcal{D}$
poly(PCL <sub>2</sub> ChMA)	1.9	430,000	770,000	1.79
poly(PCL <sub>2</sub> ChMA-AM)	1.4	522,000	939,600	1.80
poly(TMAEMC)	4.8	364,000	625,000	1.72
poly(TMAEMC-AM)	2.7	456,000	842,000	1.82

With a repeat unit with molecular weight of 207.7 Da, the charge density of the poly(TMAEMC) is 4.8 mmol/g, more than double the 1.9 mmol/g of the poly(PCL<sub>2</sub>ChMA), which has an average repeat unit with molecular weight of 527 Da. The cationic charges of poly(PCL<sub>2</sub>ChMA),



however, are located farther away from the chain backbone due to the comb-like structure formed by polymerization of the macromonomer. The charge densities are reduced to 2.7 mmol/g for poly(TMAEMC-*co*-AM) and 1.4 mmol/g for poly(PCL<sub>2</sub>ChMA-*co*-AM) by addition of 70 mol % AM as a comonomer to the chains. The addition of AM also increases the hydrophilicity of the polymer chains. High molecular weight PAM homopolymer was used as a control in this study; although of higher molecular weight (5-6 million Da), the PAM control contained no cationic charges.

The PCL<sub>2</sub>ChMA macromonomer has iodide counterions, whereas the commercial TMAEMC has chloride counterions. As the efficiency of ‘salting-out’ for iodide is greater than for chloride ions, (Mei and Ballauff, 2005) the counterion plays a role in determining the ease of adsorption of charged polymer onto the surface of the clay particles. Moreover, Tian et al. demonstrated that larger monovalent counterions led to a higher cationic density along the polymer chain (*i.e.*, less counterion condensation) and thus to more extended molecular chains that resulted in efficient adsorption on the clay surface without extending loops and tails. (Tian et al., 2007) Therefore, the iodide counterion of poly(PCL<sub>2</sub>ChMA) may be an advantage over polymers with chloride counterions.

### 5.3.2 Effect of Solids Content in MFT

The as-received MFT contained 33.5 wt. % solids and a gel-like consistency that made it difficult to mix with polymer flocculants. Flocculation attempts using the raw MFT did not result in settling of solids. Alamgir et al. have reported similar observations with MFT containing 31 wt. % solids. (Alamgir et al., 2012) Therefore, we diluted the MFT suspension to 2, 5, and 10 wt. % solids to determine the appropriate conditions for carrying out the flocculations. Deionized water was used for all dilutions to reduce the effect of water chemistry on consolidation. A concentration of 5 wt. % MFT solids was considered good enough to measure settling rates: at 2 wt. % MFT, settling was too fast to be measured consistently, and at 10 wt. % the settling was too slow, especially at lower flocculant concentrations.

The Richardson-Zaki batch settling equation (Equation 5-1) for multiparticle systems support these observations, (Masliyah, J. H, Czarnecki, J. A, Xu, 2011)

$$\frac{V_p}{V_{p\infty}} = (1 - \alpha_p)^n \quad \text{Equation 5-1}$$

where  $V_p$  is the settling velocity of a particle in suspension relative to a stationary observer in m/s,  $V_{p\infty}$  is the terminal velocity of a particle in a stagnant fluid,  $\alpha_p$  is the volume fraction of the particles, and  $n$  is an index that depends on Reynolds number, with  $n = 4.7$  in Stokes' regime. According to Equation 5-1, as the fraction of particles in the suspension increases, the settling velocity of particles decreases. In Figure 5-3, the images at 2 and 5 wt. % MFT were taken 30 min after polymer addition, whereas the image at 10 wt. % MFT was taken after 24 h.

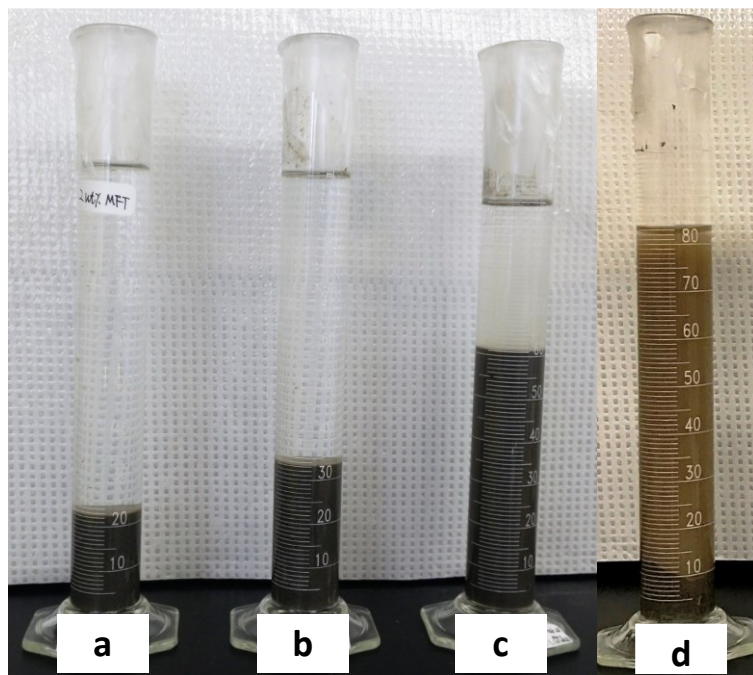


**Figure 5-3** Mudline height after flocculation using 5000 ppm of poly(PCL<sub>2</sub>ChMA) with MFT diluted to: a) 2 wt. % (30 min); b) 5 wt. % (30 min); c) 10 wt. % (24 h); and d) control sample with 5 wt. % MFT and 5000 ppm of PAM (30 min).

These three settling experiments were conducted with 5000 ppm poly(PCL<sub>2</sub>ChMA) as flocculant, and are compared to a 5 wt. % MFT settled with 5000 ppm non-ionic PAM (control) which produced a much more turbid supernatant. In contrast, the cationic poly(PCL<sub>2</sub>ChMA) destabilizes the MFT by adsorbing and neutralizing the negative charges on the clay particles, inducing floc growth and faster settling rate, as well as low supernatant turbidity. This result is supported by other studies which demonstrate that cationic polymers are better flocculants for oil

sands tailings than neutral PAM. (Lu et al., 2015, 2016; Vajihinejad et al., 2017; Wang et al., 2016)

### 5.3.3 Initial Settling Rate (ISR)

Figure 5-4 shows the ISR values measured at polymer dosages varying from 1000 to 5000 ppm. The settling rates for experiments conducted with 1000 ppm of poly(PCL<sub>2</sub>ChMA) as well as 1000 and 2000 ppm of poly(PCL<sub>2</sub>ChMA-AM) were too low to be measured, likely because of the lower charge densities of these polymers combined with their low dosages. Even though ISR does not vary with polymer dosage in a clear trend, all polymers flocculated MFT at reasonable rates. Poly(PCL<sub>2</sub>ChMA) initiated settling at 2000 ppm whereas poly(PCL<sub>2</sub>ChMA-co-AM) initiated settling at 3000 ppm, likely due to its lower charge density.

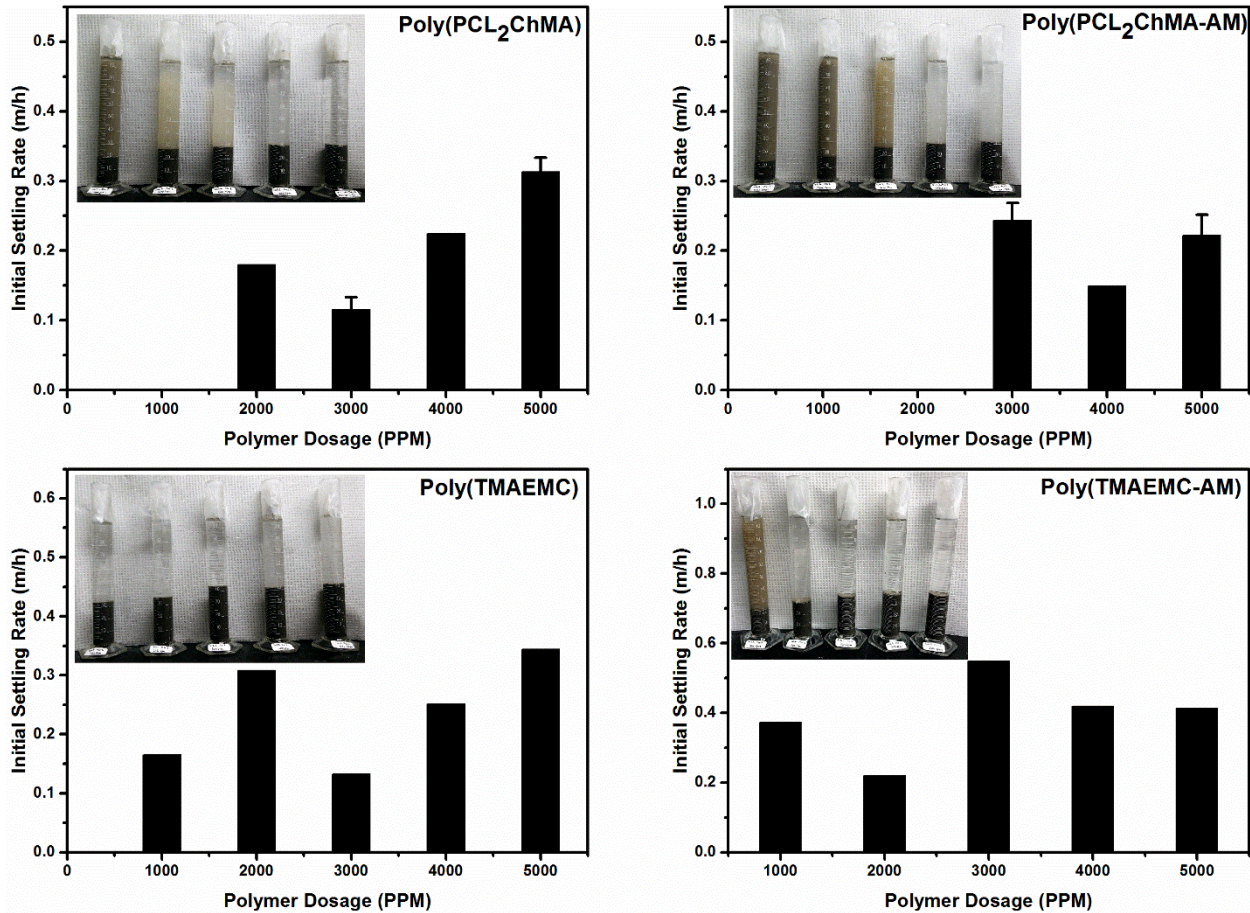


**Figure 5-4** Initial settling rates (ISR) using PCL<sub>2</sub>ChMA and TMAEMC-based polymers and copolymers at varying dosages with 5 wt. % MFT. Missing data for poly(PCL<sub>2</sub>ChMA) and poly(PCL<sub>2</sub>ChMA-AM) denotes insignificant settling. Inset images show the flocculation behavior after 24 h at respective dosages.

In addition, the AM-containing copolymers have increased hydrophilicity, which causes a decrease in floc density (and thus ISR) as the polymer concentration is increased further. The distributions of floc formation using 2000 ppm of poly(PCL<sub>2</sub>ChMA) and poly(PCL<sub>2</sub>ChMA-co-AM) are compared in the Figure A-5 of Appendix A, revealing that poly(PCL<sub>2</sub>ChMA) formed larger flocs than poly(PCL<sub>2</sub>ChMA-co-AM). Although poly(PCL<sub>2</sub>ChMA) and poly(TMAEMC) are structurally similar, the additional hydrophilicity and greater charge density of poly(TMAEMC) aids the adsorption of polymer chains to clay particles. Thus, the combination of charge neutralization and bridging increases the ISR of poly(TMAEMC) compared to poly(PCL<sub>2</sub>ChMA), especially at the lower dosages. The inset pictures in Figure 5-4 were taken after 24 h, but the settling profiles leveled off in less than 30 min. More importantly, the reported ISR values are comparable to those reported for other cationic and anionic polymers in the literature under similar conditions. (Botha et al., 2017; Feng et al., 2017; Lu et al., 2015)

The mudline heights in the insert photographs of Figure 5-4 indicate how compact the sediments are. Numerical values of final mudline heights are presented in Table A-1 of Appendix A. Although the TMAEMC homo and copolymers flocculated MFT even at 1000 PPM, the sediments are not as compact (higher final mudline height) as those flocculated with PCL<sub>2</sub>ChMA polymers, with differences seen throughout the 1000-5000 ppm concentration range. The more compact sediments generated by the PCL<sub>2</sub>ChMA flocculants may be attributed to the hydrophobicity of the polycaprolactone units in the macromonomer.

#### *5.3.4 Supernatant Turbidity*

The clarity of the water recovered after the flocculation was quantified by turbidity measurements, with a lowering of the turbidity indicating that the polymer was better able to neutralize and bridge the fine particles present in MFT. Figure 5-5 shows that the supernatant turbidity drops when the dosage of PCL<sub>2</sub>ChMA polymers increased. The turbidity for poly(PCL<sub>2</sub>ChMA-co-AM) is always higher than that of the homopolymer at the same polymer dosage, a difference that can be attributed to the lower charge density of the copolymer (1.4 versus 1.9 mmol/g). The turbidity also decreases sharply when the dosage of PCL<sub>2</sub>ChMA polymers increases from 3000 to 4000 ppm, with a smaller improvement seen at 5000 ppm.

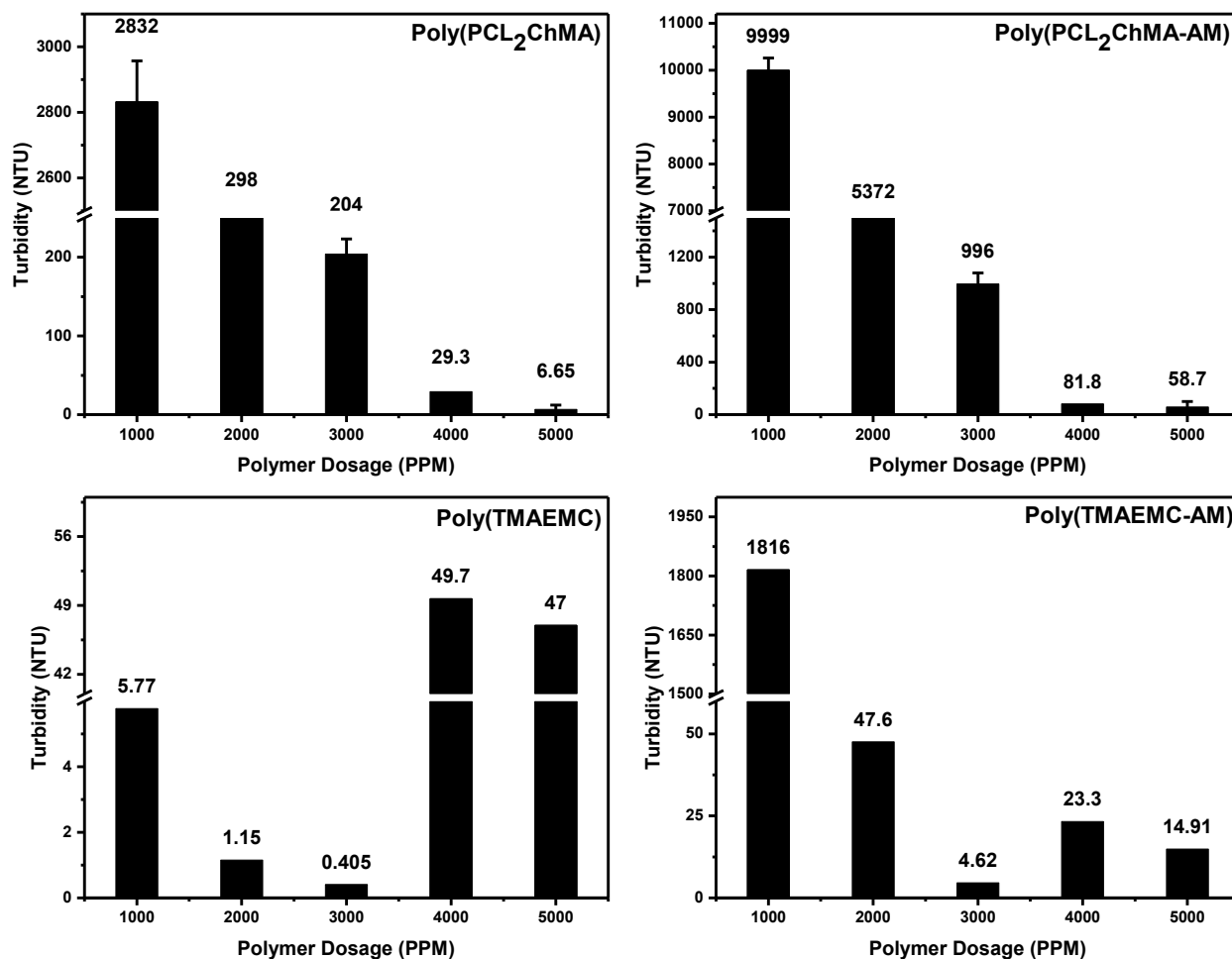


**Figure 5-5** Supernatant turbidity obtained after flocculation of 5 wt. % MFT using PCL<sub>2</sub>ChMA and TMAEMC homopolymers and copolymers at varying dosages. Turbidity values are indicated for each experiment, as the scale varies for each plot; ‘broken’ y-axes are used to visualize the relative changes among the lower turbidity values.

The influence of the dosage of TMAEMC polymers on turbidity differs in important aspects from that of PCL<sub>2</sub>ChMA polymers. With a significantly higher charge density of 4.8 mmol/g, even 1000 ppm of poly(TMAEMC) leads to a turbidity lower than 10 NTU, dropping below 1 NTU at a dosage of 3000 ppm, before increasing at higher polymer dosages. Poly(TMAEMC-co-AM) follows a similar trend, although its lowered charge density leads to higher turbidity at 1000 ppm. In addition, the increase in turbidity seen at 4000 and 5000 ppm for the TMAEMC copolymer is not as large as for the homopolymer. The increased turbidity observed at 4000 and 5000 ppm of the TMAEMC polymers may be attributed to excessive charge density that causes

the restabilization of particles above the optimum dosage, as has been noted by other researchers.(Das et al., 2013) We did not observe this type of behavior when applying the PCL<sub>2</sub>ChMA flocculants within the dosage range we investigated, as the cation charge density was tuned to neutralize clay particles in MFT, which exhibit a native zeta potential of -38 mV. (Lu et al., 2016)

Despite having significantly lower molecular weights than the commercial PAM tested in this investigation, the cationic polymers are effective in overcoming the electrostatic repulsion between negatively charged clay particles, as well as bridging between particles, both necessary features of a successful polymeric flocculating agent. (Liu et al., 2016)

### *5.3.5 Capillary Suction Time and Degradation Study*

While the four cationic polymers tested herein differed in ISR and turbidities (mostly attributable to differences in charge density), they all performed well with the challenging MFT system. The most encouraging finding is that compact sediments and clear supernatants were obtained at relatively low polymer dosages (Reis et al., 2016; Vajihinejad et al., 2017) of less than 5000 ppm (0.5 wt. %).

Capillary suction time (CST) was used to measure the dewaterability of the settled sediment. While a lower CST value indicates more efficient dewatering of sediments, previous studies in our group have shown that the CST of MFT suspensions flocculated with PAM increased for higher polymer dosages because PAM is hydrophilic. (Botha et al., 2017) Thus, we expected that the more hydrophobic PCL<sub>2</sub>ChMA polymers would make sediments with CST values lower than those of TMAEMC polymers. This expectation, however, was not met, as seen in the “Before Degradation” results in Figure 5-6: all sediments flocculated with poly(TMAEMC) and poly(TMAEMC-co-AM) had CST lower than 20 s for dosages at or above 2000 ppm, compared to 20-40 s for the most favourable 4000-5000 ppm levels of poly(PCL<sub>2</sub>ChMA) and poly(PCL<sub>2</sub>ChMA-co-AM). Since the sediments produced with PCL<sub>2</sub>ChMA were already more compact (lower mudlines in Figure 5-4, and thus lower water content), perhaps this is not surprising as it may seem at first sight. The solids content of the sediments measured before and after the flocculation showed that PCL<sub>2</sub>ChMA produced sediments with higher solid content than those produced with TMAEMC (See Table A-2 of Appendix A). Further, we also calculated the

neat Net Water Release (nNWR), which is defined as the percent of the water released that was part of the original MFT sample. The results showed that PCL<sub>2</sub>ChMA-based polymers released more water than TMAEMC-based polymers. Sawalha and Scholz have reported similar observations in their systematic study of varying solids contents on CST. (Sawalha and Scholz, 2007) The CST values measured (also summarized in Table A-3 of Appendix A) are in a similar range as those reported by other researchers for MFTs studied with either lower solid content or higher polymer dosages, (Reis et al., 2016; Zhu et al., 2017) demonstrating that our new polymers are competitive with previous flocculants.

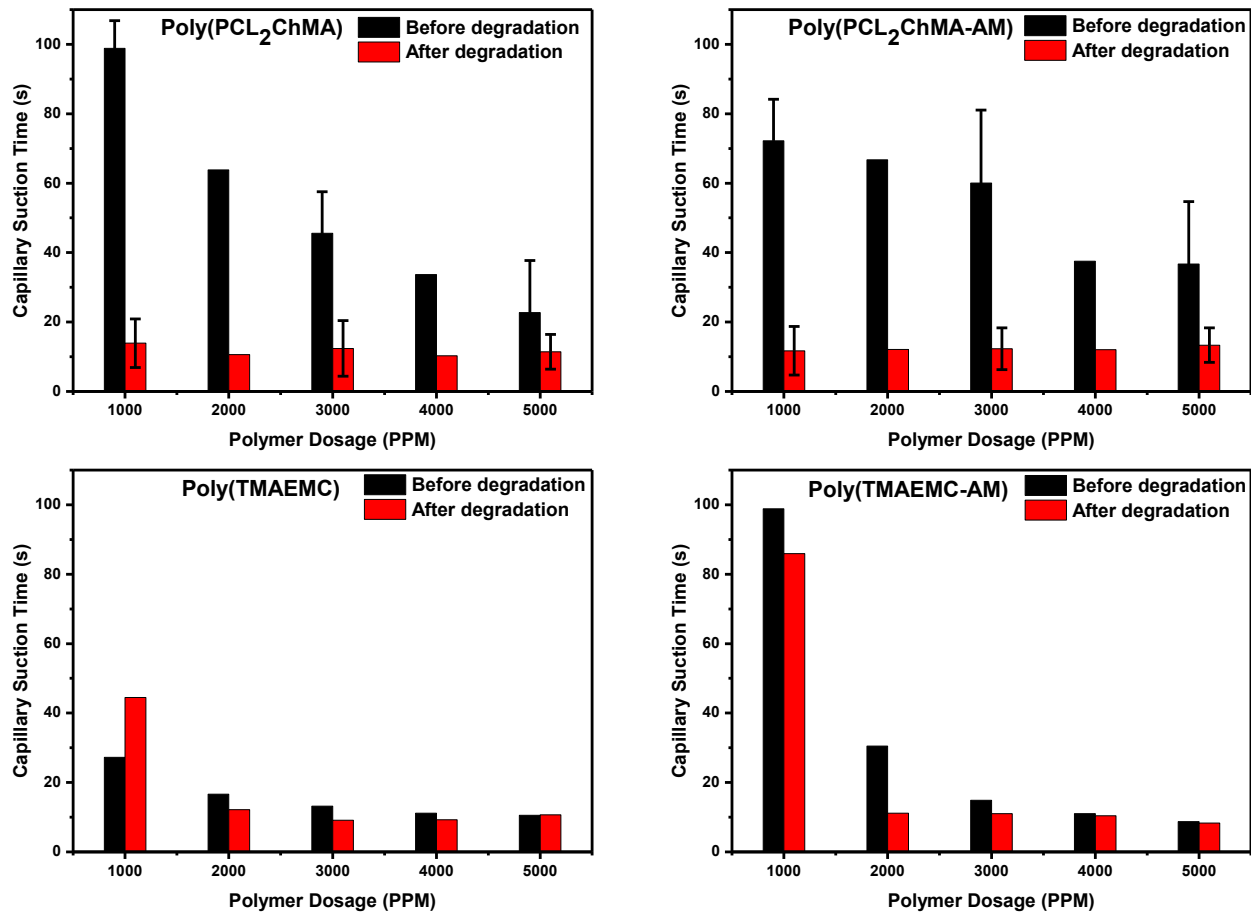


**Figure 5-6** Capillary suction times for sediments obtained from flocculation of 5 wt. % MFT using the four cationic (co)polymers, measured before and after accelerated degradation of the sediments at 85 °C for one week.

For this particular study, the best results are obtained for a poly(TMAEMC) dosage of 3000 ppm, which provides fast settling, very low supernatant turbidity, and a low CST value. Adding AM as a comonomer provides a way to control the charge density (and perhaps cost) of the polymer, but it requires a slightly increased polymer dosage (3000-4000 ppm) to achieve the same performance.

Higher levels of the poly(PCL<sub>2</sub>ChMA), 5000 ppm, are needed to achieve similar results. While the sediment mudlines are noticeably lower than for 3000 ppm poly(TMAEMC), the supernatant turbidities and CST values are slightly higher. However, an important feature of PCL<sub>2</sub>ChMA polymers is that they can degrade. As shown in our previous study, the partial hydrolysis of the polyester units reveals hydrophobic segments that reduced CST of kaolin clay sediments by 30 %. (Rooney et al., 2016) The partial hydrolytic degradation of poly(PCL<sub>2</sub>ChMA) to yield a more hydrophobic flocculant was qualitatively confirmed during an accelerated ex situ degradation study of 1 wt. % flocculant in H<sub>2</sub>O at 85 °C. As summarized by Figure A-6 of Appendix A, the decreasing pH indicates the continuous release of acidic species, while the increasing dispersion size can be attributed to an aggregation mechanism which was described in more detail by our previous work for poly(PCL<sub>3</sub>ChMA). Although a transparent solution at the beginning, the partially hydrolyzed poly(PCL<sub>2</sub>ChMA) completely precipitated from solution after 7 days at 85 °C, whereas poly(PCL<sub>3</sub>ChMA) only precipitated after 9 days – this observation confirms that both the flocculant's hydrophobicity and degradation time can be tuned by the average numbers of polyester units defined in the macromonomer synthesis. Herein we examine the impact of the increased hydrophobicity of poly(PCL<sub>2</sub>ChMA) (co)polymers on the dewaterability of the MFT sediments.

Thus, in addition to measuring CST values of the sediments after 24 h, we repeated these measurements after aging the samples for 1 week at 85 °C, as detailed in the Experimental Section. The results are also summarized in Figure 5-6, providing a direct comparison of the CST of the sediments obtained immediately after the flocculation (before degradation) and after the *in situ* accelerated degradation. A clear contrast can be seen between the sediments flocculated with the PCL<sub>2</sub>ChMA polymers, for which CST decreased remarkably after degradation, and the TMAEMC polymers, which showed no or little change in dewaterability upon aging. In all cases, irrespectively of polymer dosage or whether the sample was



poly(PCL<sub>2</sub>ChMA) or poly(PCL<sub>2</sub>ChMA-co-AM), the CST decreased to 10-15 s after one week of accelerated degradation. More importantly, these results show that increased hydrophobicity in response to hydrolysis can be achieved without the strict requirement of an external trigger such as a temperature or pH change (although these factors can certainly accelerate hydrolytic degradation).

Depending on the pH of the medium, the hydrolysis of the polyester side chains may yield degraded polymer with carboxylate or carboxylic acid functionalized pendant groups. To elicit the increased polymer hydrophobicity in response to hydrolysis documented in our previous work,<sup>27</sup> the majority of the pendant groups must be the carboxylic acid functionalized moieties obtained under acidic conditions. (Rooney et al., 2016) Even though MFT are mildly alkaline (pH 8-9), the extent of hydrolysis after the accelerated degradation test must have been sufficient to sufficiently lower the pH of the local sediment environment enough to obtain polymer with increased hydrophobicity, as inferred by the reduction in CST measurements. On the other hand, in the case of poly(TMAEMC) and poly(TMAEMC-AM) the hydrophobicity of the expected hydrolysis products under acidic conditions, poly(meth)acrylic, should not be significantly different than that of the starting material. Hence, no significant reduction in CST after the accelerated degradation study was measured for TMAEMC-based polymers.

We analyzed our hypothesis of compaction of sediments due to degradation-induced hydrophobicity using cryo-FE-SEM. Images of raw MFT are compared to the sediments obtained after the flocculation and after the degradation of 5000 ppm of poly(PCL<sub>2</sub>ChMA) in Figure 5-7. The untreated MFT exhibited a typical structure consisting of stacked layers of clay platelets bound by strong surface forces (Figure 5-7A), typical of aluminosilicate clays. (Alagha et al., 2013) The sediments of MFT treated with 5000 ppm of poly(PCL<sub>2</sub>ChMA) showed a much less ordered structure, as observed in Figure 5-7B. We speculate that poly(PCL<sub>2</sub>ChMA) synergistically assisted the exfoliation of intercalated clays in untreated MFT, as the cation charge density is sufficient to overcome the interfacial forces among the clays. At the same time, destabilized clay particles are ‘bridged’ together by polymeric chains, forming flocs of approximate dimensions 25 μm × 12 μm, as also observed by magnification of imaging inside the flocs (Figure 5-7C). The size of aggregates formed after the degradation of poly(PCL<sub>2</sub>ChMA) significantly increased to 150 μm × 50 μm (Figure 5-7D). Recently, Zhu et al.

observed similar floc morphology using dual polymer system under cryo-SEM. (Zhu et al., 2017) We observed similar structures in various flocs of varying size taken from the sediment, as shown in Figure A-5 of Appendix A.

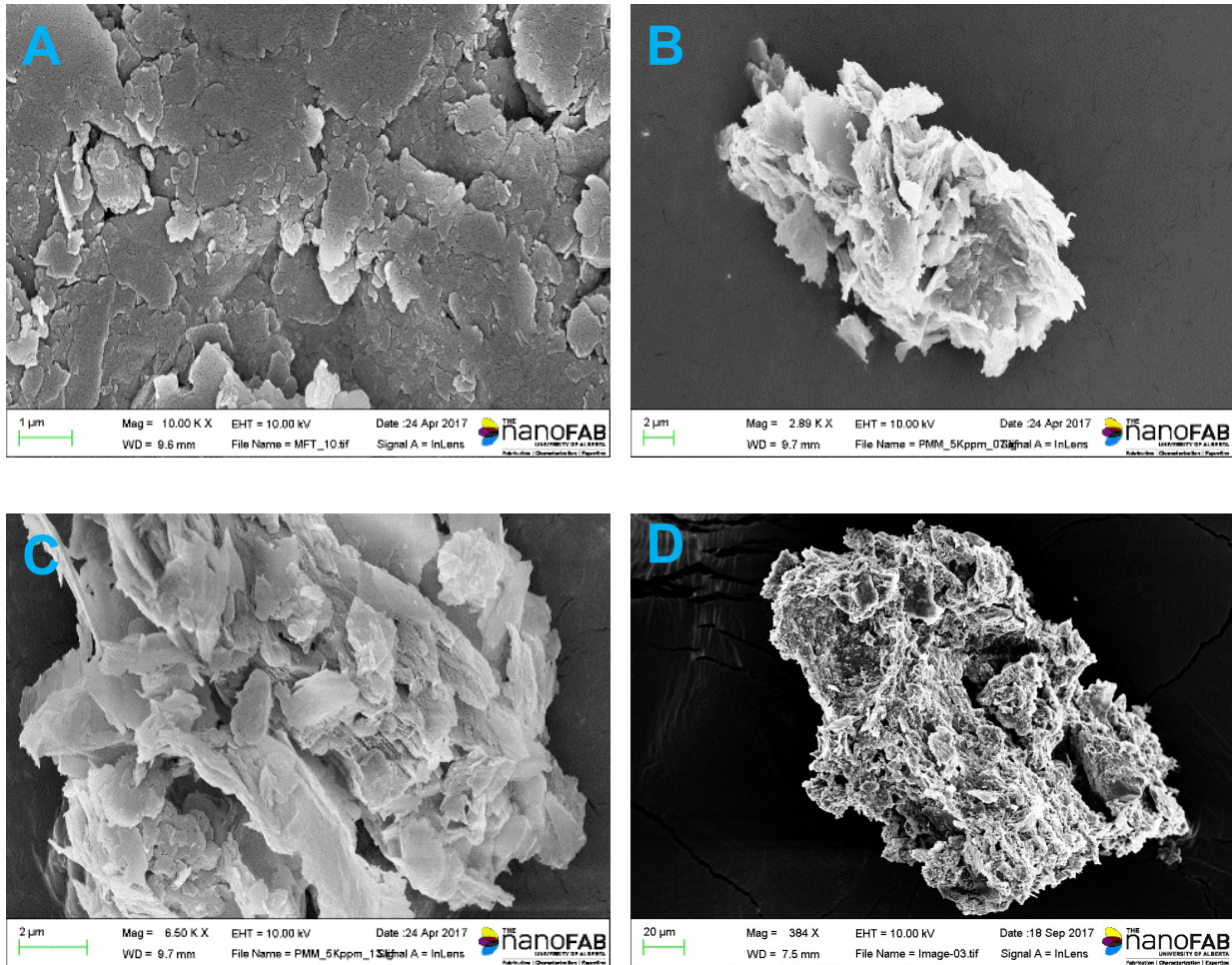


**Figure 5-7** Cryo-FE-SEM images of: A) raw MFT, B) sediments obtained after flocculation C) internal structure of a floc, and D) the sediments obtained after the polymer hydrolysis

### 5.3.6 Significance of the Current Work and Environmental Implication

This work addressed the challenge of efficient dewatering of MFT produced from oil sands extraction. The composition and water chemistry of MFT differs from other wastewater or industrial tailings due to the presence of residual bitumen in the mixture of kaolinite, illite, and interstratified illite-smectite and kaolinite-smectite clays. (Botha and Soares, 2015) Our group

has previously attempted to treat MFT using flocculants designed for other applications such as heavy metal removal, river sludge treatment, flocculation of microalgae and *E. coli*, quartz flocculation etc. (Bharti et al., 2013; Feng et al., 2017; Franks, 2005; Sharma et al., 2006; Zhang et al., 2010). However, these investigations have led us to the conclusion that it is necessary to design flocculants specifically tuned to balance the requirements of rapid settling, recovery of water with low turbidity, and ease of dewaterability of the recovered MFT sediment. Additionally, as MFT composition and physical characteristics vary depending on the bitumen extraction process and location, it is beneficial to develop a synthesis strategy that can be adapted to systematically control flocculant composition and physical characteristics by tuning its hydrophobic content and charge density.

In particular, the PCL<sub>2</sub>ChMA polymers produced in this work show promise for the long-term dewatering of MFT sediments, as the increased hydrophobicity that results from hydrolytic degradation of the polyester groups (previously demonstrated for this polymer only with kaolin (Rooney et al., 2016)) is a successful strategy for increasing the dewaterability (and thus potential land reclamation) of oil sands sediments. The novel feature of this material is that time is the trigger used to alter the properties of the polymer, a much cheaper and easier to implement solution than external triggers previously considered such as changes in temperature or pH, CO<sub>2</sub> bubbling, and UV exposure. While we accelerated the degradation process in this study by holding the sediment at 85 °C for one week, hydrolysis of similar polyester based materials is known to occur at ambient temperature, albeit over a longer time scale. (Ferrari et al., 2011) Thus, hydrolytic degradation provides a simple method to improve consolidation of the tailings sediments naturally, without the need for extra energy or equipment to be employed on the field.

In recent years, researchers have demonstrated that microbial communities in oil sands tailings can degrade the flocculant through a methanogenic process that may produce harmful monomers and oligomers from the polymer backbone. (Penner and Foght, 2010; Siddique et al., 2015) Though there are currently few investigations on this topic, it is expected that further studies will emerge. Thus it is useful to note that the expected degradation products from hydrolysis of our flocculant's PCL pendants, choline iodide and  $\omega$ -hydroxy polycaproic acid oligomers, (Rooney et al., 2016) are widely regarded as biodegradable, with similar materials being considered for biomedical applications. (Agostini et al., 2017) Both degradation products can be metabolized by

cellular mechanisms such as Krebb's cycle or enzymatic action. (Shah et al., 2008) Furthermore, the polymer concentrations required are lower (5000 ppm relative to MFT solids) relative to other cationic flocculants. Considering the promising advantages of our flocculants, we will pursue further investigations of systematically modifying its structure to optimize performance, first by changing the polyester type from polycaprolactone to polylactic acid (PLA) which hydrolytically degrades more rapidly, and thus would be more suitable for field conditions assuming equivalent settling performance. Secondly, we will prepare the acrylate analogs of the macromonomers, with this modification expected to yield flocculants of significantly higher MW, and thus potentially faster settling rates. After the relationship between optimal structure and field conditions has been established, larger scale testing is required to proceed towards field application.

#### 5.4 Conclusions

In this work, we have used a new family of cationic polyester-based polymers to flocculate oil sands MFTs. The radical polymerization of polycaprolactone choline iodide ester methacrylate (PCL<sub>2</sub>ChMA) macromonomers made comb-like polymeric flocculants with tunable charge density and hydrolytically degradable grafts that increased the hydrophobicity of the polymer with under accelerated ageing, further dewatering MFT sediments. Poly(PCL<sub>2</sub>ChMA) flocculant performed best in 5 wt. % MFT when added at a dosage of 5000 ppm, with an ISR of 0.31 m/h, turbidity of 6.65 NTU, and CST (before degradation) of 22 s. The equivalent non-degradable material used for comparison, poly(TMAEMC), had slightly improved properties at a lower level of 3000 ppm – an ISR of 0.34 m/h, turbidity of 0.405 NTU, and the lowest CST (before degradation) of 10.5 s – due to its higher charge density. However, the CST of poly(PCL<sub>2</sub>ChMA) decreased by a factor of two after degradation, while that of poly(TMAEMC) did not change. Copolymerization with acrylamide could control the performance of the flocculants, although higher dosages were needed to achieve the same performance as the corresponding homopolymers.

The study demonstrates that the dewatering efficiency of the novel PCL<sub>2</sub>ChMA flocculants, specifically designed for treatment of oil sands MFT, improved upon *in situ* hydrolytic degradation. Further work is underway to relate the performance of the flocculants to the structure of the macromonomer, and to proceed with larger-scale testing.

## References

- Agostini, A., Gatti, S., Cesana, A., Moscatelli, D., 2017. Synthesis and Degradation Study of Cationic Polycaprolactone-Based Nanoparticles for Biomedical and Industrial Applications. *Ind. Eng. Chem. Res.* 56, 5872–5880. doi:10.1021/acs.iecr.7b00426
- Alagha, L., Wang, S., Yan, L., Xu, Z., Masliyah, J., 2013. Probing Adsorption of Polyacrylamide-Based Polymers on Anisotropic Basal Planes of Kaolinite Using Quartz Crystal Microbalance. *Langmuir* 29, 3989–3998. doi:10.1021/la304966v
- Alamgir, A., Harbottle, D., Masliyah, J., Xu, Z., 2012. Al-PAM assisted filtration system for abatement of mature fine tailings. *Chem. Eng. Sci.* 80, 91–99. doi:10.1016/j.ces.2012.06.010
- Bharti, S., Mishra, S., Sen, G., 2013. Ceric ion initiated synthesis of polyacrylamide grafted oatmeal: Its application as flocculant for wastewater treatment. *Carbohydr. Polym.* 93, 528–36. doi:10.1016/j.carbpol.2012.11.072
- Botha, L., Davey, S., Nguyen, B., Swarnakar, A.K., Rivard, E., Soares, J.B.P., 2017. Flocculation of oil sands tailings by hyperbranched functionalized polyethylenes (HBfPE). *Miner. Eng.* 108, 71–82. doi:10.1016/j.mineng.2017.02.004
- Botha, L., Soares, J.B.P., 2015. The Influence of Tailings Composition on Flocculation. *Can. J. Chem. Eng.* 93, 1514–1523. doi:10.1002/cjce.22241
- Chen, C.S., Lau, Y.Y., Mercer, S.M., Robert, T., Horton, J.H., Jessop, P.G., 2013. The effect of switchable water additives on clay settling. *ChemSusChem* 6, 132–140. doi:10.1002/cssc.201200465
- Colombo, C., Dragoni, L., Gatti, S., Pesce, R.M., Rooney, T.R., Mavroudakos, E., Ferrari, R., Moscatelli, D., 2014. Tunable degradation behavior of PEGylated polyester-based nanoparticles obtained through emulsion free radical polymerization. *Ind. Eng. Chem. Res.* 53, 9128–9135. doi:10.1021/ie4036077
- Das, R., Ghorai, S., Pal, S., 2013. Flocculation characteristics of polyacrylamide grafted hydroxypropyl methyl cellulose: An efficient biodegradable flocculant. *Chem. Eng. J.* 229, 144–152. doi:10.1016/j.cej.2013.05.104
- Deng, Y., Xiao, H., Pelton, R., 1996. Temperature-Sensitive Flocculants Based on Poly(N-isopropylacrylamide-co-diallyldimethylammonium Chloride). *J. Colloid Interface Sci.* 179, 188–193. doi:10.1006/jcis.1996.0201
- Eyley, S., Vandamme, D., Lama, S., Van den Mooter, G., Muylaert, K., Thielemans, W., 2015. CO<sub>2</sub> controlled flocculation of microalgae using pH responsive cellulose nanocrystals. *Nanoscale* 7, 14413–14421. doi:10.1039/C5NR03853G
- Feng, B., Peng, J., Zhu, X., Huang, W., 2017. The settling behavior of quartz using chitosan as flocculant. *J. Mater. Res. Technol.* 6, 71–76. doi:10.1016/j.jmrt.2016.09.004
- Ferrari, R., Yu, Y., Morbidelli, M., Hutchinson, R.A., Moscatelli, D., 2011. Epsilon-

- Caprolactone-Based Macromonomers Suitable for Biodegradable Nanoparticles Synthesis Through Free Radical Polymerization. *Macromolecules* 44, 9205–9212. doi:10.1021/ma201955p
- Franks, G. V., Li, H., O'Shea, J.-P., Qiao, G.G., 2009. Temperature responsive polymers as multiple function reagents in mineral processing. *Adv. Powder Technol.* 20, 273–279. doi:10.1016/j.appt.2009.02.002
- Franks, G. V., 2005. Stimulant sensitive flocculation and consolidation for improved solid/liquid separation. *J. Colloid Interface Sci.* 292, 598–603. doi:10.1016/j.jcis.2005.06.010
- Isik, M., Fernandes, A.M., Vijayakrishna, K., Paulis, M., Mecerreyes, D., 2016. Preparation of poly(ionic liquid) nanoparticles and their novel application as flocculants for water purification. *Polym. Chem.* 7, 1668–1674. doi:10.1039/C5PY02001H
- Kaminsky, H.A.W., 2008. Characterization of an Athabasca oil sand ore and process streams. University of Alberta.
- Li, H., Long, J., Xu, Z., Masliyah, J., 2007. Flocculation of kaolinite clay suspensions using a temperature-sensitive polymer. *AIChE J.* 53, 479–488. doi:10.1002/aic
- Li, H., O'Shea, J.-P., Franks, G. V., 2009. Effect of molecular weight of poly( N -isopropyl acrylamide) temperature-sensitive flocculants on dewatering. *AIChE J.* 55, 2070–2080. doi:10.1002/aic.11859
- Li, J., Jiao, S., Zhong, L., Pan, J., Ma, Q., 2013. Optimizing coagulation and flocculation process for kaolinite suspension with chitosan. *Colloids Surfaces A Physicochem. Eng. Asp.* 428, 100–110. doi:10.1016/j.colsurfa.2013.03.034
- Li, Y., Kwak, J.C.T., 2004. Rheology of hydrophobically modified polyacrylamide-co-poly(acrylic acid) on addition of surfactant and variation of solution pH. *Langmuir* 20, 4859–4866. doi:10.1021/la036331h
- Liu, Y., Lv, C., Ding, J., Qian, P., Zhang, X., Yu, Y., Ye, S., Chen, Y., 2016. The use of the organic-inorganic hybrid polymer Al(OH)<sub>3</sub>-polyacrylamide to flocculate particles in the cyanide tailing suspensions. *Miner. Eng.* 89, 108–117. doi:10.1016/j.mineng.2016.01.018
- Lu, H., Wang, Y., Li, L., Kotsuchibashi, Y., Narain, R., Zeng, H., 2015. Temperature- and pH-Responsive Benzoboroxole-Based Polymers for Flocculation and Enhanced Dewatering of Fine Particle Suspensions. *ACS Appl. Mater. Interfaces* 7, 27176–27187. doi:10.1021/acsami.5b09874
- Lu, Q., Yan, B., Xie, L., Huang, J., Liu, Y., Zeng, H., 2016. A two-step flocculation process on oil sands tailings treatment using oppositely charged polymer flocculants. *Sci. Total Environ.* 565, 369–375. doi:10.1016/j.scitotenv.2016.04.192
- Masliyah, J. H., Czarnecki, J. A., Xu, Z., 2011. Handbook on theory and practice of bitumen recovery from Athabasca oil sands: theoretical basis, 1st ed. Kingsley Knowledge Publishing, Canada.

- Masliyah, J., Zhou, Z.J., Xu, Z., Czarnecki, J., Hamza, H., 2004. Understanding Water-Based Bitumen Extraction from Athabasca Oil Sands. *Can. J. Chem. Eng.* 82, 628–654. doi:10.1002/cjce.5450820403
- Mei, Y., Ballauff, M., 2005. Effect of counterions on the swelling of spherical polyelectrolyte brushes. *Eur. Phys. J. E* 16, 341–349. doi:10.1140/epje/i2004-10089-9
- O’Shea, J.-P., Qiao, G.G., Franks, G. V, 2011a. Temperature responsive flocculation and solid-liquid separations with charged random copolymers of poly(N-isopropyl acrylamide). *J. Colloid Interface Sci.* 360, 61–70. doi:10.1016/j.jcis.2011.04.013
- O’Shea, J.-P., Qiao, G.G., Franks, G. V, 2011b. Temperature responsive flocculation and solid-liquid separations with charged random copolymers of poly(N-isopropyl acrylamide). *J. Colloid Interface Sci.* 360, 61–70. doi:10.1016/j.jcis.2011.04.013
- Penner, T.J., Foght, J.M., 2010. Mature fine tailings from oil sands processing harbour diverse methanogenic communities. *Can. J. Microbiol.* 56, 459–470. doi:10.1139/W10-029
- Pinaud, J., Kowal, E., Cunningham, M., Jessop, P., 2012. 2-(Diethyl)aminoethyl Methacrylate as a CO<sub>2</sub>-Switchable Comonomer for the Preparation of Readily Coagulated and Redispersed Polymer Latexes. *ACS Macro Lett.* 1, 1103–1107. doi:10.1021/mz3003215
- Reis, L.G., Oliveira, R.S., Palhares, T.N., Spinelli, L.S., Lucas, E.F., Vedoy, D.R.L., Asare, E., Soares, J.B.P., 2016. Using acrylamide/propylene oxide copolymers to dewater and densify mature fine tailings. *Miner. Eng.* 95, 29–39. doi:10.1016/j.mineng.2016.06.005
- Rooney, T.R., Gumfekar, S.P., Soares, J.B.P., Hutchinson, R.A., 2016. Cationic Hydrolytically Degradable Flocculants with Enhanced Water Recovery for Oil Sands Tailings Remediation. *Macromol. Mater. Eng.* 301, 1248–1254. doi:10.1002/mame.201600230
- Sakohara, S., Kawachi, T., Gotoh, T., Iizawa, T., 2013. Consolidation of suspended particles by using dual ionic thermosensitive polymers with incorporated a hydrophobic component. *Sep. Purif. Technol.* 106, 90–96. doi:10.1016/j.seppur.2012.12.030
- Sakohara, S., Yagi, S., Iizawa, T., 2011. Dewatering of inorganic sludge using dual ionic thermosensitive polymers. *Sep. Purif. Technol.* 80, 148–154. doi:10.1016/j.seppur.2011.04.022
- Sand, A., Yadav, M., Mishra, D.K., Behari, K., 2010. Modification of alginate by grafting of N-vinyl-2-pyrrolidone and studies of physicochemical properties in terms of swelling capacity, metal-ion uptake and flocculation. *Carbohydr. Polym.* 80, 1147–1154. doi:10.1016/j.carbpol.2010.01.036
- Sawalha, O., Scholz, M., 2007. Assessment of Capillary Suction Time (CST) Test Methodologies. *Environ. Technol.* 28, 1377–1386. doi:10.1080/09593332808618898
- Shah, A.A., Hasan, F., Hameed, A., Ahmed, S., 2008. Biological degradation of plastics: A comprehensive review. *Biotechnol. Adv.* 26, 246–265. doi:10.1016/j.biotechadv.2007.12.005

- Sharma, B.R., Dhuldhoya, N.C., Merchant, U.C., 2006. Flocculants—an Ecofriendly Approach. *J. Polym. Environ.* 14, 195–202. doi:10.1007/s10924-006-0011-x
- Siddique, T., Mohamad Shahimin, M.F., Zamir, S., Semple, K., Li, C., Foght, J.M., 2015. Long-Term Incubation Reveals Methanogenic Biodegradation of C 5 and C 6 iso -Alkanes in Oil Sands Tailings. *Environ. Sci. Technol.* 49, 14732–14739. doi:10.1021/acs.est.5b04370
- Tian, B., Ge, X., Pan, G., Luan, Z., 2007. Effect of nitrate or sulfate on flocculation properties of cationic polymer flocculants. *Desalination* 208, 134–145. doi:10.1016/j.desal.2006.04.077
- Vajihinejad, V., Guillermo, R., Soares, J.B.P., 2017. Dewatering Oil Sands Mature Fine Tailings (MFTs) with Poly(acrylamide- co -diallyldimethylammonium chloride): Effect of Average Molecular Weight and Copolymer Composition. *Ind. Eng. Chem. Res.* 56, 1256–1266. doi:10.1021/acs.iecr.6b04348
- Wang, C., Han, C., Lin, Z., Masliyah, J., Liu, Q., Xu, Z., 2016. Role of Preconditioning Cationic Zetag Flocculant in Enhancing Mature Fine Tailings Flocculation. *Energy and Fuels* 30, 5223–5231. doi:10.1021/acs.energyfuels.6b00108
- Zhang, Z., Xia, S., Zhang, J., 2010. Enhanced dewatering of waste sludge with microbial flocculant TJ-F1 as a novel conditioner. *Water Res.* 44, 3087–92. doi:10.1016/j.watres.2010.02.033
- Zheng, H., Sun, Y., Guo, J., Li, F., Fan, W., Liao, Y., Guan, Q., 2014. Characterization and Evaluation of Dewatering Properties of PADB, a Highly Efficient Cationic Flocculant. *Ind. Eng. Chem. Res.* 53, 2572–2582. doi:10.1021/ie403635y
- Zheng, H., Sun, Y., Zhu, C., Guo, J., Zhao, C., Liao, Y., Guan, Q., 2013. UV-initiated polymerization of hydrophobically associating cationic flocculants: Synthesis, characterization, and dewatering properties. *Chem. Eng. J.* 234, 318–326. doi:10.1016/j.cej.2013.08.098
- Zhu, Y., Tan, X., Liu, Q., 2017. Dual polymer flocculants for mature fine tailings dewatering. *Can. J. Chem. Eng.* 95, 3–10. doi:10.1002/cjce.22628
- Zhu, Z., Jian, O., Paillet, S., Desbrières, J., Grassl, B., 2007. Hydrophobically modified associating polyacrylamide (HAPAM) synthesized by micellar copolymerization at high monomer concentration. *Eur. Polym. J.* 43, 824–834. doi:10.1016/j.eurpolymj.2006.12.016



## Chapter 6

### Conclusions and Recommendations

#### 6.1 Conclusions

I started my investigation by studying the effect of multifunctional ternary copolymers on the flocculation of kaolin suspensions. The flocculants contained different fractions of thermosensitive *N*-isopropyl acrylamide (NIPAM), anionic acrylic acid (AA), and hydrophobic *N*-*tert*-butylacrylamide (NTBM) comonomers. Higher polymer molecular weight increased the initial settling rate (ISR) of kaolin suspensions. Addition of the anionic comonomer, AA, up to a certain extent, increased ISR and lowered supernatant turbidity. Incorporation of the hydrophobic comonomer, NTBM, increased the performance of the flocculant in terms of ISR, turbidity, and dewaterability. The LCST of the ternary copolymer increased when the fraction of AA increased, but decreased when the fraction of NTBM increased. Acrylic acid in the ternary copolymer mainly neutralized the edges clay particles that are positively charged, whereas NTBM helped improve the dewaterability of the sediments.

In the next step, I focused on designing terpolymers with precise compositions taking into consideration the binary reactivity ratios of the comonomers. I synthesized hydrophobically-modified cationic ternary copolymers containing NIPAM, 2-(methacryloyloxy) ethyl trimethyl ammonium chloride (MATMAC), and *N*-*tert*-butylacrylamide (BAAM) comonomers, and used them to flocculate mature fine tailings (MFT). This approach enabled me to fine-tune the properties of the flocculant to achieve a desired performance. The cationicity of the terpolymer flocculants was optimized to 40 mol %, and their hydrophobicity was varied from 5 to 15 mol %. The hydrophobically-modified cationic ternary polymer produced the highest floc size of 200  $\mu\text{m}$ , achieved the highest ISR of 7 m/h, and the lowest capillary suction time (CST) of 20 s. The design methodology used in this work formed a framework to systematically synthesize multifunctional polymers and demonstrated the application of such hydrophobically-modified cationic terpolymers to effectively dewater MFT.

In the part segment of my thesis, I synthesized a new family of cationic polyester-based polymers to flocculate MFT. I first synthesized polycaprolactone choline iodide ester methacrylate (PCL<sub>2</sub>ChMA) macromonomers, and then polymerized them using free radical

polymerization, which yielded comb-like polymeric flocculants with tunable charge density and hydrolytically-degradable grafts. Poly(PCL<sub>2</sub>ChMA) showed cationic behavior due to the presence of choline molecule in the flocculant, and accelerated the settling rate of MFT. The flocculant became more hydrophobic in response to hydrolytic degradation, resulting in the hydrolysis of the polyester grafts that reveal the hydrophobic segments and reduce capillary suction time. This phenomenon increased the dewaterability of sediments over a longer period of time.

I also copolymerized PCL<sub>2</sub>ChMA macromonomer with acrylamide to achieve high molecular weight and compared its flocculation performance with homopolymer poly(PCL<sub>2</sub>ChMA). The dewatering efficiency of the novel PCL<sub>2</sub>ChMA-based flocculants, specifically designed for treatment of MFT, improved upon in situ hydrolytic degradation. This technology combined the material properties of polyesters with the productivity of radical polymerization to make dual functional flocculants with characteristics that can be easily tuned to control flocculation performance, such as polymeric cation density, hydrophobic content, and polymer architecture.

## **6.2 Recommendations**

This thesis work gave rise to several areas that need further investigations. I think that a better understanding of the issues encountered during this work would further enrich the current knowledge gained from this work.

The literature survey showed that there are several studies on new polymers and their flocculation performance in various types of wastewater, including clay suspensions. However, the results and knowledge produced in those works cannot be directly applied to MFT due to its complexity. Especially, the presence of various ions and residual bitumen in MFT significantly affect the performance of the flocculants used for other wastewater systems. It is highly recommended to design flocculants that suit the needs of MFT dewatering.

Polymerizable cationic surfactants (surfmers) are one of the potential candidates to achieve a balance between the polymerization kinetics and the desired properties. Such monomers are also referred as surface-active monomers and exhibit better kinetics than regular cationic monomers.

Examples of cationic surfmers are alkyl maleate trimethylamino ethyl bromide, *N,N,N',N'*-tetramethyl-*N,N'*-bis(11-methacryloyloxyundecyl)ethylene diammonium dibromide, and 1-allyl-2-methyl-5-vinyl-pyridinium bromide. Hyperbranched polymers (dendrimers) containing cationic functional groups on their surface can also effectively flocculate MFT due to the presence of higher charge density per molecule. Examples of such hyperbranched polymers are poly(*N*-acryloyl-1,2-diaminoethane hydrochloride), and poly(amidoamine) dendrimers. Flocculants synthesized using monomers that contain hydrophobic segment and positive charges can simultaneously improve dewaterability due to hydrophobicity and charge neutralization due to cationicity. 1-methyl-4-vinyl pyridinium bromide and vinyl benzyl isothiuronium chloride are a couple of examples of such dual functional polymers.

On-field flocculation is carried out with process water containing various ions, whereas lab experiments are performed with deionized water that hinders the successful translation of lab-scale results to the field trials. Sediments obtained after the lab-scale flocculation experiments do not show the channeling effects due to a lower burden of solids however, scale-up experiments produce sediments in which channeling effects are prominent. This phenomenon results in an overestimation of flocculation efficiency of polymers at lab-scale. In general, lab-scale experiments are recommended to carry out in an environment similar to on-field trials.

The ultimate aim of MFT dewatering is to reclaim the land occupied by tailing ponds and recover the water of acceptable quality. Although polymer-assisted flocculation can recover clear water, the sediments are not up to the standard requirements of land reclamation. The oil sands operators/industry process the sediments obtained after flocculation using additional mechanical operations such as thin-lift drying, centrifugation, freeze-thaw etc. The combination polymer-assisted of flocculation and mechanical operations can create sediments that match the requirements of land reclamation. The feed requirements for mechanical operations such as compactness, viscosity, shear strength may vary with the operation. In such cases, polymeric flocculants of certain nature can tune the properties of feed to the mechanical operations. The majority of the literature does not reflect on the behavior/quality of the sediments obtained after the combination of flocculation and mechanical operations. This generates a large knowledge gap and undermines the ability of novel flocculants to commercialize.

Flocculation processes involve typical parameters such as polymer dosage, the solid content of tailings, mixing rate, and polymer microstructure. These parameters need to be optimized for every new polymer used for MFT flocculation, which requires laborious work. Mathematical models describing the flocculation behavior in tailings in presence of polymeric flocculants can be very helpful to reduce the laborious optimization. A model-driven approach to predict which flocculant microstructure will achieve the desired set of performance criteria at given process conditions needs to be established. Further, various experiments or reliable literature data can “train the model” to effectively predict the output parameters.

## Bibliography

- Agostini, A., Gatti, S., Cesana, A., Moscatelli, D., 2017. Synthesis and Degradation Study of Cationic Polycaprolactone-Based Nanoparticles for Biomedical and Industrial Applications. *Ind. Eng. Chem. Res.* 56, 5872–5880. doi:10.1021/acs.iecr.7b00426
- Alagha, L., Wang, S., Yan, L., Xu, Z., Masliyah, J., 2013. Probing Adsorption of Polyacrylamide-Based Polymers on Anisotropic Basal Planes of Kaolinite Using Quartz Crystal Microbalance. *Langmuir* 29, 3989–3998. doi:10.1021/la304966v
- Alamgir, A., Harbottle, D., Masliyah, J., Xu, Z., 2012. Al-PAM assisted filtration system for abatement of mature fine tailings. *Chem. Eng. Sci.* 80, 91–99. doi:10.1016/j.ces.2012.06.010
- Beier, N., Wilson, W., Dunmola, A., Segó, D., 2013. Impact of flocculation-based dewatering on the shear strength of oil sands fine tailings. *Can. Geotech. J.* 50, 1001–1007. <https://doi.org/10.1139/cgj-2012-0262>
- Bharti, S., Mishra, S., Sen, G., 2013. Ceric ion initiated synthesis of polyacrylamide grafted oatmeal: Its application as flocculant for wastewater treatment. *Carbohydr. Polym.* 93, 528–36. doi:10.1016/j.carbpol.2012.11.072
- Bolto, B., Gregory, J., 2007. Organic polyelectrolytes in water treatment. *Water Res.* 41, 2301–2324. doi:10.1016/j.watres.2007.03.012
- Botha, L., Davey, S., Nguyen, B., Swarnakar, A.K., Rivard, E., Soares, J.B.P., 2017. Flocculation of oil sands tailings by hyperbranched functionalized polyethylenes (HBfPE). *Miner. Eng.* 108, 71–82. doi:10.1016/j.mineng.2017.02.004
- Botha, L., Soares, J.B.P., 2015. The Influence of Tailings Composition on Flocculation. *Can. J. Chem. Eng.* 93, 1514–1523. doi:10.1002/cjce.22241
- Candau, F., Selb, J., 1999. Hydrophobically-modified polyacrylamides prepared by micellar polymerization. *Adv. Colloid Interface Sci.* 79, 149–172. doi:10.1016/S0001-8686(98)00077-3
- Cengiz, I., Sabah, E., Ozgen, S., Akyildiz, H., 2009. Flocculation of fine particles in ceramic wastewater using new types of polymeric flocculants. *J. Appl. Polym. Sci.* 112, 1258–1264. <https://doi.org/10.1002/app.29508>
- Chen, C.S., Lau, Y.Y., Mercer, S.M., Robert, T., Horton, J.H., Jessop, P.G., 2013. The effect of switchable water additives on clay settling. *ChemSusChem* 6, 132–140. doi:10.1002/cssc.201200465
- Clark, K.A., Pasternack, D.S., 1932. Hot Water Separation of Bitumen from Alberta Bituminous Sand. *Ind. Eng. Chem.* 24, 1410–1416. doi:10.1021/ie50276a016
- Colombo, C., Dragoni, L., Gatti, S., Pesce, R.M., Rooney, T.R., Mavroudakís, E., Ferrari, R., Moscatelli, D., 2014. Tunable degradation behavior of PEGylated polyester-based nanoparticles obtained through emulsion free radical polymerization. *Ind. Eng. Chem. Res.*

53, 9128–9135. doi:10.1021/ie4036077

Das, R., Ghorai, S., Pal, S., 2013. Flocculation characteristics of polyacrylamide grafted hydroxypropyl methyl cellulose: An efficient biodegradable flocculant. *Chem. Eng. J.* 229, 144–152. doi:10.1016/j.cej.2013.05.104

Deng, Y., Xiao, H., Pelton, R., 1996. Temperature-Sensitive Flocculants Based on Poly(N-isopropylacrylamide-co-diallyldimethylammonium Chloride). *J. Colloid Interface Sci.* 179, 188–193. doi:10.1006/jcis.1996.0201

Dimitrov, I., Trzebicka, B., Muller, A.H.E., Dworak, A., Tsvetanov, C.B., 2007. Thermosensitive water-soluble copolymers with doubly responsive reversibly interacting entities. *Prog. Polym. Sci.* 32, 1275–1343. <https://doi.org/10.1016/j.progpolymsci.2007.07.001>

Divakaran, R., Sivasankara Pillai, V.N., 2001. Flocculation of kaolinite suspensions in water by chitosan. *Water Res.* 35, 3904–3908. doi:10.1016/S0043-1354(01)00131-2

Energy Resources Conservation Board, 2009. Alberta's Energy Reserves 2008 and Supply/Demand Outlook 2009-2018, Outlook.

Escudero Sanz, F.J., Ochoa Gómez, J.R., Sasia, P.M., De Apodaca, E.D., Río, P., 2007. Synthesis of cationic flocculants by the inverse microemulsion copolymerization of acrylamide with 60% 2-acryloxyethyltrimethyl ammonium chloride in the monomer feed. I. Initiation by ammonium persulfate/sodium disulfite redox system. *J. Appl. Polym. Sci.* 103, 2826–2836. doi:10.1002/app.24381

Eyley, S., Vandamme, D., Lama, S., Van den Mooter, G., Muylaert, K., Thielemans, W., 2015. CO<sub>2</sub> controlled flocculation of microalgae using pH responsive cellulose nanocrystals. *Nanoscale* 7, 14413–14421. doi:10.1039/C5NR03853G

Feng, B., Peng, J., Zhu, X., Huang, W., 2017. The settling behavior of quartz using chitosan as flocculant. *J. Mater. Res. Technol.* 6, 71–76. doi:10.1016/j.jmrt.2016.09.004

Ferrari, R., Yu, Y., Morbidelli, M., Hutchinson, R.A., Moscatelli, D., 2011. Epsilon-Caprolactone-Based Macromonomers Suitable for Biodegradable Nanoparticles Synthesis Through Free Radical Polymerization. *Macromolecules* 44, 9205–9212. doi:10.1021/ma201955p

Fineman, M., Ross, S.D., 1950. Linear method for determining monomer reactivity ratios in copolymerization. *J. Polym. Sci.* 5, 259–262. doi:10.1002/pol.1950.120050210

Franks, G. V., 2005. Stimulant sensitive flocculation and consolidation for improved solid/liquid separation. *J. Colloid Interface Sci.* 292, 598–603. doi:10.1016/j.jcis.2005.06.010

Franks, G. V., Li, H., O'Shea, J.-P., Qiao, G.G., 2009. Temperature responsive polymers as multiple function reagents in mineral processing. *Adv. Powder Technol.* 20, 273–279. <https://doi.org/10.1016/j.appt.2009.02.002>

Franks, G., Sepulveda, C., Jameson, G., 2006. pH sensitive flocculation: Settling rates and

- sediment densities. *AIChE J.* 52, 2774–2782. <https://doi.org/10.1002/aic>
- Gao, C., Chen, B., Möhwald, H., 2006. Thermosensitive poly(allylamine)-g-poly(N-isopropylacrylamide) copolymers: Salt-tuned phase separation, particle formation and their applicability on curved surface. *Colloids Surfaces A Physicochem. Eng. Asp.* 272, 203–210. doi:10.1016/j.colsurfa.2005.07.023
- Gao, C., Möhwald, H., Shen, J., 2005. Thermosensitive poly(allylamine)-g-poly(N-isopropylacrylamide): synthesis, phase separation and particle formation. *Polymer (Guildf)*. 46, 4088–4097. doi:10.1016/j.polymer.2005.02.115
- Glinel, K., Sukhorukov, G.B., Möhwald, H., Khrenov, V., Tauer, K., 2003. Thermosensitive Hollow Capsules Based on Thermoresponsive Polyelectrolytes. *Macromol. Chem. Phys.* 204, 1784–1790. doi:10.1002/macp.200350033
- Gouveia, L.M., Paillet, S., Khoukh, A., Grassl, B., Muller, A.J., 2008. The effect of the ionic strength on the rheological behavior of hydrophobically modified polyacrylamide aqueous solutions mixed with sodium dodecyl sulfate (SDS) or cetyltrimethylammonium p-toluenesulfonate (CTAT). *Colloids Surfaces A Physicochem. Eng. Asp.* 322, 211–218. doi:10.1016/j.colsurfa.2008.03.008
- Gregory, J., 2009. Monitoring particle aggregation processes. *Adv. Colloid Interface Sci.* 147–148, 109–123. doi:10.1016/j.cis.2008.09.003
- Gregory, J., Barany, S., 2011. Adsorption and flocculation by polymers and polymer mixtures. *Adv. Colloid Interface Sci.* 169, 1–12. doi:10.1016/j.cis.2011.06.004
- Griot, O., Kitchener, J.A., 1963. “Ageing” of Silica Suspensions in Water and its Influence on Flocculation by Polyacrylamide. *Nature* 200, 1004–1005. <https://doi.org/10.1038/2001004b0>
- Gumfekar, S.P., Rooney, T.R., Hutchinson, R.A., Soares, J.B.P., 2017. Dewatering Oil Sands Tailings with Degradable Polymer Flocculants. *ACS Appl. Mater. Interfaces* 9, 36290–36300. doi:10.1021/acsami.7b10302
- Gumfekar, S.P., Soares, J.B.P., 2018. A novel hydrophobically-modified polyelectrolyte for enhanced dewatering of clay suspension. *Chemosphere* 194, 422–431. doi:10.1016/j.chemosphere.2017.12.009
- Guo, D., Xie, G., Luo, J., 2014. Mechanical properties of nanoparticles: basics and applications. *J. Phys. D. Appl. Phys.* 47, 13001. <https://doi.org/10.1088/0022-3727/47/1/013001>
- Hagiopol, C., 1999. Copolymerization. Springer US, Boston, MA. doi:10.1007/978-1-4615-4183-7
- Han, D.-M., Matthew Zhang, Q., Serpe, M.J., 2015. Poly (N-isopropylacrylamide)-co-(acrylic acid) microgel/Ag nanoparticle hybrids for the colorimetric sensing of H<sub>2</sub>O<sub>2</sub>. *Nanoscale* 7, 2784–2789. doi:10.1039/C4NR06093H
- Inchausti, I., Sasia, P.M., Katime, I., 2005. Copolymerization of dimethylaminoethylacrylate-

- methyl chloride and acrylamide in inverse emulsion. *J. Mater. Sci.* 40, 4833–4838.  
<https://doi.org/10.1007/s10853-005-2003-y>
- Isik, M., Fernandes, A.M., Vijayakrishna, K., Paulis, M., Mecerreyes, D., 2016. Preparation of poly(ionic liquid) nanoparticles and their novel application as flocculants for water purification. *Polym. Chem.* 7, 1668–1674. doi:10.1039/C5PY02001H
- Jain, K., Vedarajan, R., Watanabe, M., Ishikiriya, M., Matsumi, N., 2015. Tunable LCST behavior of poly(N-isopropylacrylamide/ionic liquid) copolymers. *Polym. Chem.* 6, 6819–6825. doi:10.1039/C5PY00998G
- Jia, S., Yang, Z., Yang, W., Zhang, T., Zhang, S., Yang, X., Dong, Y., Wu, J., Wang, Y., 2016. Removal of Cu(II) and tetracycline using an aromatic rings-functionalized chitosan-based flocculant: Enhanced interaction between the flocculant and the antibiotic. *Chem. Eng. J.* 283, 495–503. doi:10.1016/j.cej.2015.08.003
- Kaminsky, H.A.W., 2008. Characterization of an Athabasca oil sand ore and process streams. University of Alberta.
- Kelen, T., Tüd[Otilde]s, F., 1975. Analysis of the Linear Methods for Determining Copolymerization Reactivity Ratios. I. A New Improved Linear Graphic Method. *J. Macromol. Sci. Part A - Chem.* 9, 1–27. doi:10.1080/00222337508068644
- Klein, C., Harbottle, D., Alagha, L., Xu, Z., 2013. Impact of fugitive bitumen on polymer-based flocculation of mature fine tailings. *Can. J. Chem. Eng.* 91, 1427–1432.  
<https://doi.org/10.1002/cjce.21863>
- Konan, K.L., Peyratout, C., Bonnet, J.P., Smith, A., Jacquet, A., Magnoux, P., Ayrault, P., 2007. Surface properties of kaolin and illite suspensions in concentrated calcium hydroxide medium. *J. Colloid Interface Sci.* 307, 101–108. <https://doi.org/10.1016/j.jcis.2006.10.085>
- Lee, K.E., Morad, N., Poh, B.T., Teng, T.T., 2011. Comparative study on the effectiveness of hydrophobically modified cationic polyacrylamide groups in the flocculation of kaolin. *Desalination* 270, 206–213. doi:10.1016/j.desal.2010.11.047
- Li, H., Long, J., Xu, Z., Masliyah, J.H., 2008. Effect of molecular weight and charge density on the performance of polyacrylamide in low-grade oil sand ore processing. *Can. J. Chem. Eng.* 86, 177–185. <https://doi.org/10.1002/cjce.20029>
- Li, H., O'Shea, J.-P., Franks, G. V., 2009. Effect of molecular weight of poly(N-isopropyl acrylamide) temperature-sensitive flocculants on dewatering. *AIChE J.* 55, 2070–2080.  
<https://doi.org/10.1002/aic.11859>
- Li, J., Jiao, S., Zhong, L., Pan, J., Ma, Q., 2013. Optimizing coagulation and flocculation process for kaolin suspension with chitosan. *Colloids Surfaces A Physicochem. Eng. Asp.* 428, 100–110. doi:10.1016/j.colsurfa.2013.03.034
- Li, Y., Kwak, J.C.T., 2004. Rheology of hydrophobically modified polyacrylamide-co-poly(acrylic acid) on addition of surfactant and variation of solution pH. *Langmuir* 20,



4859–4866. doi:10.1021/la036331h

- Li, H., Long, J., Xu, Z., Masliyah, J., 2007. Flocculation of kaolinite clay suspensions using a temperature-sensitive polymer. *AIChE J.* 53, 479–488. doi:10.1002/aic
- Liu, B., Zheng, H., Deng, X., Xu, B., Sun, Y., Liu, Y., Liang, J., 2017. Formation of cationic hydrophobic micro-blocks in P(AM-DMC) by template assembly: characterization and application in sludge dewatering. *RSC Adv.* 7, 6114–6122. doi:10.1039/C6RA27400E
- Liu, P., 2007. Polymer modified clay minerals: A review. *Appl. Clay Sci.* 38, 64–76. doi:10.1016/j.clay.2007.01.004
- Liu, Y., Lv, C., Ding, J., Qian, P., Zhang, X., Yu, Y., Ye, S., Chen, Y., 2016. The use of the organic-inorganic hybrid polymer Al(OH)<sub>3</sub>-polyacrylamide to flocculate particles in the cyanide tailing suspensions. *Miner. Eng.* 89, 108–117. doi:10.1016/j.mineng.2016.01.018
- Liao, Y., Zheng, H., Qian, L., Sun, Y., Dai, L., Xue, W., 2014. UV-Initiated Polymerization of Hydrophobically Associating Cationic Polyacrylamide Modified by a Surface-Active Monomer: A Comparative Study of Synthesis, Characterization, and Sludge Dewatering Performance. *Ind. Eng. Chem. Res.* 53, 11193–11203. <https://doi.org/10.1021/ie5016987>
- Long, J., Li, H., Xu, Z., Masliyah, J.H., 2006. Role of colloidal interactions in oil sand tailings treatment. *AIChE J.* 52, 371–383. doi:10.1002/aic.10603
- Lowe, T.L., Virtanen, J., Tenhu, H., 1999. Hydrophobically modified responsive polyelectrolytes. *Langmuir* 15, 4259–4265. doi:10.1021/la981194n
- Lu, H., Wang, Y., Li, L., Kotsuchibashi, Y., Narain, R., Zeng, H., 2015. Temperature- and pH-Responsive Benzoboroxole-Based Polymers for Flocculation and Enhanced Dewatering of Fine Particle Suspensions. *ACS Appl. Mater. Interfaces* 7, 27176–27187. <https://doi.org/10.1021/acsami.5b09874>
- Lu, H., Xiang, L., Cui, X., Liu, J., Wang, Y., Narain, R., Zeng, H., 2016. Molecular Weight Dependence of Synthetic Glycopolymers on Flocculation and Dewatering of Fine Particles. *Langmuir* 32, 11615–11622. <https://doi.org/10.1021/acs.langmuir.6b03072>
- Lu, Q., Yan, B., Xie, L., Huang, J., Liu, Y., Zeng, H., 2016. A two-step flocculation process on oil sands tailings treatment using oppositely charged polymer flocculants. *Sci. Total Environ.* 565, 369–375. <https://doi.org/10.1016/j.scitotenv.2016.04.192>
- Masliyah, J.H., Bhattacharjee, S., 2006. *Electrokinetic and Colloid Transport Phenomena*. John Wiley & Sons, Inc., Hoboken, NJ, USA. <https://doi.org/10.1002/0471799742>
- Masliyah, J. H., Czarnecki, J. A., Xu, Z., 2011. *Handbook on theory and practice of bitumen recovery from Athabasca oil sands: theoretical basis*, 1st ed. Kingsley Knowledge Publishing, Canada.
- Masliyah, J., Zhou, Z.J., Xu, Z., Czarnecki, J., Hamza, H., 2004. Understanding Water-Based Bitumen Extraction from Athabasca Oil Sands. *Can. J. Chem. Eng.* 82, 628–654. doi:10.1002/cjce.5450820403

- Maximova, N., Dahl, O., 2006. Environmental implications of aggregation phenomena: Current understanding. *Curr. Opin. Colloid Interface Sci.* 11, 246–266. <https://doi.org/10.1016/j.cocis.2006.06.001>
- Mayo, F.R., Lewis, F.M., 1944. Copolymerization. I. A Basis for Comparing the Behavior of Monomers in Copolymerization; The Copolymerization of Styrene and Methyl Methacrylate. *J. Am. Chem. Soc.* 66, 1594–1601. doi:10.1021/ja01237a052
- Mei, Y., Ballauff, M., 2005. Effect of counterions on the swelling of spherical polyelectrolyte brushes. *Eur. Phys. J. E* 16, 341–349. doi:10.1140/epje/i2004-10089-9
- O’Shea, J.-P., Qiao, G.G., Franks, G. V, 2011. Temperature responsive flocculation and solid-liquid separations with charged random copolymers of poly(N-isopropyl acrylamide). *J. Colloid Interface Sci.* 360, 61–70. doi:10.1016/j.jcis.2011.04.013
- Pal, S., Sen, G., Ghosh, S., Singh, R.P., 2012. High performance polymeric flocculants based on modified polysaccharides—Microwave assisted synthesis. *Carbohydr. Polym.* 87, 336–342. <https://doi.org/10.1016/j.carbpol.2011.07.052>
- Penner, T.J., Foght, J.M., 2010. Mature fine tailings from oil sands processing harbour diverse methanogenic communities. *Can. J. Microbiol.* 56, 459–470. doi:10.1139/W10-029
- Pinaud, J., Kowal, E., Cunningham, M., Jessop, P., 2012. 2-(Diethyl)aminoethyl Methacrylate as a CO<sub>2</sub>-Switchable Comonomer for the Preparation of Readily Coagulated and Redispersed Polymer Latexes. *ACS Macro Lett.* 1, 1103–1107. doi:10.1021/mz3003215
- Quinlan, P.J., Tam, K.C., 2015. Water treatment technologies for the remediation of naphthenic acids in oil sands process-affected water. *Chem. Eng. J.* 279, 696–714. doi:10.1016/j.cej.2015.05.062
- Reis, L.G., Oliveira, R.S., Palhares, T.N., Spinelli, L.S., Lucas, E.F., Vedoy, D.R.L., Asare, E., Soares, J.B.P., 2016. Using acrylamide/propylene oxide copolymers to dewater and densify mature fine tailings. *Miner. Eng.* 95, 29–39. doi:10.1016/j.mineng.2016.06.005
- Rani, G.U., Mishra, S., Sen, G., Jha, U., 2012. Polyacrylamide grafted Agar: synthesis and applications of conventional and microwave assisted technique. *Carbohydr. Polym.* 90, 784–91. <https://doi.org/10.1016/j.carbpol.2012.05.069>
- Ren, H., Li, Y., Zhang, S., Wang, J., Luan, Z., 2008. Flocculation of kaolin suspension with the adsorption of N,N-disubstituted hydrophobically modified polyacrylamide. *Colloids Surfaces A Physicochem. Eng. Asp.* 317, 388–393. <https://doi.org/10.1016/j.colsurfa.2007.11.007>
- Roussy, J., Van Vooren, M., Dempsey, B.A., Guibal, E., 2005. Influence of chitosan characteristics on the coagulation and the flocculation of bentonite suspensions. *Water Res.* 39, 3247–3258. <https://doi.org/10.1016/j.watres.2005.05.039>
- Rooney, T.R., Gumfekar, S.P., Soares, J.B.P., Hutchinson, R.A., 2016. Cationic Hydrolytically Degradable Flocculants with Enhanced Water Recovery for Oil Sands Tailings

- Remediation. *Macromol. Mater. Eng.* 301, 1248–1254. doi:10.1002/mame.201600230
- Sakohara, S., Hinago, R., Ueda, H., 2008. Compaction of TiO<sub>2</sub> suspension by using dual ionic thermosensitive polymers. *Sep. Purif. Technol.* 63, 319–323. <https://doi.org/10.1016/j.seppur.2008.05.014>
- Sakohara, S., Kawachi, T., Gotoh, T., Iizawa, T., 2013. Consolidation of suspended particles by using dual ionic thermosensitive polymers with incorporated a hydrophobic component. *Sep. Purif. Technol.* 106, 90–96. <https://doi.org/10.1016/j.seppur.2012.12.030>
- Sakohara, S., Nishikawa, K., 2004. Compaction of TiO<sub>2</sub> suspension utilizing hydrophilic/hydrophobic transition of cationic thermosensitive polymers. *J. Colloid Interface Sci.* 278, 304–9. <https://doi.org/10.1016/j.jcis.2004.06.002>
- Sakohara, S., Yagi, S., Iizawa, T., 2011. Dewatering of inorganic sludge using dual ionic thermosensitive polymers. *Sep. Purif. Technol.* 80, 148–154. <https://doi.org/10.1016/j.seppur.2011.04.022>
- Sand, A., Yadav, M., Mishra, D.K., Behari, K., 2010. Modification of alginate by grafting of N-vinyl-2-pyrrolidone and studies of physicochemical properties in terms of swelling capacity, metal-ion uptake and flocculation. *Carbohydr. Polym.* 80, 1147–1154. doi:10.1016/j.carbpol.2010.01.036
- Sawalha, O., Scholz, M., 2007. Assessment of Capillary Suction Time (CST) Test Methodologies. *Environ. Technol.* 28, 1377–1386. doi:10.1080/09593332808618898
- Senaputra, A., Jones, F., Fawell, P.D., Smith, P.G., 2014. Focused beam reflectance measurement for monitoring the extent and efficiency of flocculation in mineral systems. *AIChE J.* 60, 251–265. doi:10.1002/aic.14256
- Sinha Ray, S., Okamoto, M., 2003. Polymer/layered silicate nanocomposites: a review from preparation to processing. *Prog. Polym. Sci.* 28, 1539–1641. doi:10.1016/j.progpolymsci.2003.08.002
- Shah, A.A., Hasan, F., Hameed, A., Ahmed, S., 2008. Biological degradation of plastics: A comprehensive review. *Biotechnol. Adv.* 26, 246–265. doi:10.1016/j.biotechadv.2007.12.005
- Shaikh, S.M.R., Nasser, M.S., Hussein, I.A., Benamor, A., 2017. Investigation of the effect of polyelectrolyte structure and type on the electrokinetics and flocculation behavior of bentonite dispersions. *Chem. Eng. J.* 311, 265–276. <https://doi.org/10.1016/j.cej.2016.11.098>
- Shaikh, S.M.R., Nasser, M.S., Hussein, I., Benamor, A., Onaizi, S.A., Qiblawey, H., 2017. Influence of polyelectrolytes and other polymer complexes on the flocculation and rheological behaviors of clay minerals: A comprehensive review. *Sep. Purif. Technol.* 187, 137–161. doi:10.1016/j.seppur.2017.06.050
- Sharma, B.R., Dhuldhoya, N.C., Merchant, U.C., 2006. Flocculants—an Ecofriendly Approach.

- J. Polym. Environ. 14, 195–202. doi:10.1007/s10924-006-0011-x
- Siddique, T., Mohamad Shahimin, M.F., Zamir, S., Semple, K., Li, C., Foght, J.M., 2015. Long-Term Incubation Reveals Methanogenic Biodegradation of C 5 and C 6 iso -Alkanes in Oil Sands Tailings. *Environ. Sci. Technol.* 49, 14732–14739. doi:10.1021/acs.est.5b04370
- Sun, W., Zhang, G., Pan, L., Li, H., Shi, A., 2013. Synthesis, Characterization, and Flocculation Properties of Branched Cationic Polyacrylamide. *Int. J. Polym. Sci.* 2013, 1–10. <https://doi.org/10.1155/2013/397027>
- Sylvester, N.D., Toure, M.P., 1978. Effect of Shear on Polymer Aided Flocculation of Suspensions. *Ind. Eng. Chem. Prod. Res. Dev.* 17, 347–351. <https://doi.org/10.1021/i360068a012>
- Sworska, A., Laskowski, J., Cymerman, G., 2000. Flocculation of the Syncrude fine tailings. *Int. J. Miner. Process.* 60, 143–152. doi:10.1016/S0301-7516(00)00012-0
- Tombácz, E., Szekeres, M., 2006. Surface charge heterogeneity of kaolinite in aqueous suspension in comparison with montmorillonite. *Appl. Clay Sci.* 34, 105–124. <https://doi.org/10.1016/j.clay.2006.05.009>
- Tian, B., Ge, X., Pan, G., Luan, Z., 2007. Effect of nitrate or sulfate on flocculation properties of cationic polymer flocculants. *Desalination* 208, 134–145. doi:10.1016/j.desal.2006.04.077
- Tripathy, T., De, B., 2006. Flocculation: a new way to treat the waste water. *J. Phys. Sci.* 10, 93–127.
- Vajihinejad, V., Guillermo, R., Soares, J.B.P., 2017. Dewatering Oil Sands Mature Fine Tailings (MFTs) with Poly(acrylamide- co -diallyldimethylammonium chloride): Effect of Average Molecular Weight and Copolymer Composition. *Ind. Eng. Chem. Res.* 56, 1256–1266. <https://doi.org/10.1021/acs.iecr.6b04348>
- Vedoy, D.R.L., Soares, J.B.P., 2015. Water-soluble polymers for oil sands tailing treatment: A Review. *Can. J. Chem. Eng.* 93, 888–904. doi:10.1002/cjce.22129
- Wang, L.-J., Wang, J.-P., Zhang, S.-J., Chen, Y.-Z., Yuan, S.-J., Sheng, G.-P., Yu, H.-Q., 2009. A water-soluble cationic flocculant synthesized by dispersion polymerization in aqueous salts solution. *Sep. Purif. Technol.* 67, 331–335. <https://doi.org/10.1016/j.seppur.2009.03.044>
- Wang, Y., Kotsuchibashi, Y., Liu, Y., Narain, R., 2014. Temperature-Responsive Hyperbranched Amine-Based Polymers for Solid–Liquid Separation. *Langmuir* 30, 2360–2368. <https://doi.org/10.1021/la5003012>
- Wang, C., Harbottle, D., Liu, Q., Xu, Z., 2014. Current state of fine mineral tailings treatment: A critical review on theory and practice. *Miner. Eng.* 58, 113–131. doi:10.1016/j.mineng.2014.01.018
- Wang, C., Han, C., Lin, Z., Masliyah, J., Liu, Q., Xu, Z., 2016. Role of Preconditioning Cationic Zetag Flocculant in Enhancing Mature Fine Tailings Flocculation. *Energy and Fuels* 30,

5223–5231. doi:10.1021/acs.energyfuels.6b00108

- Wilkinson, N., Metaxas, A., Bricchetto, E., Wickramaratne, S., Reineke, T.M., Dutcher, C.S., 2017. Ionic strength dependence of aggregate size and morphology on polymer- clay flocculation. *Colloids Surfaces A* 529, 1037–1046. doi:10.1016/j.colsurfa.2017.06.085
- Wu, H., Liu, Z., Yang, H., Li, A., 2016. Evaluation of chain architectures and charge properties of various starch-based flocculants for flocculation of humic acid from water. *Water Res.* 96, 126–135. <https://doi.org/10.1016/j.watres.2016.03.055>
- Yang, Z., Wu, H., Yuan, B., Huang, M., Yang, H., Li, A., Bai, J., Cheng, R., 2014. Synthesis of amphoteric starch-based grafting flocculants for flocculation of both positively and negatively charged colloidal contaminants from water. *Chem. Eng. J.* 244, 209–217. <https://doi.org/10.1016/j.cej.2014.01.083>
- Yang, Z.L., Gao, B.Y., Li, C.X., Yue, Q.Y., Liu, B., 2010. Synthesis and characterization of hydrophobically associating cationic polyacrylamide. *Chem. Eng. J.* 161, 27–33. doi:10.1016/j.cej.2010.04.015
- Yingchoncharoen, P., Kalinowski, D.S., Richardson, D.R., 2016. Lipid-Based Drug Delivery Systems in Cancer Therapy: What Is Available and What Is Yet to Come. *Pharmacol. Rev.* 68, 701–787. <https://doi.org/10.1124/pr.115.012070>
- Zhang, D., Thundat, T., Narain, R., 2017. Flocculation and Dewatering of Mature Fine Tailings Using Temperature-Responsive Cationic Polymers. *Langmuir* 33, 5900–5909. <https://doi.org/10.1021/acs.langmuir.7b01160>
- Zhang, Z., Zheng, H., Huang, F., Li, X., He, S., Zhao, C., 2016. Template Polymerization of a Novel Cationic Polyacrylamide: Sequence Distribution, Characterization, and Flocculation Performance. *Ind. Eng. Chem. Res.* 55, 9819–9828. doi:10.1021/acs.iecr.6b01894
- Zhang, Z., Xia, S., Zhang, J., 2010. Enhanced dewatering of waste sludge with microbial flocculant TJ-F1 as a novel conditioner. *Water Res.* 44, 3087–92. doi:10.1016/j.watres.2010.02.033
- Zheng, H., Sun, Y., Guo, J., Li, F., Fan, W., Liao, Y., Guan, Q., 2014. Characterization and Evaluation of Dewatering Properties of PADB, a Highly Efficient Cationic Flocculant. *Ind. Eng. Chem. Res.* 53, 2572–2582. <https://doi.org/10.1021/ie403635y>
- Zheng, H., Sun, Y., Zhu, C., Guo, J., Zhao, C., Liao, Y., Guan, Q., 2013. UV-initiated polymerization of hydrophobically associating cationic flocculants: Synthesis, characterization, and dewatering properties. *Chem. Eng. J.* 234, 318–326. doi:10.1016/j.cej.2013.08.098
- Zhou, Y., Franks, G. V., 2006. Flocculation mechanism induced by cationic polymers investigated by light scattering. *Langmuir* 22, 6775–86. <https://doi.org/10.1021/la060281+>
- Zhou, Y., Gan, Y., Wanless, E.J., Jameson, G.J., Franks, G. V., 2008. Interaction forces between silica surfaces in aqueous solutions of cationic polymeric flocculants: effect of polymer

charge. *Langmuir* 24, 10920–8. <https://doi.org/10.1021/la801109n>

Zhu, Y., Tan, X., Liu, Q., 2017. Dual polymer flocculants for mature fine tailings dewatering. *Can. J. Chem. Eng.* 95, 3–10. doi:10.1002/cjce.22628

Zhu, Z., Jian, O., Paillet, S., Desbrières, J., Grassl, B., 2007. Hydrophobically modified associating polyacrylamide (HAPAM) synthesized by micellar copolymerization at high monomer concentration. *Eur. Polym. J.* 43, 824–834. doi:10.1016/j.eurpolymj.2006.12.016

Zintchenko, A., Ogris, M., Wagner, E., 2006. Temperature Dependent Gene Expression Induced by PNIPAM-Based Copolymers: Potential of Hyperthermia in Gene Transfer. *Bioconjug. Chem.* 17, 766–772. doi:10.1021/bc050292z

## Appendix A

### Supplementary Information for Chapter 5

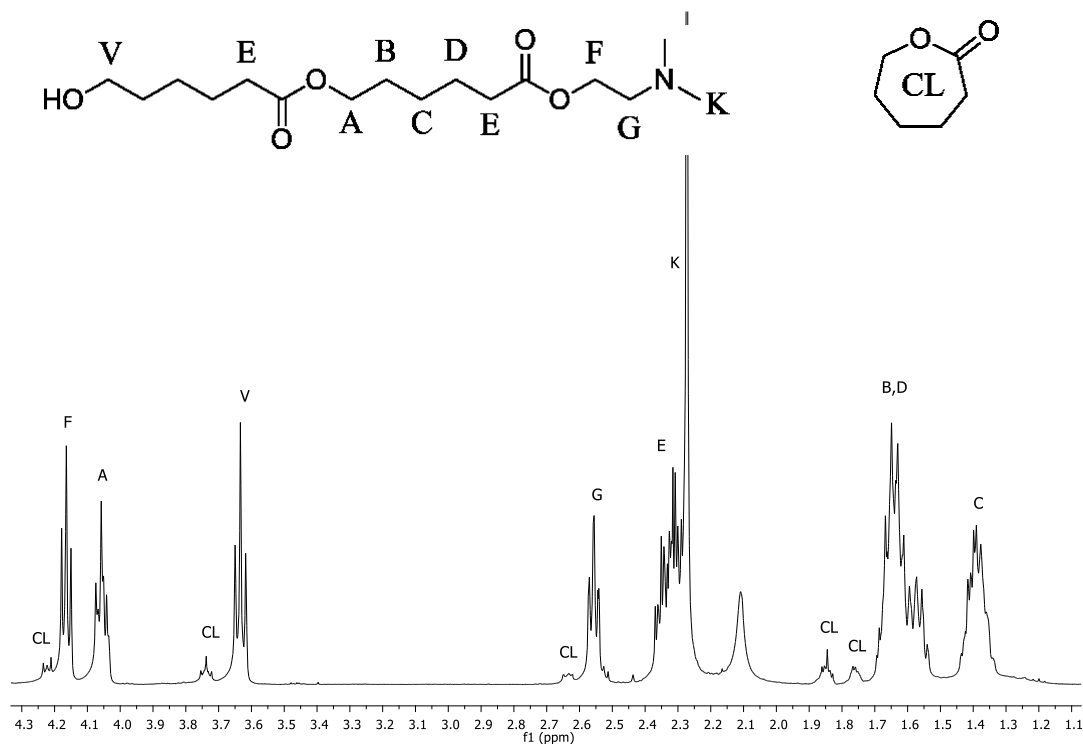


**Figure A-1**  $^1\text{H-NMR}$  spectrum and peak assignment for the average chain length of  $\text{PCL}_2\text{De}$  in  $\text{CDCl}_3$  at  $25\text{ }^\circ\text{C}$ .

$\text{PCL}_2\text{De}$   $^1\text{H-NMR}$  ( $\text{CDCl}_3$ , 400 MHz) with integrations relative to Peak V:  $\delta = 4.16$  ppm (t, 1.9H, F),  $\delta = 4.06$  ppm (t, 2.0H, A),  $\delta = 3.63$  ppm (t, 2.0H, V),  $\delta = 2.56$  ppm (t, 1.9H, G),  $\delta = 2.40\text{--}2.22$  ppm (m, 10.0H, E+K),  $\delta = 1.85$  ppm (m, 0.25H, CL),  $\delta = 1.72\text{--}1.51$  ppm (m, 8.0H, B+D),  $\delta = 1.47\text{--}1.31$  ppm (m, 4.0H, C).

$$n = \frac{\text{Integral (A + V)}}{\text{Integral (V)}} = \frac{2.0 + 2.0}{2.0} = 2.0$$

$$\% \text{CL conversion} = \frac{\text{Integral (A + V)}}{\text{Integral (A + V + CL)}} = \frac{2.0 + 2.0}{2.0 + 2.0 + 0.25} = 94\%$$

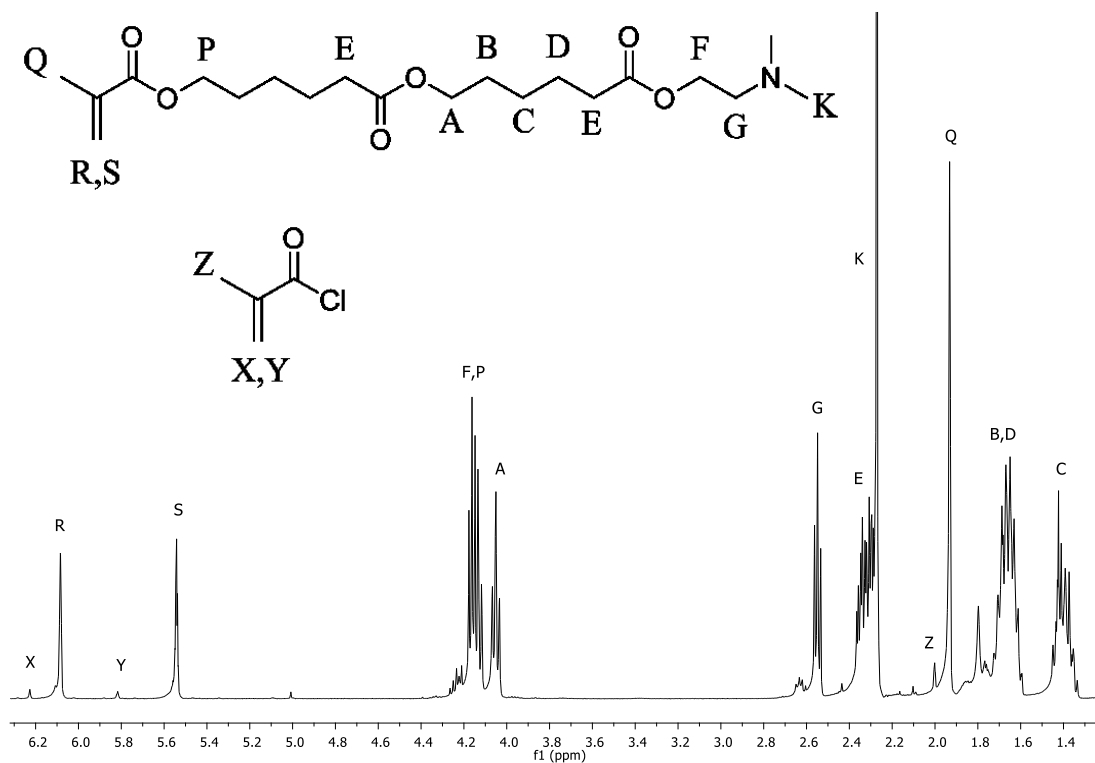


**Figure A-2**  $^1\text{H}$  NMR spectrum and peak assignment for  $\text{PCL}_2\text{DeMA}$  in  $\text{CDCl}_3$  at  $25\text{ }^\circ\text{C}$ .

$\text{PCL}_2\text{DeMA}$   $^1\text{H}$ -NMR ( $\text{CDCl}_3$ , 400 MHz) with integrations relative to Peak S:  $\delta = 6.23$  ppm (s, 0.04H, X),  $\delta = 6.08$  ppm (s, 1.0H, R),  $\delta = 5.82$  ppm (s, 0.04H, Y),  $\delta = 5.54$  ppm (s, 1.0H, S),  $\delta = 4.21\text{--}4.10$  ppm (m, 4.0H, F+P),  $\delta = 4.05$  ppm (t, 2.0H, A),  $\delta = 2.55$  ppm (t, 2.0H, G),  $\delta = 2.41\text{--}2.25$  ppm (m, 10.2H, E+K),  $\delta = 2.00$  ppm (s, 0.12H, Z),  $\delta = 1.93$  ppm (s, 3.0H, Q),  $\delta = 1.74\text{--}1.58$  ppm (m, 8.1H, B+D),  $\delta = 1.50\text{--}1.33$  ppm (m, 4.1H, C).

$$n = \frac{\text{Integral (A + G)}/2}{\text{Integral (S)}} = \frac{(2.0 + 2.0)/2}{1.0} = 2.0$$



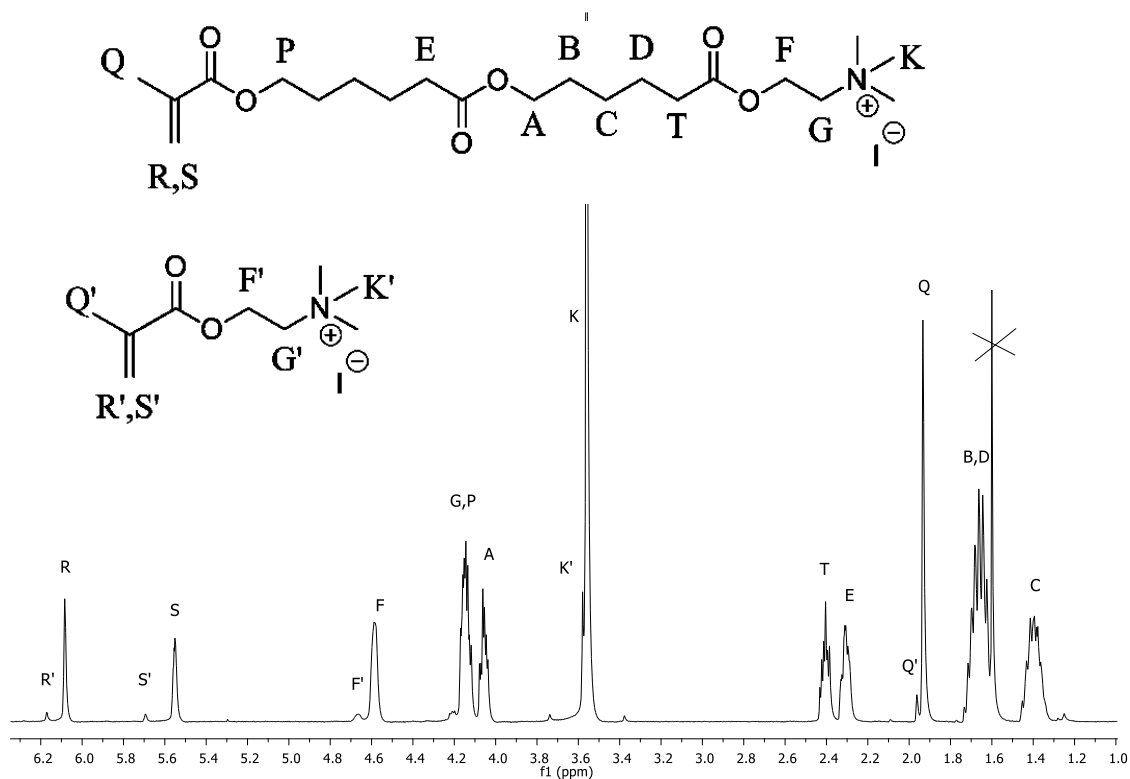


**Figure A-3**  $^1\text{H}$  NMR spectrum and peak assignment for  $\text{PCL}_2\text{ChMA}$  in  $\text{CDCl}_3$  at  $25\text{ }^\circ\text{C}$ .

$\text{PCL}_2\text{ChMA}$   $^1\text{H}$ -NMR ( $\text{CDCl}_3$ , 400 MHz) with integrations relative to Peak (S+S'):  $\delta = 6.17$  ppm (s, 0.1H, R'),  $\delta = 6.09$  ppm (s, 0.9H, R),  $\delta = 5.70$  ppm (s, 0.1H, S'),  $\delta = 5.56$  ppm (s, 0.9H, S),  $\delta = 4.67$  ppm (t, 0.2H, F'),  $\delta = 4.59$  ppm (t, 1.8H, F),  $\delta = 4.23\text{--}4.11$  ppm (m, 4.0H, G+P),  $\delta = 4.06$  ppm (t, 2.0H, A),  $\delta = 3.57$  ppm (s, -, K'),  $\delta = 3.56$  ppm (s, 9.0H, K+K'),  $\delta = 2.45\text{--}2.37$  ppm (t, 2.0H, T),  $\delta = 2.36\text{--}2.27$  ppm (t, 2.0H, E),  $\delta = 1.97$  ppm (s, -, Q'),  $\delta = 1.94$  ppm (s, 3.0H, Q+Q'),  $\delta = 1.74\text{--}1.61$  ppm (m, 8.0H, B+D),  $\delta = 1.47\text{--}1.33$  ppm (m, 4.0H, C).

$$n = \frac{\text{Integral}(E + T)/2}{\text{Integral}(S + S')} = \frac{(2.0 + 2.0)/2}{1.0} = 2.0$$

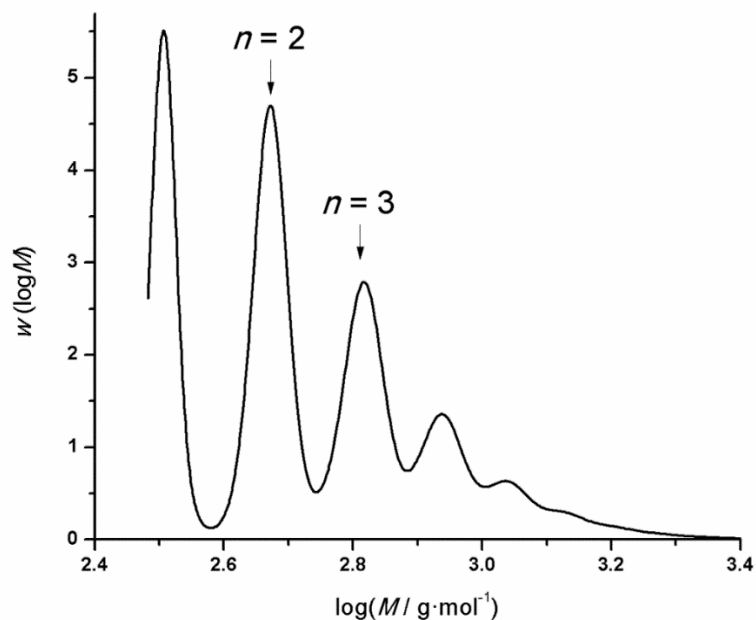


**Figure A-4** Molecular weight distributions for cationic macromonomer precursors measured in polyMMA equivalents by SEC with THF as eluent.

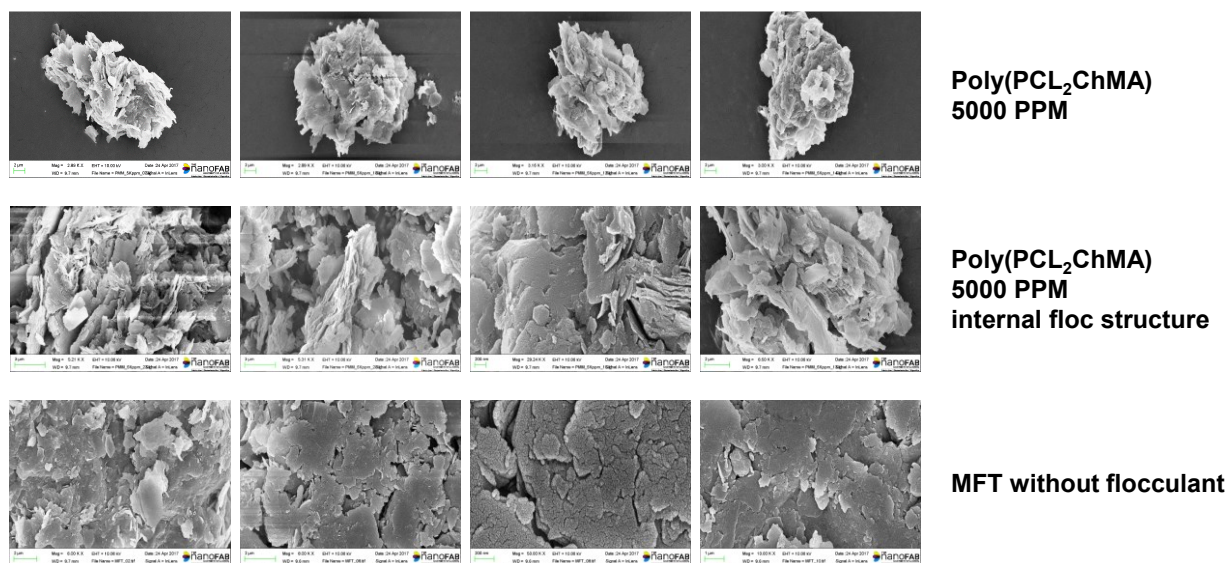


**Figure A-5** Additional Cryo-FE-SEM images show the multiple similar microstructures across the sample

**Table A-1** Tabular format of CST values measured before the degradation of polymer (s)

Dosage (PPM)	Poly(PCL <sub>2</sub> ChMA)	Poly(PCL <sub>2</sub> ChMA-AM)	Poly(TMAEMC)	Poly(TMAEMC-AM)
1000	98.85	72.2	27.25	98.85
2000	63.85	66.7	16.65	30.5
3000	45.55	60.05	13.15	14.9
4000	33.7	37.5	11.15	11
5000	22.75	36.7	10.55	8.7

**Table A-2** Tabular format of CST values measured before the degradation of polymer (s)

Dosage (PPM)	Poly(PCL <sub>2</sub> ChMA)	Poly(PCL <sub>2</sub> ChMA-AM)	Poly(TMAEMC)	Poly(TMAEMC-AM)
1000	13.9	11.7	44.5	85.9
2000	10.6	12.1	12.15	11.15
3000	12.4	12.3	9.1	11.05
4000	10.3	12.05	9.25	10.4
5000	11.45	13.35	10.65	8.3

## Appendix B

### Terpolymer Composition using the Reactivity Ratios Calculated by Different Methods

**Table B-1** Feed and terpolymer composition of the flocculants estimated using the reactivity ratios calculated by Fineman-Ross method.

Terpolymer	NIPAM		MATMAC		BAAM	
	<i>f</i>	<i>F</i>	<i>f</i>	<i>F</i>	<i>f</i>	<i>F</i>
P(NMB-5)	0.775	0.55	0.200	0.40	0.025	0.05
P(NMB-10)	0.74	0.50	0.205	0.40	0.055	0.10
P(NMB-15)	0.69	0.45	0.22	0.40	0.09	0.15

**Table B-2** Feed and terpolymer composition of the flocculants estimated using the reactivity ratios calculated by Kelen-Tudos method.

Terpolymer	NIPAM		MATMAC		BAAM	
	<i>f</i>	<i>F</i>	<i>f</i>	<i>F</i>	<i>f</i>	<i>F</i>
P(NMB-5)	0.750	0.55	0.220	0.40	0.030	0.05
P(NMB-10)	0.700	0.50	0.230	0.40	0.070	0.10
P(NMB-15)	0.660	0.45	0.240	0.40	0.100	0.15

**Table B-3** Feed and terpolymer composition of the flocculants estimated using the reactivity ratios calculated by Yezrielev - Brokhina – Roskin method.

Terpolymer	NIPAM		MATMAC		BAAM	
	<i>f</i>	<i>F</i>	<i>f</i>	<i>F</i>	<i>f</i>	<i>F</i>
P(NMB-5)	0.740	0.55	0.230	0.40	0.030	0.05
P(NMB-10)	0.700	0.50	0.235	0.40	0.065	0.10
P(NMB-15)	0.650	0.45	0.245	0.40	0.105	0.15